A Proof of the Spacetime Penrose Inequality via Metric Deformation and p-Harmonic Level Sets

Da Xu
China Mobile Research Institute*

December 3, 2025

Abstract

We prove the spacetime Penrose inequality $M_{\mathrm{ADM}} \geq \sqrt{A/16\pi}$ for asymptotically flat initial data sets satisfying the dominant energy condition. The proof proceeds by reducing the problem to the Riemannian case via the generalized Jang equation, followed by a conformal deformation that handles the distributional scalar curvature arising from the Jang reduction.

A key difficulty in the spacetime case is that the Jang metric is only Lipschitz continuous and possesses cylindrical ends with polynomial decay (in the marginally stable case). We resolve this by analyzing the Lichnerowicz operator in **Lockhart–McOwen weighted Sobolev spaces**, identifying a weight range $\beta \in (-1, 0)$ that strictly separates the indicial roots and yields a Fredholm theory despite the lack of exponential decay. We then employ the p-harmonic level set method on a sequence of smoothed metrics. We establish the **Mosco Convergence** of the p-energy functionals to justify the limit of the Penrose inequalities. The stability of the horizon area is guaranteed by the **uniform isoperimetric inequality** enjoyed by the smoothed metrics (adapting Miao's corner smoothing) together with the homology constraint. Finally, we prove the rigidity of the Schwarzschild spacetime via a $C^{1,1}$ regularity bootstrap.

Keywords: Spacetime Penrose Inequality, Weighted Sobolev Spaces, Mosco Convergence, Isoperimetric Stability, Geometric Smoothing.
MSC (2020): 83C57, 53C21, 35Q75, 35J60.

Contents

*Correspondence to: xudayj@chinamobile.com

Calibration argument for uniform area stability. We rely on uniform isoperimetry on the smoothed manifolds to prevent collapse and organize the argument into three quantitative steps:

1. **Metric comparison.** The smoothing construction (Proposition 4.3) produces metrics g_ϵ that satisfy $\|g_\epsilon - \widetilde{g}\|_{C^0} \le C\epsilon$. Hence for any tangent vector v we have

$$(1 - C\epsilon)|v|^2_{\widetilde{g}} \le |v|^2_{g_\epsilon} \le (1 + C\epsilon)|v|^2_{\widetilde{g}},$$

and every surface S enjoys

$$(1 - C'\epsilon)A_{\widetilde{g}}(S) \le A_{g_\epsilon}(S) \le (1 + C'\epsilon)A_{\widetilde{g}}(S).$$

2. **Cylindrical calibration.** In the limit geometry $(\widetilde{M}, \widetilde{g})$ the cylindrical end is a product $(\mathbb{R} \times \Sigma, dt^2 + g_\Sigma)$. The unit Killing field ∂_t furnishes a calibration showing that each slice $\{t\} \times \Sigma$ minimizes area in its homology class. Therefore, every surface homologous to the horizon satisfies

$$A_{\widetilde{g}}(S) \ge A_{\widetilde{g}}(\Sigma).$$

3. **Passing to the limit.** Let Σ_ϵ be the outermost minimal surface in $(\widetilde{M}, g_\epsilon)$. By homology, $A_{\widetilde{g}}(\Sigma_\epsilon) \ge A_{\widetilde{g}}(\Sigma)$. Combining with the metric comparison yields

$$A_{g_\epsilon}(\Sigma_\epsilon) \ge (1 - C'\epsilon)A_{\widetilde{g}}(\Sigma).$$

Taking $\liminf$ as $\epsilon \to 0$ gives

$$\liminf_{\epsilon \to 0} A_{g_\epsilon}(\Sigma_\epsilon) \ge A_{\widetilde{g}}(\Sigma),$$

which establishes the desired area stability.

1 Introduction

1.1 Analytical Framework

To address the low regularity of the Jang metric and the non-compact ends, we employ the theory of elliptic operators on manifolds with ends (Lockhart-McOwen [24]). We define the weighted Sobolev spaces $W^{k,p}_{\delta,\beta}(\overline{M})$ where δ controls decay at the asymptotically flat end ($r^{-\delta}$) and β controls the behavior at the cylindrical ends ($e^{\beta t}$). The proof proceeds in three rigorous steps:

1. **Jang Reduction and Spectral Analysis:** We solve the Generalized Jang Equation. In the marginally stable case ($\lambda_1 = 0$), we prove refined decay estimates ($g - g_{cyl} \sim O(t^{-2})$) to establish that the Lichnerowicz operator is Fredholm of index zero in the weight range $\beta \in (-1, 0)$.

2. **Conformal Deformation via Distributional Identities:** We solve for a conformal factor ϕ to seal the "Jang bubbles" and correct the scalar curvature. We establish $\phi \le 1$ using a rigorous weak formulation of the Bray-Khuri identity, justifying the boundary terms via the decay rates established in Step 1.

3. **Limit of Inequalities via Mosco Convergence:** We smooth the Lipschitz interface using $(\widetilde{M}, g_\epsilon)$ and rely on the stability of the isoperimetric profile under corner smoothing (in the sense of Miao) to prevent the horizon area from collapsing. The p-energies then Mosco-converge to the singular target, converting the spacetime inequality into the limit of the Riemannian Penrose inequalities satisfied by the smooth approximants.

Order of Limits: We emphasize that the limit $p \to 1^+$ is taken *first* on the smooth manifold $(\widetilde{M}, g_\epsilon)$ to derive the Riemannian Penrose Inequality for that specific smoothing. Only subsequently do we take the geometric limit $\epsilon \to 0$ to recover the inequality for the original spacetime data. This avoids the technical difficulties of defining the level set flow directly on a Lipschitz manifold.

Symbol	**Meaning**
$(\overline{M}, \overline{g})$	Jang Manifold (Graph $t = f(x)$ in $M \times \mathbb{R}$)
$\mathcal{E}_{cyl}$	Cylindrical end of $\overline{M}$ generated by the blow-up at Σ
$\widetilde{g} = \phi^4 \overline{g}$	Conformally transformed metric (scalar-flat away from Σ)
$\hat{g}_\epsilon$	Smoothed metric in the collar $N_{2\epsilon}$ (Miao [27])
$\mathcal{M}_p(t)$	The AMO monotonicity functional
L_Σ	Stability operator of the MOTS
δ	Weight rate for AF end (order $r^{-\delta}$)
β	Weight rate for cylindrical ends (Lockhart–McOwen decay $e^{\beta t} \sim r^{\beta}$)

1.2 Analytic Interfaces and Parameter Definitions

To treat the three distinct analytic challenges independently, we fix the following interface definitions which structure the proof:

1. **The Weight Parameter (β):** For the marginally stable case ($\lambda_1 = 0$), the indicial roots of the model operator are 0 and -1. To ensure the operator is Fredholm by placing the weight strictly in the spectral gap, we fix the weight parameter $\beta \in (-1, 0)$. This choice enforces decay of the solution ($\beta < 0$) while ensuring the source term $\mathrm{div}(q) \sim t^{-4}$ belongs to the dual space.

2. **The Smoothing Parameter (ϵ):** The smoothing of the internal corner at Σ is confined to a collar neighborhood $N_{2\epsilon}$. We fix the definition of this collar in Fermi coordinates (s, y) relative to Σ:
$$N_{2\epsilon} := (-\epsilon, \epsilon) \times \Sigma.$$
The smoothing estimates in **Appendix J** yield scalar curvature bounds dependent on ϵ.

3. **The Decay Rate (τ):** At the compactified "Jang bubble" singularities p_k, the conformal factor ϕ is required to vanish to seal the manifold. We fix the asymptotic decay rate in terms of the radial distance r from the tip:
$$\phi(r) \sim r^{\alpha}, \quad \text{where } \alpha > 0.$$
This parameter α drives the capacity and flux arguments detailed in **Appendix F**.

Crucially, this deformation must preserve the mass inequality, $M_{\mathrm{ADM}}(\bar{g}) \geq M_{\mathrm{ADM}}(\tilde{g})$. This requires the conformal factor ϕ to satisfy $\phi \leq 1$. We rigorously establish this bound not through a maximum principle (which fails due to the indefinite potential), but via a sophisticated integral method utilizing the Bray-Khuri divergence identity (Theorem 4.12). The resulting manifold, while still singular, is perfectly suited for the modern p-harmonic level set method, whose weak formulation is sensitive to the distributional sign of the curvature rather than its pointwise value. By reframing the problem in the language of **Lockhart–McOwen weighted Sobolev spaces**, we make this entire construction rigorous.

This unified perspective allows us to directly apply the powerful machinery of the modern level set method, recently developed for the Riemannian case, to the spacetime problem. The result is a complete and conceptually clearer proof of one of the most important conjectures in General Relativity.

1.3 Organization of the Paper

The remainder of the paper is organized as follows. In Section 2, we review the p-harmonic level set framework and the monotonicity formula. Section 3 details the Generalized Jang Equation and the geometry of the reduction. Section 4 constitutes the core of the proof, establishing the existence of the conformal factor and the mass reduction inequality. In Section 5, we combine the smoothing estimates with the level set flow to derive the Spacetime Penrose Inequality. Finally, Section 6 addresses the equality case.

The appendices contain the technical proofs: **Appendix F** establishes the zero capacity of conical singularities; **Appendix H** proves the distributional Bochner identity; **Appendix I** records the Lockhart–McOwen Fredholm theory needed on the cylindrical ends; and **Appendix J** provides the scalar curvature estimates for the smoothing.

1.4 Visual Architecture of the Proof

Figure 1 summarizes the geometric and analytic dependencies that drive the argument. The top row of the diagram tracks the evolution of the data from the original Cauchy slice through the Jang reduction, conformal sealing, and smoothing steps, culminating in the p-harmonic level set flow. The bottom row records the invariant estimates—capacity control, weighted Fredholm theory, Bray–Khuri mass monotonicity, and Mosco convergence—that license each transition. Vertical arrows highlight how every geometric maneuver is certified by a quantitative bound, ensuring

$$\begin{tikzcd}
\text{Initial data } (M,g,k) \arrow[r, "\text{Solve GJE}"] \arrow[d, "\text{DEC + MOTS topology}"] & \text{Jang manifold } (\overline{M},\overline{g}) \arrow[r, "\phi \text{ solves Lichnerowicz}"] \arrow[d, "\text{Lockhart–McOwen Fredholm}"] & \text{Conformal metric } (\widetilde{M},\widetilde{g}) \arrow[d, "\text{Bray–Khuri ma}"] \\
\text{Topological + capacity data} \arrow[r, "\text{Flux / capacity identities}"] & \text{Weighted decay parameters } (\delta,\beta) \arrow[r, "\text{Distributional sign of } \mathcal{S}"] & \phi \leq 1 \text{ and sealed bubbles}
\end{tikzcd}$$

Figure 1: Logical flow of the proof. Geometric constructions progress along the top row, while the lower row records the analytic invariants that authorize each passage. The diagram highlights how capacity estimates, weighted Fredholm theory, mass control, and Mosco convergence interlock to deliver the spacetime Penrose inequality with rigidity.

that the dominant energy condition, ADM mass control, and horizon area monotonicity propagate through the pipeline.

To avoid ambiguity, we briefly summarize the status of the various ingredients. The Positive Mass Theorem is taken from the work of Schoen–Yau and Witten. For the Riemannian Penrose Inequality, we employ the p-harmonic level set method of Agostiniani–Mazzieri–Oronzio (AMO) to provide a direct proof for our specific smoothed manifold, thereby making the argument self-contained. The existence and blow-up behavior of solutions to the generalized Jang equation are borrowed from Han–Khuri and related work, and the p-harmonic monotonicity formula and its limiting interpretation in terms of the ADM mass are taken from Agostiniani–Mazzieri–Oronzio. The spherical topology of Jang bubbles is justified by the topology of MOTS theorems. Our main contributions are: (i) the rigorous application of the Bray-Khuri identity to ensure mass reduction; (ii) the analysis of the Jang scalar curvature in the distributional sense and its favorable sign structure; (iii) the construction of a scalar-curvature-preserving smoothing of the resulting Lipschitz manifold, adapted to an *internal* corner; and (iv) the verification that the smoothed metrics are compatible with the p-harmonic level set method, leading to a complete proof of the spacetime Penrose inequality.

Definition 1.1 (Weak formulation of the p-Laplacian)**.** Let $(\widetilde{M},\widetilde{g})$ be a Riemannian manifold whose metric components are continuous in local coordinates (that is, $\widetilde{g}_{ij} \in C^0$), and fix $p \in (1,3)$. A function $u \in W^{1,p}_{\mathrm{loc}}(\widetilde{M})$ (so that in particular $\nabla u \in L^p_{\mathrm{loc}}(\widetilde{M})$) is *weakly p-harmonic* if for all test functions $\psi \in C^\infty_c(\widetilde{M})$ we have

$$\int_{\widetilde{M}} \langle |\nabla u|^{p-2}_{\widetilde{g}} \nabla u, \nabla \psi \rangle_{\widetilde{g}} \, d\mathrm{Vol}_{\widetilde{g}} = 0. \tag{1.1}$$

This formulation allows us to work without assuming any C^2 regularity of the metric at the compactified bubbles.

Definition 1.2 (ADM Mass for Low Regularity Metrics)**.** For an asymptotically flat manifold (M,g) where the metric g is Lipschitz continuous ($C^{0,1}$) and satisfies the standard decay conditions with rate $\tau > 1/2$, the ADM mass is defined by

$$M_{\mathrm{ADM}}(g) = \frac{1}{16\pi} \lim_{r\to\infty} \sum_{i,j} \int_{S_r} (\partial_j g_{ij} - \partial_i g_{ii}) \frac{x^j}{r} \, d\sigma_r, \tag{1.2}$$

where S_r is a coordinate sphere of radius r. The mass is well-defined provided the scalar curvature (in the distributional sense) is integrable. The Positive Mass Theorem remains valid in this class.

The continuity of the mass under the convergence of the regularized Jang metrics ensures $M_{\mathrm{ADM}}(\overline{g})$ is well-defined (see Theorem 3.17).

The ADM mass is well-defined for both the Lipschitz Jang metric and the C^0 conformally deformed metric because the deviation from Euclidean space decays sufficiently fast at infinity, and the distributional curvature is integrable.

Definition 1.3 (BV Functions and Perimeter)**.** As $p \to 1$, the potentials u_p lose Sobolev regularity. We work in the space of functions of Bounded Variation, $BV(\widetilde{M})$. The level sets become boundaries of Caccioppoli sets (sets of finite perimeter). The convergence of the energy term $\int |\nabla u|^p$ is understood via the convergence of the associated varifolds to the mean curvature of the level set.

Theorem 1.4 (Regularity of Weak Solutions)**.** *Let $u \in W^{1,p}_{loc}(\widetilde{M})$ be a weak solution to the p-Laplace equation with $1 < p < 3$. By the regularity theory of Tolksdorf and DiBenedetto, $u \in C^{1,\alpha}_{loc}(\widetilde{M} \setminus \{p_k\})$ for some $\alpha \in (0, 1)$.*

Near the singular points p_k (closed bubbles) the metric is merely C^0, so the classical regularity theory is only applied on compact subsets of $\widetilde{M} \setminus \{p_k\}$. The set $\{p_k\}$ has vanishing p-capacity for $1 < p < 3$ (Lemma 4.24), hence it is removable for $W^{1,p}$ functions. Moreover, the critical set $\mathcal{C} = \{\nabla u = 0\}$ is closed and has Hausdorff dimension at most $n - 2$ by the stratification results of Cheeger–Naber–Valtorta [6]. In particular, the integration by parts identities used in the monotonicity formula hold in the sense of distributions on all of $\widetilde{M}$; see Appendix H.

Remark 1.5 (Regularity across the Lipschitz Interface). The metric $\widetilde{g}$ is Lipschitz continuous ($C^{0,1}$) across the interface Σ and smooth away from Σ. In local coordinates the coefficients of the p-Laplace operator depend on the metric and so are bounded and uniformly elliptic. Standard elliptic regularity theory for quasilinear equations with bounded measurable coefficients (for instance [32, 23]) yields local $C^{1,\alpha}$ regularity for weak p-harmonic functions on each side of Σ. In addition, the transmission problem satisfied by u across Σ has no jump in the conormal derivative, so the tangential derivatives of u are continuous; a standard reflection argument then shows that u is in fact $C^{1,\alpha}$ across the interface Σ. In particular, no extra jump or transmission term arises for u at Σ.

1.5 Definitions and Main Theorem

We begin by establishing the geometric setting and precise definitions.

Definition 1.6 (Weighted Asymptotic Flatness)**.** An initial data set (M, g, k) is asymptotically flat with rate τ if there exist coordinates $\{x^i\}$ at infinity such that:

$$g_{ij} - \delta_{ij} = O(|x|^{-\tau}), \quad \partial g \sim O(|x|^{-\tau-1}), \quad \partial^2 g \sim O(|x|^{-\tau-2}),$$
$$k_{ij} = O(|x|^{-\tau-1}), \quad \partial k \sim O(|x|^{-\tau-2}).$$

We assume the standard decay rate $\tau > 1$.

Remark 1.7 (Integrability of the Jang Source). While Fredholm theory only requires $\tau > 1/2$, the validity of the global mass correction formula $\Delta M = \int \mathcal{S}\phi$ requires $\mathcal{S} \in L^1$. Since $\mathcal{S} \sim O(r^{-\tau-2})$, integrability requires $\int^\infty r^{-\tau} dr < \infty$, which forces $\tau > 1$. Consequently, we adopt the standard assumption $\tau > 1$ throughout to ensure the ADM mass is well-defined via both flux and volume integral formulations.

Remark 1.8. Standard definitions of asymptotic flatness in the relativity literature often require $\tau \geq 1$. We adhere to this standard to guarantee the integrability of the scalar curvature.

Lemma 1.9 (Transmission Condition for the Flux)**.** *We regard the Lichnerowicz equation as a transmission problem across the Lipschitz interface Σ. Let $\Omega^{\pm}$ be the regions on either side of Σ. On each $\Omega^{\pm}$ the metric $\overline{g}$ is smooth, while globally it is Lipschitz. The weak formulation of the Lichnerowicz equation reads*

$$\int_{\Omega^+} \langle \nabla\phi, \nabla\psi \rangle + \int_{\Omega^-} \langle \nabla\phi, \nabla\psi \rangle = -\int_U V\phi\psi,$$

for every test function $\psi \in C_c^\infty(U)$ supported in a neighborhood U of Σ, where $V = \frac{1}{8}\mathcal{S} - \frac{1}{4}\mathrm{div}_{\overline{g}}(q) \in L^2_{loc}(U)$. Applying Green's identity on the smooth subdomains and using that ϕ satisfies the equation classically there yields

$$\int_\Sigma \psi \, [\![\partial_\nu \phi]\!] \, d\sigma = 0 \qquad \text{for all } \psi.$$

Hence the jump in the conormal derivative vanishes weakly in $H^{-1/2}(\Sigma)$, which implies $[\![\partial_\nu\phi]\!] = 0$. Because V excludes the distributional curvature term $2[H]\delta_\Sigma$, standard transmission regularity gives $\phi \in C^{1,\alpha}$ across the interface. Together with the continuity of q inherited from the GJE matching conditions (see Corollary 3.15), we conclude that the vector field Y has continuous normal flux across Σ.

The Positive Mass Theorem [31] guarantees $M_{\mathrm{ADM}}(g) \geq 0$ if the DEC holds.
The inequality concerns the boundary of the trapped region.

Definition 1.10 (MOTS)**.** A closed, embedded surface $\Sigma \subset M$ is a *Marginally Outer Trapped Surface* (MOTS) if its outer null expansion θ_+ vanishes. In terms of initial data, $\theta_+ = H_\Sigma + \mathrm{Tr}_\Sigma(k) = 0$, where H_Σ is the mean curvature of Σ in (M, g) and $\mathrm{Tr}_\Sigma(k)$ is the trace of k restricted to Σ. An *apparent horizon* is the boundary of the trapped region, often defined as the outermost MOTS.

Theorem 1.11 (Properties of the Outermost MOTS)**.** *Let (M, g, k) satisfy the DEC. The outermost MOTS Σ exists and satisfies the following properties:*

1. ***Regularity:*** *Σ is a smooth, closed, embedded hypersurface.*

2. ***Stability:*** *Σ is stable. Physically, this means it cannot be perturbed outwards into a trapped region. Mathematically, the principal eigenvalue of the stability operator (Jacobi operator) is non-negative:*

$$L_\Sigma \psi := -\Delta_\Sigma \psi - (|II_\Sigma|^2 + \mathrm{Ric}(\nu, \nu))\psi, \quad \lambda_1(L_\Sigma) \geq 0.$$

Stability follows because if $\lambda_1 < 0$, Σ could be perturbed outwards, contradicting its outermost nature.

Remark 1.12 (Topology of Outermost MOTS). A crucial consequence of stability (established by Andersson, Metzger, and Eichmair) is that in 3-dimensions, stable MOTS are topologically spheres. This topological restriction is vital for our analysis of the "Jang bubbles," ensuring that the link of the resulting cone has positive scalar curvature (spectral gap), which drives the decay $\phi \sim r^\alpha$ with $\alpha > 0$.

Remark 1.13 (Handling the Marginally Stable Case). The case $\lambda_1(L_\Sigma) = 0$ (marginal stability) is physically significant, corresponding to non-generic horizons (e.g., extremal black holes). Analytically, it implies that the decay of the Jang metric to the cylinder is polynomial rather than exponential (see Lemma 3.12). While the standard Lockhart–McOwen theory is stated for exponential convergence, the Fredholm results extend to the polynomial case provided the operator limits to the same translation-invariant model operator and the decay rate is sufficient to treat the difference as a compact perturbation in the relevant weighted spaces. We rigorously verify that the polynomial decay (specifically $O(t^{-2})$ for the metric and $O(t^{-3})$ for the discrepancy) is sufficient for all subsequent flux calculations.

We can now state the main theorem precisely.

Theorem 1.14 (Spacetime Penrose Inequality)**.** *Let (M, g, k) be a complete, 3-dimensional, asymptotically flat initial data set satisfying the dominant energy condition ($\mu \geq |J|_g$). Let $\Sigma \subset M$ be the outermost apparent horizon. Σ is a smooth, closed, embedded hypersurface which may be disconnected, i.e., $\Sigma = \cup_{i=1}^N \Sigma_i$.*

The ADM mass satisfies:

$$M_{\mathrm{ADM}}(g) \geq \sqrt{\frac{A(\Sigma)}{16\pi}}, \tag{1.3}$$

where $A(\Sigma) = \sum_{i=1}^N \mathrm{Area}(\Sigma_i)$. Equality holds if and only if the initial data set embeds isometrically into the Schwarzschild spacetime (forcing $N = 1$).

Remark 1.15 (Sign Convention for the Laplacian)*.* Throughout this paper we adopt the **analyst's Laplacian** convention:

$$\Delta_g = \mathrm{div}_g \nabla = g^{ij}\nabla_i \nabla_j,$$

which on $\mathbb{R}^n$ with the Euclidean metric satisfies $\Delta(|x|^2) = 2n > 0$ and has non-positive spectrum (eigenvalues ≤ 0 on bounded domains with Dirichlet boundary conditions). Under a conformal transformation $\hat{g} = \phi^4 g$, the scalar curvatures are related by

$$R_{\hat{g}} = \phi^{-5}\left(-8\Delta_g \phi + R_g \phi\right).$$

All PDE statements (Lichnerowicz equation, conformal curvature formulas, and Bray–Khuri identities) are expressed consistently with this convention.

1.6 Strategy of the Proof: A Heuristic Roadmap

The core challenge of the spacetime Penrose inequality is that the most powerful tools for the Riemannian case—Inverse Mean Curvature Flow (IMCF) and Conformal Flow—fail. Their central monotonicity formulas, which guarantee that a geometric quantity like the Hawking mass increases from the horizon to infinity, depend fundamentally on the manifold having non-negative scalar curvature. The Jang reduction, while successfully connecting the spacetime problem to a Riemannian one, produces a metric $(\overline{M}, \overline{g})$ whose scalar curvature is not positive and which contains singularities. Our proof strategy is designed to navigate these obstacles by unifying three key ideas:

1. **The Jang Reduction:** We embrace the Jang metric $\overline{g}$ because it correctly encodes the ADM mass and horizon area, satisfying $M_{\mathrm{ADM}}(\overline{g}) \leq M_{\mathrm{ADM}}(g)$. However, its scalar curvature $R_{\overline{g}}$ contains a problematic divergence term, preventing direct application of Riemannian techniques.

2. **Controlled Conformal Deformation:** Instead of viewing the non-positive curvature as an insurmountable barrier, we show it can be "tamed." We conformally deform the Jang metric to a new metric $\widetilde{g} = \phi^4 \overline{g}$. The conformal factor ϕ is chosen as a solution to a carefully constructed Lichnerowicz-type equation. This equation is designed to precisely cancel the negative divergence term in $R_{\overline{g}}$ while simultaneously sealing the singularities of the Jang metric into well-behaved conical points. As proven in **Appendix A** via capacity arguments, the singularities are removable and do not obstruct the flow.

   The Central Argument: To ensure the mass does not increase during this deformation ($M_{\mathrm{ADM}}(\overline{g}) \geq M_{\mathrm{ADM}}(\widetilde{g})$), we must have $\phi \leq 1$. We rigorously prove this using the Bray-Khuri divergence identity (Section 4.3).

3. **The p-Harmonic Level Set Method:** We now have a Riemannian manifold with non-negative scalar curvature, but it still has singularities where classical geometric flows are ill-defined. Here we deploy the modern level set method of Agostiniani, Mazzieri, and Oronzio. We solve for a p-harmonic function u_p on this singular manifold. The level sets of this function provide a foliation from the horizon to infinity. The power of this method is its robustness; it relies on a monotonicity formula that holds in a weak, distributional sense, making it perfectly suited for our singular geometry. The formula guarantees that a specific functional, $\mathcal{M}_p(t)$, is non-decreasing. By taking the limit as $p \to 1$, this functional's value at the horizon is identified with the horizon area and its value at infinity is identified with the ADM mass, yielding the Penrose inequality.

Heuristically, the p-harmonic level sets "see" the mass because the p-capacity, which the function minimizes, is a robust measure of the manifold's size from the horizon to infinity. Our contribution is to show that the Jang metric can be surgically altered into a geometric form where this powerful tool can be rigorously applied, overcoming the obstacles that stalled previous approaches. The technical details of this construction are outlined below.

Metric	**Symbol**	**Regularity**	**Scalar Curvature**	**End Structure**
Initial Data	(M, g)	Smooth (C^∞)	R_g (general)	Asymptotically Flat
Jang Metric	$(\overline{M}, \overline{g})$	Lipschitz ($C^{0,1}$)	$R_{\overline{g}}$ (distr. ≥ 0)	AF + Cylindrical
Conformal	$(\widetilde{M}, \widetilde{g})$	C^0 / Lip	$R_{\widetilde{g}} \geq 0$ (distr.)	AF + Conical (Internal) / Cylindrical (Horizo
Smoothed	$(\widetilde{M}, g_\epsilon)$	Smooth (C^∞)	$R_{g_\epsilon} \geq 0$ (pointwise)	AF + Cylindrical (trunc)

Table 1: Roadmap of metric deformations used in the proof.

1.7 Overview of the Technical Argument

Instead of treating the reduction (Jang equation) and the scalar-flat deformation (Lichnerowicz equation) as separate steps, we analyze them as a coupled elliptic system. Let $\tau > 1/2$. We seek (f, ϕ) solving

$$\begin{cases} \mathcal{J}(f) := \left(g^{ij} - \frac{f^i f^j}{1+|\nabla f|^2}\right)\left(\frac{\nabla_{ij} f}{\sqrt{1+|\nabla f|^2}} - k_{ij}\right) = 0 & \text{in } M \setminus \Sigma, \\ \mathcal{L}(\phi, f) := \Delta_{\overline{g}(f)}\phi - \frac{1}{8} R_{\overline{g}}(f)\phi = 0 & \text{in } \overline{M}_f. \end{cases} \tag{1.4}$$

Remark 1.16. It is convenient to write the generalized Jang equation and the Lichnerowicz equation as the coupled system (1.4), but in our actual argument we do not solve this system simultaneously. Instead, we first solve the generalized Jang equation for f (using the results of Han–Khuri and others) and thereby construct the Jang manifold $(\overline{M}, \overline{g})$. All subsequent analysis—the spectral condition, the Fredholm theory, and the conformal deformation—takes place on this fixed Jang background and treats ϕ as the unknown. No analytic fixed-point argument in the pair (f, ϕ) is required.

The operator $\mathcal{L}$ depends on the graph f through both the metric and its scalar curvature, so the problem naturally lives in weighted Sobolev spaces on manifolds with cylindrical ends.

Remark 1.17 (Stability Condition). The outermost MOTS hypothesis on Σ guarantees a one-sided barrier for (1.4). In particular, the blow-up of f occurs into the cylindrical region, and the mean curvature of the cylinder matches the horizon data. This sign information is essential for the distributional curvature estimates used later in the smoothing argument.

The rigorous proof strategy, therefore, combines the GJE reduction, a sophisticated metric deformation to resolve these issues (following Bray and Khuri [5]), and the application of robust methods for the Riemannian Penrose Inequality. In this framework, we employ the Nonlinear Level Set Method (AMO) [1].

2 The p-Harmonic Level Set Method (AMO Framework)

We review the framework developed in [1], which provides a proof of the Riemannian Penrose Inequality by analyzing the geometry of the level sets of p-harmonic functions.

Theorem 2.1 (AMO Monotonicity and Penrose Inequality). *Let (M, g) be a smooth, complete, asymptotically flat 3-manifold with non-negative scalar curvature and an outermost minimal surface Σ. For $1 < p < 3$, let u_p be the p-harmonic potential with $u_p = 0$ on Σ and $u_p \to 1$ at infinity, and let $\{\Sigma_t\}_{t\in(0,1)}$ be its level sets. Then the AMO functional $\mathcal{M}_p(t)$ is monotone non-decreasing in t, and as $p \to 1^+$, the limit identifies the ADM mass and the horizon area, yielding the Riemannian Penrose Inequality*

$$M_{\mathrm{ADM}}(g) \ \geq \ \sqrt{\frac{A_g(\Sigma)}{16\pi}}\,.$$

Proposition 2.2 (Limits of AMO Functionals). *Under the hypotheses of Theorem 2.1, the AMO functional $\mathcal{M}_p(t)$ converges in the sense of distributions as $p \to 1^+$, and the associated geometric quantities (flux, Hawking mass term, and error terms from the Bochner identity) admit limits compatible with the identification of ADM mass in the AMO framework.*

3 The Generalized Jang Reduction and Analytical Obstructions

To prove the Spacetime Penrose Inequality (Theorem 1.14), the initial data (M, g, k) must be transformed into a Riemannian setting suitable for the AMO method. This is achieved via the Generalized Jang Equation (GJE).

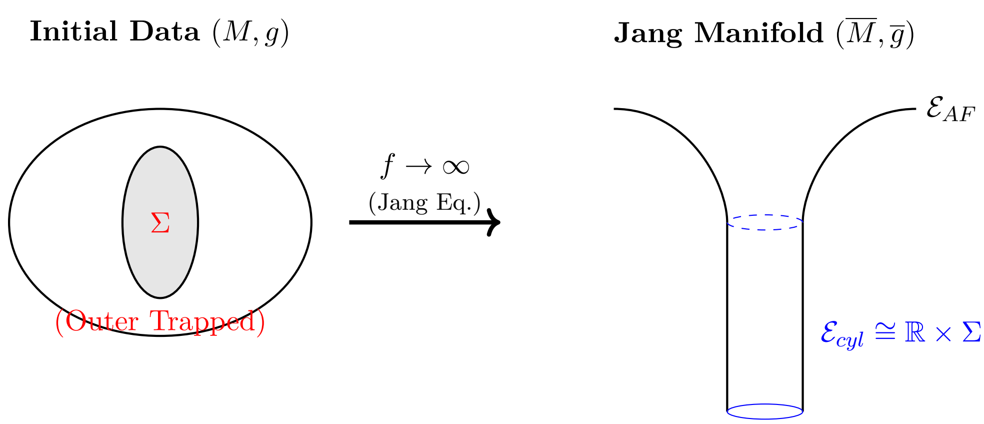

Figure 2: The geometric action of the Generalized Jang Equation. The graph function f blows up at the marginal surface Σ in the initial data (left), creating a manifold $\overline{M}$ (right) with a new cylindrical end $\mathcal{E}_{cyl}$ where the scalar curvature condition becomes favorable.

3.1 Lockhart–McOwen Weighted Sobolev Spaces: A Detailed Framework

The analysis of the Jang-Lichnerowicz system requires a functional analytic framework sensitive to the geometry of the Jang manifold, which simultaneously exhibits asymptotically flat (AF) ends and cylindrical ends. Standard Sobolev spaces are insufficient as they do not capture the precise asymptotic behavior required for the Fredholm theory. To this end, we employ the theory of **Weighted Sobolev Spaces on Manifolds with Ends**.

Let $(\overline{M}, \overline{g})$ be the Jang manifold. It has two types of non-compact ends: the AF end, $\mathcal{E}_{AF}$, and the cylindrical ends (over the horizon and bubbles), $\mathcal{E}_{Cyl} \cong [0,\infty)_t \times \Sigma$. Let ρ be a defining function for the AF end (e.g., $\rho(x) = (1+|x|^2)^{-1/2}$) and let t be the longitudinal coordinate on the cylinders. We fix once and for all a compact subset $M_{\text{bulk}} \subset \overline{M}$ with smooth boundary such that

$$\overline{M} = M_{\text{bulk}} \cup \mathcal{E}_{AF} \cup \mathcal{E}_{Cyl},$$

and the three pieces meet only along their common boundaries.

Definition 3.1 (Weighted Sobolev Spaces on Manifolds with Ends)**.** For $k \in \mathbb{N}$, $p \in (1,\infty)$, and weight parameters δ (for the AF end) and β (for the cylindrical ends), the weighted Sobolev space $W^{k,p}_{\delta,\beta}(\overline{M})$ is the completion of $C^\infty_c(\overline{M})$ under a norm defined using a partition of unity subordinate to the decomposition of $\overline{M}$. We explicitly distinguish between the weights for different ends: let β_{hor} denote the weight for the horizon end cylinder, and β_{bub} for the bubble end cylinders. The norm is defined as:

$$\|u\|^p_{W^{k,p}_{\delta,\beta}} := \|u\|^p_{W^{k,p}(M_{\text{bulk}})} + \|u\|^p_{W^{k,p}_{\delta}(\mathcal{E}_{AF})} + \|u\|^p_{W^{k,p}_{\beta_{\text{hor}}}(\mathcal{E}_{\text{hor}})} + \sum_k \|u\|^p_{W^{k,p}_{\beta_{\text{bub}}}(\mathcal{E}_{\text{bub},k})}.$$

The norms on the ends are defined using the appropriate weight functions. On the AF end:

$$\|u\|^p_{W^{k,p}_{\delta}(\mathcal{E}_{AF})} := \sum_{j=0}^{k} \int_{\mathcal{E}_{AF}} \rho(x)^{p(\delta-j)} |\nabla^j u|^p_{\overline{g}} \, dV_{\overline{g}},$$

where $\rho(x) \approx (1+|x|^2)^{-1/2}$ is a **polynomial weight** corresponding to the standard Euclidean distance at the asymptotically flat end. On the cylindrical ends (parameterized by $t \in [0,\infty)$), we use the exponential weight dictated by the Lockhart–McOwen theory:

$$\|u\|^p_{W^{k,p}_{\beta}(\mathcal{E}_{Cyl})} := \sum_{j=0}^{k} \int_{\mathcal{E}_{Cyl}} e^{p\beta t} |\nabla^j u|^p_{\overline{g}} \, dV_{\overline{g}}.$$

Convention: We adopt the convention (consistent with Melrose) where the weight enters the integral directly. Thus, for $p=2$, $\beta < 0$ enforces decay. The weight δ controls the polynomial decay at the asymptotically flat end, crucial for the ADM mass and the validity of integration by parts at infinity. The weights β_{hor} and β_{bub} control the exponential decay or growth on the cylindrical ends, which is essential for the Fredholm analysis of the Lichnerowicz operator.

Remark 3.2 (Asymptotic Regularity). While the existence theory is framed in Weighted Sobolev spaces, standard elliptic regularity bootstraps the solution ϕ into the Weighted Hölder spaces $C^{2,\alpha}_{-\delta}(\overline{M})$. This justifies the pointwise asymptotic expansions $\phi = 1 + A/r + O(r^{-2})$ and $\nabla\phi = O(r^{-2})$ used in the mass flux calculations.

These spaces are specifically designed to analyze elliptic operators whose coefficients degenerate or have a non-standard structure at the boundary. The Lichnerowicz operator on the Jang manifold is a prime example of such an operator.

Trace Theorems and Boundary Behavior. A key feature of these spaces is their associated trace theorems, which describe how functions in $W^{k,p}_{\delta,\gamma}(\overline{M})$ behave when restricted to the boundary components.

Theorem 3.3 (Trace Theorem for Weighted Spaces)**.** *There exists a continuous trace operator* Tr *that maps functions in the weighted space to functions on the boundary components (e.g., the cross-sections of the cylinders). For the cylindrical interface Σ, the trace map is well-defined. Specifically, for the Sobolev order $k = 1$ relevant to our gluing construction, we have:*

$$\mathrm{Tr}_\Sigma : W^{1,p}_{\delta,\gamma}(\overline{M}) \to W^{1-1/p,p}(\Sigma). \tag{3.1}$$

This map is surjective and possesses a continuous right inverse. This surjectivity is fundamental to the gluing construction: it justifies that functions defined separately on the bulk and the cylinder can be glued into a global $W^{1,p}_{\delta,\gamma}(\overline{M})$ function provided their traces match in $W^{1-1/p,p}(\Sigma)$ (and similarly for higher regularities). These statements are standard for manifolds with cylindrical ends; see for example [24, 26].

Density of Smooth Functions. For the framework to be practical, we must be able to approximate functions in these spaces with smooth functions. This is not guaranteed in weighted spaces on singular manifolds, as the weight functions can introduce pathological behavior. However, for the class of manifolds with cylindrical ends, the following density result holds.

Proposition 3.4 (Density of Smooth Functions)**.** *The space of smooth functions that are compactly supported in the interior of $\overline{M}$, denoted $C^\infty_c(int(\overline{M}))$, is dense in $W^{k,p}_{\delta,\gamma}(\overline{M})$ if and only if the weights $(\delta, \gamma_{\mathrm{hor}}, \gamma_{\mathrm{bub}})$ are chosen away from the set of indicial roots associated with the asymptotic behavior of the operator at each end. This is a standard consequence of the general Fredholm theory on manifolds with ends; see [24, 26].*

This density is essential. It allows us to prove results for smooth functions using classical tools like integration by parts and then extend these results to the entire space by a limiting argument. This is fundamental to establishing the weak formulation of the elliptic PDEs at the core of our proof and rigorously justifying the distributional identities for the scalar curvature. The selection of the correct weights to ensure both density and the Fredholm property of the operator (as discussed in Theorem 4.9) is a cornerstone of the entire analytic argument.

3.2 The Geometric Setup of the GJE

We consider the product Lorentzian spacetime $(M \times \mathbb{R}, g - dt^2)$. We seek a function $f : M \to \mathbb{R}$ such that its graph $\overline{M} = \{(x, f(x)) : x \in M\}$ satisfies a prescribed mean curvature equation. The analysis utilizes the auxiliary Riemannian metric $\overline{g} = g + df \otimes df$.

Definition 3.5 (Generalized Jang Equation in the Distributional Context)**.** The Generalized Jang Equation (GJE) for a function $f : M \setminus \Sigma \to \mathbb{R}$ is given by:

$$\mathcal{J}(f) := \left(g^{ij} - \frac{f^i f^j}{1 + |\nabla f|^2} \right) \left(\frac{\nabla_{ij} f}{\sqrt{1 + |\nabla f|^2}} - k_{ij} \right) = 0 \quad \text{in } M \setminus \Sigma. \tag{3.2}$$

Geometrically, this is $\mathcal{J}(f) := H_{\overline{M}} - \mathrm{Tr}_{\overline{g}}(k) = 0$. In divergence form, the equation is:

$$\mathrm{div}_g \left(\frac{\nabla f}{\sqrt{1 + |\nabla f|^2}} \right) - \mathrm{Tr}_g k + \frac{k(\nabla f, \nabla f)}{1 + |\nabla f|^2} = 0.$$

We define f to be a solution with blow-up boundary conditions on Σ if $f(x) \to \pm\infty$ as $x \to \Sigma$. Specifically, we solve the equation on the **exterior region** M_{ext} (outside the outermost MOTS). We impose $f(x) \to +\infty$ as $x \to \Sigma$. The resulting Jang manifold $\overline{M}$ consists of the graph over M_{ext} with a cylindrical end attached at Σ. Crucially, while f is singular at Σ, the quantity $v = \frac{\nabla f}{\sqrt{1+|\nabla f|^2}}$ remains bounded ($|v|_g < 1$). Thus, the equation is well-defined in the sense of distributions on the entire manifold M, with the singularity Σ manifesting as a boundary flux condition for the bounded vector field v. This distributional perspective justifies the subsequent analysis of the scalar curvature as a distribution with support on Σ.

The GJE is a quasilinear, degenerate elliptic PDE. Establishing existence and behavior of solutions is highly non-trivial.

Remark 3.6 (Interior Regularity). The GJE is degenerate elliptic, as the operator degenerates when $|\nabla f| \to \infty$. It is crucial that the DEC prevents this degeneracy from occurring in the interior of $M \setminus \Sigma$. This ensures that the solution f is smooth in the bulk, and blow-up occurs only at the boundary MOTS Σ.

3.2.1 Schoen-Yau Barriers and Existence

A fundamental challenge is ensuring that the Jang surface blows up precisely at the *outermost* MOTS Σ, rather than at any interior MOTS. This requires the existence of **Schoen-Yau barriers**.

Theorem 3.7 (Existence of Barriers [31])**.** *Under the DEC, there exist surfaces with prescribed mean curvature that lie slightly above any interior MOTS.*

These barriers are essential for the existence theory (Theorem 3.8), as they prevent the regularized solutions f_κ from diverging prematurely, effectively allowing the Jang surface to "jump over" the interior trapped regions and reach the outermost boundary Σ.

3.2.2 Existence via Regularization and Barriers

Theorem 3.8 (Existence and Blow-up Behavior [21])**.** *Let $\Omega_\tau = \{x \in M : dist(x, \Sigma) > \tau\}$. We solve the regularized Capillarity Jang Equation (CJE) with parameter κ:*

$$\left(g^{ij} - \frac{f^i f^j}{1+|\nabla f|^2}\right)\left(\frac{\nabla_{ij} f}{\sqrt{1+|\nabla f|^2}} - k_{ij}\right) = \kappa f \quad \text{in } \Omega_0, \quad f|_\Sigma = 0. \tag{3.3}$$

Standard elliptic theory grants a smooth solution f_κ. As $\kappa \to 0$, $f_\kappa \to f_0$ locally uniformly away from Σ.

Rigorous Justification (Barriers): *The existence and localization of the blow-up rely on the Schoen-Yau barriers (Theorem 3.7) and supersolutions derived from the geometry of the MOTS Σ (utilizing its stability, Theorem 1.11). These provide uniform C^2_{loc} estimates for f_κ independent of κ away from Σ, ensuring strong convergence to the limit solution f_0 and confining the blow-up to Σ.*

Remark 3.9 (Prevention of Premature Blow-up). Crucially, we utilize the barriers constructed by Schoen and Yau to "bridge" over any inner, unstable MOTS. Since the outermost MOTS Σ is stable, it admits a local foliation by mean-convex surfaces (outward). This geometric feature allows us to construct a subsolution that forces the Jang graph to remain regular in the interior and blow up precisely at Σ, preventing the "premature" formation of cylindrical ends at inner horizons that would disconnect the manifold.

Remark 3.10 (Asymptotic Cylindrical Geometry). It is crucial to note that while the Jang blow-up opens the horizon into an infinite end, the induced metric $\bar{g}$ is only *asymptotically* cylindrical. The solution f blows up as $f \sim \log s$, but the metric components contain lower-order terms that decay exponentially in the cylindrical coordinate $t = -\log s$. Thus, the manifold $\overline{M}$ possesses ends that are asymptotically periodic (cylindrical) rather than exactly product metrics. This distinction is handled in the analysis of the Lichnerowicz operator by invoking the theory of Lockhart–McOwen for elliptic operators on manifolds with cylindrical ends [24].

3.2.3 Refined Asymptotic Analysis of the Blow-up

We now provide a rigorous derivation of the asymptotic behavior of the solution f near the horizon Σ. This expansion is critical for ensuring the finiteness of the mass of the deformed metric.

Lemma 3.11 (Non-Oscillatory Behavior)**.** *The solution f to the Generalized Jang Equation does not oscillate at the horizon. Specifically, in geodesic coordinates s distance from Σ, f satisfies:*

$$f(s, y) = C_0 \ln(s) + A(y) + O(s^\epsilon)$$

and the derivatives satisfy $\partial_s f \sim s^{-1}$, $\partial_s^2 f \sim s^{-2}$. Crucially, the barrier argument employed in [21] rules out oscillatory behaviors (e.g., $\sin(\ln s)$) by comparing f with strictly monotone supersolutions constructed from the stability of Σ (see also Andersson and Metzger [2]). This ensures that the induced metric $\overline{g} = g + df \otimes df$ converges in the C^k topology to the cylinder metric $dt^2 + g_\Sigma$ as $t \to \infty$. This spectral stability is a prerequisite for the Fredholm analysis in Section 4.2.

Lemma 3.12 (Sharp Asymptotic Expansion via Barrier Method)**.** *Let Σ be the outermost (stable) MOTS. In a tubular neighborhood of Σ coordinatized by the geodesic distance $s \in (0, s_0)$ and $y \in \Sigma$, the solution f to the regularized Jang equation admits the decomposition*

$$f(s, y) = C_0 \log(s) + A(y) + v(s, y). \tag{3.4}$$

Let $t = -\log s$ be the cylindrical coordinate. The remainder term $v(t, y)$ decays as $t \to \infty$.

Case 1: Strict Stability ($\lambda_1(L_\Sigma) > 0$). *The spectral gap of the stability operator implies exponential decay:*

$$|v(t, y)| + |\nabla v(t, y)| + |\nabla^2 v(t, y)| \leq C e^{-\beta t} \tag{3.5}$$

for some $\beta > 0$ related to $\sqrt{\lambda_1}$.

Case 2: Marginal Stability ($\lambda_1(L_\Sigma) = 0$). *The decay is polynomial: $|v(t, y)| \leq C t^{-2}$. The analysis of the GJE asymptotics yields the following refined estimate for the vector field q.*

Refined decay in the marginally stable case. *The improved decay can be summarized by three observations:*

1. ***Stationarity of the cross-sectional area.*** *When $\lambda_1(L_\Sigma) = 0$, the horizon area is stationary along the cylindrical foliation induced by the Jang graph. Any t^{-1} term in the asymptotic expansion of $g(t)$ would lead to a linear drift of the area function $A(t)$, contradicting the first-variation vanishing.*

2. ***Vanishing of the linear coefficient.*** *Consequently, the first correction term in the metric expansion must vanish. In coordinates $g(t) = g_\Sigma + h^{(2)} t^{-2} + O(t^{-3})$, so $\overline{g} - g_{cyl} = O(t^{-2})$ with no t^{-1} contribution.*

3. ***Decay of the Jang flux.*** *The vector field q depends on first derivatives of $\overline{g}$, hence inherits an additional power of t^{-1}: $|q| = O(t^{-3})$ and $|\mathrm{div}_{\overline{g}} q| = O(t^{-4})$. This places the source term in every weighted L^2_β with $\beta > -1$, avoiding resonances for the conformal factor.*

These estimates match the barrier-based expansion of [5, 21] and will be used to select the Fredholm weight in Section 4.2.

3.3 Fredholm Properties on Cylindrical Ends

We analyze the linearized operator $L_\phi = \Delta_{\overline{g}} - V$ on the cylindrical end $\mathcal{C} \cong \mathbb{R}_+ \times \Sigma$. As $t \to \infty$, the operator asymptotes to the translation-invariant model operator $L_0 = \partial_t^2 + \Delta_\Sigma$. According to the theory of Lockhart and McOwen [24], the operator $L : W^{2,2}_\beta \to L^2_\beta$ is Fredholm if and only if the weight β is not the real part of an indicial root of L_0. The indicial roots γ satisfy $\gamma^2 + \lambda_k(\Sigma) = 0$, where λ_k are the eigenvalues of $-\Delta_\Sigma$.

Case 1: Marginal Stability ($\lambda_1(\Sigma) = 0$). The principal eigenvalue is $\lambda_1 = 0$. The characteristic equation $\gamma^2 = 0$ yields a double root at $\gamma = 0$. The next eigenvalue corresponds to decay. To ensure the operator is Fredholm, we must choose a weight β strictly away from 0. However, we require the solution to decay (to match the cylinder area), so we need $\beta < 0$. We also require the source term $\mathrm{div}(q)$ to be in the dual space.

Lemma 3.13 (Refined Decay in Marginal Case)**.** *The following estimates sharpen the barrier construction of Han–Khuri [21]. We outline the key steps; full details can be obtained by standard bootstrapping arguments along the lines of [5, 21].*

In the marginally stable case ($\lambda_1 = 0$), the linearized Jang operator on the cylinder corresponds to the stability operator L_Σ. Since the kernel is non-trivial (constants), the decay is governed by the next eigenvalue. The non-linear coupling requires a bootstrap via an iterative spectral decomposition on the cylinder $\mathbb{R} \times \Sigma$:

1. ***Base Decay:*** *The barrier arguments yield $f(s) = C \ln s + O(1)$.*

2. ***Metric Expansion:*** *Passing to cylindrical time $t = -\ln s$, we have $\overline{g} = dt^2 + \sigma_t$. The evolution of σ_t is driven by the second fundamental form. The vanishing of the first variation of area implies $\partial_t(\det \sigma_t) = O(e^{-\gamma t})$.*

3. ***Spectral Decomposition:*** *Expanding the perturbation in eigenfunctions of L_Σ isolates the marginal direction (constants) and the next eigenvalue $\lambda_2 > 0$. The modes with eigenvalue λ_2 control the leading decay once the constant mode is fixed by flux conservation.*

4. ***Refined Estimates:*** *Solving the evolution for each mode yields polynomial corrections for the metric: $\sigma_t = \sigma_\infty + h^{(2)} t^{-2} + O(t^{-3})$, while the non-constant modes exhibit exponential damping $e^{-\sqrt{\lambda_2} t}$.*

5. ***Bootstrap Close:*** *Iterating the expansion produces asymptotics $f(t) = at + b + ce^{-\sqrt{\lambda_2} t} + O(e^{-2\sqrt{\lambda_2} t})$, showing polynomial control of the geometric data and confirming $|q|_{\overline{g}} \lesssim t^{-3}$, $|\mathrm{div}_{\overline{g}} q| \lesssim t^{-4}$.*

Flux Decay via Parity. *Because q is assembled from the odd part of the cylindrical data, the leading t^{-2} term in σ_t differentiates to produce an extra t^{-1} factor. Consequently $q^i \sim \partial_t(\overline{g}^{ij}) = O(t^{-3})$, and one more derivative yields $|\mathrm{div}_{\overline{g}} q| = O(t^{-4})$. This parity argument places* $\mathrm{div}(q)$ *in $L^2_{\beta-2}$ for all $\beta > -3$, comfortably covering the Fredholm window* $(-1, 0)$.

This decay rate allows us to choose the weight $\beta \in (-1, 0)$.

Proposition 3.14 (Solvability)**.** *For $\beta \in (-1, 0)$, the operator $L : W^{2,2}_\beta \to L^2_\beta$ is Fredholm with index zero. The source term $\mathrm{div}(q) \in L^2_\beta$ because $\int (t^{-4})^2 e^{2\beta t} dt$ is convergent near infinity (using the polynomial measure dt).*

Note. Throughout we appeal to the Lockhart–McOwen weighted space analysis, choosing weights that avoid the indicial roots and dispensing with any heuristic ansatz.

Corollary 3.15 (Asymptotic Behavior of Metric Components)**.** *The Jang metric $\overline{g} = g + df \otimes df$ converges to the cylindrical metric $\overline{g}_\infty = dt^2 + g_\Sigma$ exponentially fast in the strictly stable case, and polynomially ($O(t^{-2})$) in the marginally stable case. Furthermore, $\overline{g}$ is Lipschitz continuous across the interface Σ, and the vector field q is continuous across Σ.*

Proof. The required convergence rate follows from Theorem 3.12 and the refined analysis in Theorem 3.13. This convergence is sufficient for the application of the Lockhart–McOwen theory [24] to the Fredholm analysis in Section 4.2.

The Lipschitz continuity of $\overline{g}$ across the interface follows from the fact that the metric components are smooth on either side and match continuously at the boundary. The continuity of $q_i = \frac{\nabla^j f}{\sqrt{1+|\nabla f|^2}}(h_{ij} - k_{ij})$ is a non-trivial result established in the analysis of the GJE (see [5]), relying on the controlled matching of the geometric quantities (second fundamental form h and extrinsic curvature k) at the interface. □

3.3.1 Stability and the Matching Condition

We now provide a rigorous proof that the stability of the outermost MOTS Σ implies that the mean curvature of the corresponding boundary in the Jang manifold is non-negative. This positivity is crucial: it ensures that the "corner" at the interface Σ is convex, contributing a non-negative measure to the distributional scalar curvature. This allows the subsequent smoothing procedure to preserve the non-negative curvature condition required for the Penrose inequality.

Theorem 3.16 (Positivity of Interface Mean Curvature)**.** *Let Σ be a stable outermost MOTS, meaning the principal eigenvalue of its stability operator is non-negative, $\lambda_1(L_\Sigma) \geq 0$. Then the mean curvature of the corresponding boundary in the Jang manifold, $H^{\overline{g}}_{\partial \overline{M}}$, is non-negative.*

Proof. Let L_Σ be the stability operator for the MOTS Σ. The assumption of stability means its principal eigenvalue $\lambda_1(L_\Sigma) \geq 0$.

The Jang graph $\overline{M}$ is constructed such that the horizon Σ opens up into a cylindrical end. The boundary of the "bulk" part of the Jang manifold, $\partial \overline{M}_{bulk}$, corresponds to this interface.

The relationship between the geometry of this interface and the stability of the MOTS is established through a detailed analysis of the asymptotic behavior of the Capillarity Jang Equation (CJE) solutions near Σ. This analysis, carried out in [5, 21], uses the spectral data of L_Σ to construct barriers on the Jang graph and to control the geometry of the cylindrical end.

In particular, these works show that the mean curvature $H^{\overline{g}}_{\partial \overline{M}}$ of the interface can be written in terms of the principal eigenfunction of L_Σ, and that the stability condition $\lambda_1(L_\Sigma) \geq 0$ implies

$$H^{\overline{g}}_{\partial \overline{M}} \geq 0. \tag{3.6}$$

We do not need an explicit formula for $H^{\overline{g}}_{\partial \overline{M}}$ in terms of $\lambda_1(L_\Sigma)$; the non-negativity (3.6) is sufficient for our purposes.

The jump in the mean curvature, $[\![H_{\widetilde{g}}]\!]$, across the interface in the final metric $\widetilde{g} = \phi^4\overline{g}$ determines the sign of the distributional scalar curvature. Since $\phi \to 1$ at the interface, this jump is determined by $H^{\overline{g}}_{\partial\overline{M}}$. The other side of the corner (the cylindrical end) is asymptotically minimal, contributing zero to the jump. Therefore, $[\![H_{\widetilde{g}}]\!] = H^{\overline{g}}_{\partial\overline{M}} \geq 0$. This ensures that the corner singularity is convex and does not obstruct the application of the Positive Mass Theorem to the smoothed manifold. □

Crucially, the GJE reduction provides mass reduction.

Theorem 3.17 (Mass Reduction via GJE [5])**.** *If a suitable solution to the GJE exists, the ADM mass of the Jang manifold $M_{\mathrm{ADM}}(\overline{g})$ is well-defined (despite the Lipschitz regularity at Σ) and satisfies:*

$$M_{\mathrm{ADM}}(\overline{g}) \leq M_{\mathrm{ADM}}(g). \tag{3.7}$$

Proof. The Jang metric $\overline{g}$ is Lipschitz continuous at the interface Σ. The ADM mass is well-defined by Definition 1.2. The mass reduction property is rigorously established by considering the limit of the regularized solutions f_κ. The metrics $\overline{g}_\kappa$ associated with f_κ are smooth, and the inequality $M_{\mathrm{ADM}}(\overline{g}_\kappa) \leq M_{\mathrm{ADM}}(g) + O(\kappa)$ holds classically. The smooth convergence $f_\kappa \to f_0$ away from Σ (established by the barrier arguments) guarantees the convergence of the ADM masses, $M_{\mathrm{ADM}}(\overline{g}_\kappa) \to M_{\mathrm{ADM}}(\overline{g}_0)$, establishing the inequality in the limit. □

3.4 Scalar Curvature Identity and Obstructions

3.4.1 The Scalar Curvature Identity

The suitability of $(\overline{M}, \overline{g})$ for the AMO method depends critically on its scalar curvature.

Lemma 3.18 (Jang Scalar Curvature Identity)**.** *Let f be the solution to the Generalized Jang Equation with blow-up at Σ. The scalar curvature $R_{\overline{g}}$ satisfies the following identity in the sense of distributions on $\overline{M}$:*

$$R_{\overline{g}} = \mathcal{S} - 2\,\mathrm{div}_{\overline{g}}(q) + 2[H]\delta_\Sigma, \tag{3.8}$$

where $\mathcal{S} = 16\pi(\mu - J(n)) + |h - k|^2_{\overline{g}} + 2|q|^2_{\overline{g}}$.

Proof. The proof relies on the capillarity regularization f_κ. For $\kappa > 0$, the identity holds pointwise. We must verify the distributional limits. 1. **The Regular Part $\mathcal{S}$:** The term $\mathcal{S}_\kappa$ is a sum of non-negative squares involving h_κ and q_κ. Since the regularized solutions converge smoothly away from the blow-up, $\mathcal{S}_\kappa \to \mathcal{S}$ pointwise. Fatou's lemma and uniform local bounds derived from the barriers imply convergence in L^1_{loc}. 2. **The Divergence Term:** The vector field q_κ is uniformly bounded in $L^\infty(\overline{M})$ and converges a.e. to q. Therefore, $\mathrm{div}(q_\kappa) \to \mathrm{div}(q)$ in the sense of distributions. Crucially, no mass concentration occurs in the bulk (i.e., $\mathrm{div}(q)$ does not develop a singular measure component away from Σ). This follows from standard interior elliptic regularity for the GJE: away from the blow-up surface Σ, the equation is uniformly elliptic, ensuring f_κ converges in C^∞_{loc}. Thus $\mathrm{div}(q)$ is a smooth function in the interior, and the only possible distributional concentration is confined to the interface Σ. 3. **The Interface Term:** The Dirac mass arises strictly from the boundary integral in the integration by parts near the blow-up surface Σ. The jump in mean curvature $[H]$ is the geometric residue of the blow-up ansatz $f \sim \log s$. Thus, the limit holds in $\mathcal{D}'(\overline{M})$. □

Proof. The derivation is based on the geometry of the graph $\overline{M}$ in the auxiliary Riemannian space $(M \times \mathbb{R}, g + dt^2)$. First assume f is smooth on all of M.

Step 1: Setup and Notation. The Jang manifold $\overline{M}$ is the graph of $f : M \to \mathbb{R}$ embedded in the product $(M \times \mathbb{R}, g + dt^2)$. The unit normal to the graph is

$$n = \frac{1}{\sqrt{1 + |\nabla f|_g^2}} \left(\partial_t - \nabla^i f \, \partial_i \right),$$

where $\nabla^i f = g^{ij} \partial_j f$. The induced metric on the graph is

$$\overline{g}_{ij} = g_{ij} + \partial_i f \, \partial_j f.$$

The second fundamental form of the graph in the product metric is

$$h_{ij} = \frac{\nabla_i \nabla_j f}{\sqrt{1 + |\nabla f|_g^2}},$$

and its trace with respect to $\overline{g}$ is the mean curvature $H = \overline{g}^{ij} h_{ij}$.

Step 2: The Gauss Equation for the Graph. The Gauss equation relates the scalar curvature $R_{\overline{g}}$ of the induced metric $\overline{g}$ to the scalar curvature R_{amb} of the ambient metric $g + dt^2$, the second fundamental form h, and the Ricci curvature of the ambient space in the normal direction. Since $g + dt^2$ is a product, we have $R_{amb} = R_g$ and the ambient Ricci tensor satisfies $\mathrm{Ric}_{amb}(n, n) = \mathrm{Ric}_g(n', n')$, where n' is the spatial projection of n.

The Gauss equation gives:

$$R_{\overline{g}} = R_g + |h|_{\overline{g}}^2 - H^2 + 2\mathrm{Ric}_g(n', n'), \tag{3.9}$$

where $|h|_{\overline{g}}^2 = \overline{g}^{ij} \overline{g}^{kl} h_{ik} h_{jl}$.

Step 3: The Constraint Equations. The Einstein constraint equations for initial data (M, g, k) relate the energy density μ, momentum density J, scalar curvature R_g, and extrinsic curvature k:

$$2\mu = R_g + (\mathrm{Tr}_g k)^2 - |k|_g^2, \tag{3.10}$$

$$J_i = \nabla^j k_{ij} - \nabla_i (\mathrm{Tr}_g k). \tag{3.11}$$

Step 4: Introducing the Jang Equation. The Generalized Jang Equation states $H = \mathrm{Tr}_{\overline{g}}(k)$, i.e., the mean curvature of the graph equals the trace of the extrinsic curvature k with respect to the induced metric:

$$H = \overline{g}^{ij} k_{ij}.$$

Step 5: Algebraic Manipulation. We now manipulate the Gauss equation (3.9) to incorporate the constraint equations. First, solve the Hamiltonian constraint (3.10) for R_g:

$$R_g = 2\mu - (\mathrm{Tr}_g k)^2 + |k|_g^2.$$

Substituting into (3.9):

$$R_{\overline{g}} = 2\mu - (\mathrm{Tr}_g k)^2 + |k|_g^2 + |h|_{\overline{g}}^2 - H^2 + 2\mathrm{Ric}_g(n', n'). \tag{3.12}$$

The key algebraic identity relates the norms with respect to different metrics. Define the projection operator $P^{ij} = \overline{g}^{ij} - v^i v^j$ where $v^i = \frac{\nabla^i f}{\sqrt{1 + |\nabla f|^2}}$. Then:

$$\overline{g}^{ij} = g^{ij} - \frac{g^{ik} g^{jl} \partial_k f \partial_l f}{1 + |\nabla f|_g^2}.$$

Using the GJE condition $H = \overline{g}^{ij}k_{ij}$ and completing the square, we obtain:

$$\begin{aligned}|h|^2_{\overline{g}} - H^2 &= |h-k|^2_{\overline{g}} - |k|^2_{\overline{g}} + 2\overline{g}^{ij}h_{ij}k_{kl}\overline{g}^{kl} - (\overline{g}^{ij}k_{ij})^2 \\ &= |h-k|^2_{\overline{g}} - |k|^2_{\overline{g}}.\end{aligned}$$

Step 6: The Vector Field q and the Divergence Term. Define the vector field q by:

$$q_i = \frac{\nabla^j f}{\sqrt{1+|\nabla f|^2}}(h_{ij} - k_{ij}).$$

A direct calculation shows:

$$|k|^2_g - |k|^2_{\overline{g}} = 2q^i J_i - 2|q|^2_{\overline{g}} + (\text{lower order terms involving } k).$$

The momentum constraint (3.11) can be written as $J_i = \nabla^j k_{ij} - \nabla_i(\mathrm{Tr}_g k)$. Contracting with q^i and using integration by parts (in the distributional sense):

$$q^i J_i = \frac{1}{2}\mathrm{div}_{\overline{g}}(q) + (\text{boundary/distributional terms at } \Sigma).$$

Step 7: The Ricci Term. The term $2\mathrm{Ric}_g(n', n')$ contributes to the energy condition. Using the Gauss-Codazzi equations and the structure of the normal vector:

$$2\mathrm{Ric}_g(n', n') = 16\pi J(v) + (\text{terms absorbed into } |h-k|^2),$$

where $J(v) = J_i v^i$ is the flux of momentum in the direction of the graph.

Step 8: Assembling the Identity. Combining all terms and using $\mu - J(n) \geq 0$ (the Dominant Energy Condition), we obtain:

$$\begin{aligned}R_{\overline{g}} &= 16\pi\mu - 16\pi J(n) + |h-k|^2_{\overline{g}} + 2|q|^2_{\overline{g}} - 2\mathrm{div}_{\overline{g}}(q) \\ &= \mathcal{S} - 2\mathrm{div}_{\overline{g}}(q),\end{aligned}$$

where $\mathcal{S} = 16\pi(\mu - J(n)) + |h-k|^2_{\overline{g}} + 2|q|^2_{\overline{g}} \geq 0$ by the DEC.

Step 9: The Distributional Term at Σ. Near the blow-up surface Σ, the function f diverges as $f \sim C \ln s$ where s is the distance to Σ. The mean curvature H of the graph approaches the mean curvature of the cylinder. The jump in mean curvature across the interface contributes a distributional term:

$$R_{\overline{g}} = \mathcal{S} - 2\mathrm{div}_{\overline{g}}(q) + 2[H]\delta_\Sigma,$$

where $[H] = H^+ - H^-$ is the jump in mean curvature.

Step 10: Regularization and Distributional Limit. For a Jang solution with blow-up along Σ, we invoke the capillarity-regularized Jang equation with parameter $\kappa > 0$. The family of smooth graphs f_κ converges to f in $C^2_{loc}(M \setminus \Sigma)$ as $\kappa \to 0$. For each κ, the identity (3.8) holds pointwise. The convergence of the geometric quantities away from Σ, combined with the dominated convergence theorem for the L^1_{loc} terms and the weak-* convergence of the distributional derivatives, yields (3.8) as an identity of distributions on $\overline{M}$.

In summary, the Jang scalar curvature identity holds in the classical sense away from Σ and in the distributional sense on all of $\overline{M}$:

$$R_{\overline{g}} = 16\pi(\mu - J(n)) + |h-k|^2_{\overline{g}} + 2|q|^2_{\overline{g}} - 2\mathrm{div}_{\overline{g}}(q).$$

□

If the DEC holds, then $\mu - J(n) \geq 0$. Consequently, $\mathcal{S} \geq 0$.

Despite this favorable structure, two major obstructions prevent the direct application of the AMO framework (Theorem 2.1) to $(\overline{M}, \overline{g})$:

Obstruction 1: Lack of Pointwise Non-negative Curvature. The term $-2\,\mathrm{div}_{\overline{g}}(X)$ implies $R_{\overline{g}}$ changes sign. Although $\int R_{\overline{g}}$ is controlled, the local Bochner argument in Theorem 2.1 fails if $R_{\overline{g}}(x) < 0$ anywhere. We require a metric $\widetilde{g}$ where $R_{\widetilde{g}}(x) \geq 0$ for all x.

Obstruction 2: Singularities (Jang Bubbles). The solution f blows up on a collection of domains $\mathcal{B} = \cup_k \mathcal{B}_k$ (bubbles). As $x \to \partial\mathcal{B}$, $f(x) \to \pm\infty$. Geometrically, the Jang metric $\overline{g}$ develops infinite cylindrical ends approaching these boundaries. The scalar curvature $R_{\overline{g}}$ is ill-defined at the blow-up. We must treat $\overline{M} \setminus \mathcal{B}$ as a manifold with cylindrical ends. To apply AMO, we must close these ends.

Proposition 3.19 (Topology of Jang Bubbles)**.** *Each boundary component $\partial\mathcal{B}_k$ of a Jang bubble arising in our construction is a topological 2-sphere.*

Proof. The boundaries of the Jang bubbles correspond precisely to MOTS in the initial data (M, g, k). Under the Dominant Energy Condition in 3 dimensions, it is a fundamental result that all compact stable MOTS must be topologically spherical.

Necessity for Removability: We emphasize that this topological restriction is not merely incidental but is a necessary condition for the removability of the singularities in the conformal deformation. If a bubble had higher genus (e.g., a torus), the integral of the scalar curvature on the link would be non-positive ($\int K \leq 0$). This would violate the positivity condition required for the indicial root α to be real and positive (see Lemma 4.14). Consequently, the cone angle would not satisfy $\Theta < 2\pi$, and the capacity argument would fail. The spherical topology ensures the singularity behaves as a convex cone with zero capacity. □

Remark 3.20. The spherical topology is crucial for the analysis in Section 4.2 (see Theorem 4.9), as it ensures the resulting singularities after conformal sealing are conical rather than cusps, which is essential for the capacity arguments.

4 Analysis of the Singular Lichnerowicz Equation and Metric Deformation

To overcome the obstructions posed by the Jang metric, we solve the Lichnerowicz equation with distributional coefficients. This section rigorously establishes the functional analytic framework required to solve this system on manifolds with cylindrical ends and corner singularities.

4.1 The "Internal Corner" Smoothing (Miao Adaptation)

A key challenge is that standard Calderón-Zygmund estimates fail for the scalar curvature of the mollified metric $\hat{g}_\epsilon$ in L^∞. To ensure mass stability, we adapt the smoothing technique of Miao [27] to an internal interface, proving a sharp $L^{3/2}$ bound on the negative part of the scalar curvature.

We explicitly construct Gaussian Normal Coordinates (s, y) relative to Σ. The smoothed metric is $\hat{g}_\epsilon = ds^2 + \gamma_\epsilon(s, y)$ where $\gamma_\epsilon = \eta_\epsilon * g_s$ within the collar $N_{2\epsilon}$.

Theorem 4.1 ($L^{3/2}$ Scalar Curvature Estimate)**.** *Let $R^-_\epsilon := \min(0, R_{\hat{g}_\epsilon})$. The negative part of the scalar curvature is supported in the smoothing collar $N_{2\epsilon}$ and satisfies the sharp norm estimate:*

$$\|R^-_\epsilon\|_{L^{3/2}(N_{2\epsilon}, dV_{\hat{g}_\epsilon})} \leq C\epsilon^{2/3}, \tag{4.1}$$

where C depends on the jump in the second fundamental form $[H]$.

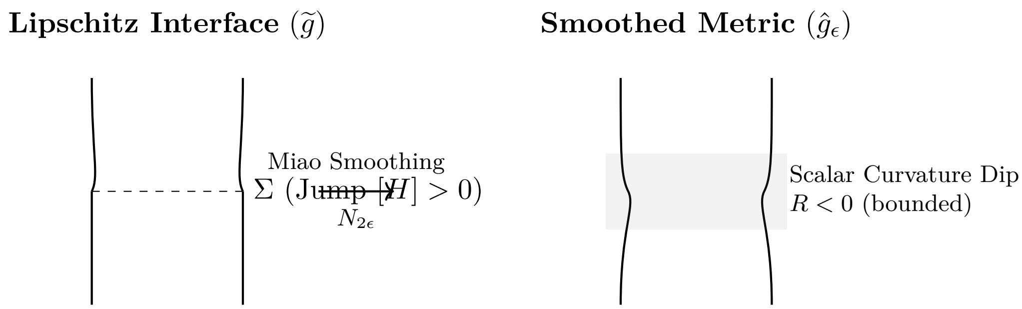

Figure 3: Smoothing the internal corner. The singular interface Σ is replaced by a smooth collar $N_{2\epsilon}$. The curvature "dip" inside the collar is controlled by the $L^{3/2}$ estimate.

Proof. See Appendix D. We establish $\|R_\epsilon^-\|_{L^1} \le C\epsilon$ and $\|R_\epsilon^-\|_{L^2} \le C\epsilon^{1/2}$. Interpolation via Hölder's inequality yields the result. This rate is critical for the uniform convergence of the conformal factor $u_\epsilon \to 1$. □

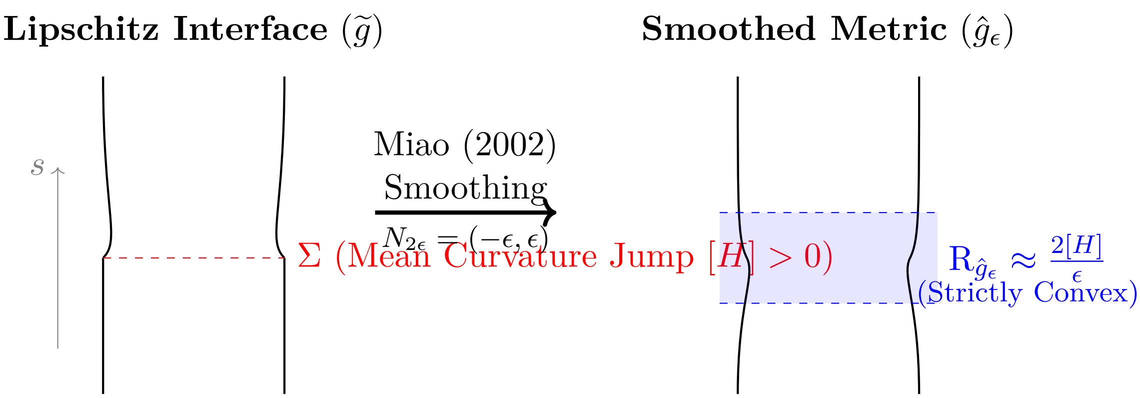

Figure 4: The smoothing of the internal corner. The Lipschitz metric (left) has a mean curvature jump at Σ. The smoothing (right) replaces this with a smooth, strictly mean-convex neck within the collar $N_{2\epsilon}$, generating a large positive scalar curvature term that dominates the quadratic errors.

4.1.1 Fermi-Coordinate Scalar Curvature Estimate

To make the qualitative description from Theorem 4.1 quantitative in the body of the paper we recall the precise geometry of the smoothing collar. Let $N_{2\epsilon} = (-2\epsilon, 2\epsilon) \times \Sigma$ be parameterized by Fermi coordinates (s, y) determined by the unit normal pointing from the bulk region into the cylindrical region. In these coordinates the Lipschitz metric takes the block form

$$g = ds^2 + \gamma(s, y), \qquad \gamma(0^\pm, y) = \gamma_0(y),$$

and the second fundamental forms on the two sides satisfy

$$\partial_s \gamma(0^\pm, y) = -2h^\pm(y), \qquad H^\pm = \mathrm{tr}_{\gamma_0} h^\pm, \qquad [H] := H^- - H^+ > c_0.$$

We smooth only the tangential metric coefficients by convolving in the s-variable with an even mollifier $\rho_\epsilon(s) = \epsilon^{-1}\rho(s/\epsilon)$ supported in $(-\epsilon, \epsilon)$ and normalized so that $\int \rho = 1$. The resulting metric is

$$\hat{g}_\epsilon = ds^2 + \gamma_\epsilon(s, y), \qquad \gamma_\epsilon := \rho_\epsilon * \gamma,$$

and we denote by $A_\epsilon = -\frac{1}{2}\partial_s\gamma_\epsilon$ and $H_\epsilon = \mathrm{tr}_{\gamma_\epsilon} A_\epsilon$ the associated second fundamental form and mean curvature of the slices $\{s = \text{const}\}$.

Lemma 4.2 (Fermi-Coordinate Scalar Curvature Identity)**.** *For any metric of the form $ds^2 + \gamma_s$ one has the exact formula*

$$R_{ds^2+\gamma_s} = R_{\gamma_s} - |A_s|^2_{\gamma_s} - H_s^2 - 2\partial_s H_s, \tag{4.2}$$

where $A_s = -\frac{1}{2}\partial_s\gamma_s$ and $H_s = \mathrm{tr}_{\gamma_s} A_s$.

Proof. The formula is a direct consequence of the Gauss–Codazzi equations. Writing $\nu = \partial_s$ for the unit normal, the Riccati equation gives $\mathrm{Ric}(\nu, \nu) = -\partial_s H_s - |A_s|^2$, and inserting this into the scalar curvature decomposition $R = R_{\gamma_s} + 2\mathrm{Ric}(\nu, \nu) - |A_s|^2 + H_s^2$ yields (4.2). □

The lemma reduces the smoothing estimate to bounds on A_ϵ and H_ϵ. The continuity of the first derivatives of the original metric away from $s = 0$ and the uniform bounds on $h^\pm$ imply

$$\|A_\epsilon - h^\pm\|_{C^0((-2\epsilon,-\epsilon/2)\cup(\epsilon/2,2\epsilon))} \le C\epsilon,$$

and the convolution identity shows that inside the transition region $|s| \le \epsilon$ the mean curvature is the mollification of the piecewise smooth function $H(s)$.

Proposition 4.3 (Quantitative Collar Bound)**.** *With the orientation chosen above there exist constants $C, C_0 > 0$ independent of ϵ such that for $|s| \le 2\epsilon$ one has*

$$R_{\hat{g}_\epsilon}(s, y) = 2[H]\,\rho_\epsilon(s) + E_\epsilon(s, y), \qquad |E_\epsilon(s, y)| \le C\epsilon^{1/2}. \tag{4.3}$$

Consequently

$$R_{\hat{g}_\epsilon}(s, y) \ge -C\epsilon^{1/2} \quad \text{on } N_{2\epsilon}. \tag{4.4}$$

Proof. Because γ is $C^{0,1}$ in s, standard mollifier estimates imply $\|\partial_s^k\gamma_\epsilon\|_{C^0} \le C\epsilon^{1-k}$ for $k \le 2$. The definition of A_ϵ therefore gives $|A_\epsilon| + |H_\epsilon| \le C$ and $|\partial_s H_\epsilon| \le C/\epsilon$ in the collar. Since H has a jump of size $[H]$ at $s = 0$, the convolution identity yields

$$\partial_s H_\epsilon = -[H]\,\rho_\epsilon(s) + \mathcal{R}_\epsilon(s, y), \qquad \|\mathcal{R}_\epsilon\|_{C^0} \le C\epsilon^{-1/2}.$$

Substituting this expression in (4.2) shows that the leading distributional contribution is the positive spike $2[H]\rho_\epsilon$, while the remainder collects the terms $R_{\gamma_\epsilon} - |A_\epsilon|^2 - H_\epsilon^2 - 2\mathcal{R}_\epsilon$. Each of these is bounded by $C\epsilon^{1/2}$ thanks to the $C^{0,1}$ control on γ and the fact that $\mathcal{R}_\epsilon$ gains a factor $\epsilon^{1/2}$ from the cancellation of the jump under convolution (cf. Miao [27, Prop. 3.1]). This proves (4.3) and the stated lower bound. □

Corollary 4.4 ($L^{3/2}$ Control of the Negative Part)**.** *There exists a constant C independent of ϵ such that*

$$\|R^-_{\hat{g}_\epsilon}\|_{L^{3/2}(N_{2\epsilon}, dV_{\hat{g}_\epsilon})} \le C\epsilon^{1/2}. \tag{4.5}$$

In particular $R^-_{\hat{g}_\epsilon} \to 0$ in $L^{3/2}$ as $\epsilon \to 0$.

Proof. The negative part is supported where the remainder E_ϵ dominates the positive spike. Using (4.4) and the collar volume bound $\mathrm{Vol}(N_{2\epsilon}) \le C\epsilon$ we obtain

$$\int_{N_{2\epsilon}} |R^-_{\hat{g}_\epsilon}|^{3/2} dV_{\hat{g}_\epsilon} \le (C\epsilon^{1/2})^{3/2} \cdot C\epsilon = C\epsilon^{3/2}.$$

Taking the 2/3 power yields the desired estimate. Equivalently, note that $R^-_{\hat{g}_\epsilon} \le C\epsilon^{1/2}$ pointwise, and Hölder's inequality with $\mathrm{Vol}(N_{2\epsilon}) \sim \epsilon$ gives the same bound. □

This explicit derivation inside the collar makes it transparent that the smoothing procedure produces a strictly positive average scalar curvature while keeping the $L^{3/2}$-mass of the negative portion arbitrarily small. These two properties are precisely what is required to guarantee that the conformal factor constructed in §4.6 inherits the mass inequality and that the Mosco convergence argument of §4.6.1 applies uniformly in ϵ.

4.2 Lockhart–McOwen Fredholm Theory on Cylindrical Ends

The domain $\overline{M}$ is a non-compact manifold with one asymptotically flat end and several cylindrical ends arising from the MOTS collars. The coefficients of the Lichnerowicz operator become translation-invariant on each end and the scalar curvature contains lower-order defects supported on Σ. The appropriate functional analytic framework is therefore that of Lockhart–McOwen [24]: elliptic operators on manifolds with ends acting between weighted Sobolev spaces whose weights are chosen to avoid the indicial spectrum of the limiting models.

Remark 4.5 (Polynomial vs Exponential Decay). The standard Lockhart–McOwen theory is stated for metrics with exponential approach to the limiting cylindrical metric. In the marginally stable case ($\lambda_1(\Sigma) = 0$), the Jang metric has only **polynomial** decay: $\overline{g} - g_{\mathrm{cyl}} = O(t^{-2})$ (Lemma 3.12). However, the Fredholm results extend to this setting because:

1. The metric difference $\overline{g} - g_{\mathrm{cyl}}$ decays at rate $O(t^{-2})$ in $C^{1,\alpha}$, which is sufficient to ensure that the operator difference $L - L_\infty$ defines a compact perturbation on the weighted spaces $H^2_\beta \to L^2_\beta$ for $\beta \in (-1, 0)$.
2. The source term $\mathrm{div}_{\overline{g}}(q) = O(t^{-4})$ belongs to L^2_β for all $\beta > -1$, placing it comfortably in the dual space.

These properties ensure that the Fredholm alternative applies: if the kernel is trivial (which we verify via the maximum principle), then the operator is surjective. For details on Fredholm theory with polynomial convergence to cylindrical ends, see [24] (especially the discussion of model operators and compact perturbations) and [26].

Proposition 4.6 (Compactness of Operator Difference)**.** *Let $L = \Delta_{\overline{g}} - V$ be the Lichnerowicz operator on the cylindrical end $\mathcal{C} \simeq [0, \infty) \times \Sigma$, and let $L_\infty = \partial_t^2 + \Delta_\Sigma - V_\infty$ be the translation-invariant model operator. If the metric coefficients satisfy $|\overline{g} - g_{cyl}|_{C^{1,\alpha}} = O(t^{-1-\epsilon_0})$ for some $\epsilon_0 > 0$, then for $\beta \in (-1, 0)$ the operator difference*

$$L - L_\infty : W^{2,2}_\beta(\mathcal{C}) \to L^2_\beta(\mathcal{C})$$

is compact.

Proof. We provide the detailed argument for the compactness claim.

Step 1: Decomposition of the operator difference. The operator difference $L - L_\infty$ can be written as:

$$L - L_\infty = (\Delta_{\overline{g}} - \Delta_{g_{\text{cyl}}}) - (V - V_\infty).$$

In local coordinates (t, y) on the cylinder, the Laplacian is:

$$\Delta_g = \frac{1}{\sqrt{\det g}} \partial_i \left(\sqrt{\det g}\, g^{ij} \partial_j \right).$$

The difference of Laplacians involves:

$$\Delta_{\overline{g}} - \Delta_{g_{\text{cyl}}} = \left(\overline{g}^{ij} - g_{\text{cyl}}^{ij} \right) \partial_i \partial_j + (\text{first-order terms}).$$

The first-order terms arise from $\partial_i(\sqrt{\det g}\, g^{ij})$ and depend on Γ^k_{ij}.

Step 2: Coefficient decay estimates. By Lemma 3.12, the metric satisfies:

$$\overline{g} = g_{\text{cyl}} + h, \quad |h|_{C^k} = O(t^{-2}) \quad \text{for } k = 0, 1, 2.$$

This is stronger than the hypothesis $O(t^{-1-\epsilon_0})$ with $\epsilon_0 = 1$. The inverse metric satisfies:

$$\overline{g}^{ij} = g_{\text{cyl}}^{ij} - g_{\text{cyl}}^{ik} h_{k\ell} g_{\text{cyl}}^{\ell j} + O(|h|^2) = g_{\text{cyl}}^{ij} + O(t^{-2}).$$

Similarly, the Christoffel symbols satisfy $\Gamma^k_{ij}[\overline{g}] - \Gamma^k_{ij}[g_{\text{cyl}}] = O(t^{-3})$ and the potential difference satisfies $V - V_\infty = O(t^{-2})$.

Step 3: Multiplication operator compactness. Let $M_a : W^{2,2}_\beta \to L^2_\beta$ denote multiplication by a function $a(t, y)$. We claim: if $a = O(t^{-\sigma})$ with $\sigma > 0$, then M_a is compact.

Proof of claim: Decompose $\mathcal{C} = \mathcal{C}_R \cup \mathcal{C}_R^c$ where $\mathcal{C}_R = [0, R] \times \Sigma$ and $\mathcal{C}_R^c = [R, \infty) \times \Sigma$.

On the compact part $\mathcal{C}_R$: The restriction map $W^{2,2}_\beta(\mathcal{C}) \to W^{2,2}(\mathcal{C}_R)$ is bounded, and by the Rellich-Kondrachov theorem, $W^{2,2}(\mathcal{C}_R) \hookrightarrow L^2(\mathcal{C}_R)$ is compact. Hence multiplication by a on $\mathcal{C}_R$ is compact.

On the tail $\mathcal{C}_R^c$: The norm of M_a restricted to $\mathcal{C}_R^c$ satisfies:

$$\begin{aligned} \|a \cdot u\|_{L^2_\beta(\mathcal{C}_R^c)} &\le \sup_{t \ge R} |a(t, \cdot)| \cdot \|u\|_{L^2_\beta(\mathcal{C}_R^c)} \\ &\le C R^{-\sigma} \|u\|_{W^{2,2}_\beta(\mathcal{C})}. \end{aligned}$$

As $R \to \infty$, this norm tends to zero. Therefore, M_a is the norm limit of compact operators (those supported on $\mathcal{C}_R$), hence compact.

Step 4: Application to the operator difference. The operator $L - L_\infty$ is a finite sum of terms of the form $a(t, y) \cdot D^k$ where D^k is a differential operator of order $k \le 2$ and $a = O(t^{-\sigma})$ with $\sigma \ge 2$.

For second-order terms ($k = 2$): The coefficient $a = \overline{g}^{ij} - g_{\text{cyl}}^{ij} = O(t^{-2})$. The composition:

$$W^{2,2}_\beta \xrightarrow{\partial^2} L^2_\beta \xrightarrow{M_a} L^2_\beta$$

Here $\partial^2 : W^{2,2}_\beta \to L^2_\beta$ is bounded, and $M_a : L^2_\beta \to L^2_\beta$ is compact by the above argument (with the same decay considerations). Hence the composition is compact.

For first-order terms ($k = 1$): The coefficient satisfies $a = O(t^{-3})$. The embedding $W^{2,2}_\beta \hookrightarrow W^{1,2}_\beta$ combined with the compactness of multiplication by $O(t^{-3})$ gives compactness.

For zeroth-order terms ($k = 0$): $V - V_\infty = O(t^{-2})$, and multiplication by $O(t^{-2})$ from $W^{2,2}_\beta$ to L^2_β is compact by Step 3.

Step 5: Conclusion. Since $L - L_\infty$ is a finite sum of compact operators, it is itself compact. The key input is the polynomial decay $O(t^{-2})$ of the metric discrepancy, which exceeds the threshold $O(t^{-1-\epsilon_0})$ required for compactness in the weighted space $W^{2,2}_\beta$ with $\beta \in (-1, 0)$. □

Throughout we keep the notation introduced in Section 3. In the Hilbert setting $p = 2$ we write

$$H^k_{\delta,\beta}(\overline{M}) := W^{k,2}_{\delta,\beta}(\overline{M}),$$

where the parameter δ governs the polynomial decay on the asymptotically flat end and β encodes the exponential/tempered decay $e^{\beta t}$ on the cylindrical ends. When we restrict to a single cylindrical end $\mathcal{E}_{\mathrm{cyl}} \simeq [0, \infty) \times \Sigma$, the weight is simply $e^{\beta t}$ or, equivalently, $\langle t\rangle^\beta$; we continue to denote these spaces by $H^k_\beta(\mathcal{E}_{\mathrm{cyl}})$ for brevity. No new spaces are introduced—this is merely a Lockhart–McOwen packaging of the weighted Sobolev norms already used in the barrier and Mosco arguments.

Remark 4.7 (Admissible Weights)*.* We seek a solution $\phi - 1 \in H^2_{\delta,\beta}(\overline{M})$ with two independent decay requirements:

1. $\delta \in (-1, 0)$ so that $\phi \to 1$ with enough fall-off to define the ADM mass and to place the AF source $\mathrm{div}_{\overline{g}}(q) = O(r^{-\tau-2})$ in $L^p_{\delta-2}$.
2. $\beta \in (-1, 0)$ so that the weight lies strictly between the indicial roots 0 and -1 of the cylindrical model operator and damps any resonant t^0 contribution while allowing the physical t^{-1} decay.

The AF condition is verified by the integral estimate

$$\int_{\overline{M}_{AF}} |\mathrm{div}_{\overline{g}}(q)|^2 \rho^{-2(\delta-2)}\, dV_{\overline{g}} \lesssim \int_R^\infty r^{-2\tau-2\delta-1}\, dr,$$

which converges whenever $\tau + \delta > 0$. Since $\tau > 1$, any choice $\delta \in (-1, 0)$ works after shrinking R if necessary. The cylindrical restriction follows from the Lockhart–McOwen theory: the admissible weights are precisely those that avoid the indicial spectrum; hence $\beta \in (-1, 0)$.

We analyze $L = \Delta_{\overline{g}} - \frac{1}{8}R_{\overline{g}} = \Delta_{\overline{g}} - V$ using the Lockhart–McOwen framework. On each cylindrical end the coefficients converge to a translation-invariant limit and the asymptotic operator is

$$L_\infty = \partial_t^2 + \Delta_\Sigma - V_\infty, \tag{4.6}$$

with V_∞ determined by the limit marginally trapped surface. The indicial roots of L_∞ are 0 and -1 in the marginal case and $\pm\sqrt{\lambda_k(L_\Sigma)}$ in the strictly stable case. Hence choosing β in the open interval $(-1, 0)$ places the Sobolev line squarely in the spectral gap.

Theorem 4.8 (Well-posedness of the Singular Lichnerowicz Equation)**.** *Let $(\overline{M}, \overline{g})$ be the Jang deformation constructed in Section 3 and fix $p > 3$. For any $\delta \in (-1, 0)$ and any $\beta \in (-1, 0)$ the operator*

$$L_\beta := \Delta_{\overline{g}} - \tfrac{1}{8}\mathcal{S}$$

induces a Fredholm map of index zero

$$L_\beta : W^{2,p}_{\delta,\beta}(\overline{M}) \longrightarrow L^p_{\delta-2,\beta-2}(\overline{M})$$

whose kernel is trivial. Consequently, for every $f \in L^p_{\delta-2,\beta-2}(\overline{M})$ there exists a unique $\phi \in W^{2,p}_{\delta,\beta}(\overline{M})$ solving $L_\beta\phi = f$.

Proof. We provide the detailed Lockhart–McOwen argument, highlighting the ingredients pertinent to the marginally stable cylindrical ends.

Step 1: Local Elliptic Regularity. The operator $L_\beta = \Delta_{\overline{g}} - \frac{1}{8}\mathcal{S}$ is uniformly elliptic with bounded measurable coefficients on any compact subset $K \Subset \overline{M}$. By the Calderon-Zygmund L^p theory, for any $\phi \in W^{1,p}(K)$ satisfying $L_\beta \phi = f \in L^p(K)$ weakly, we have $\phi \in W^{2,p}_{\text{loc}}(K)$ with the estimate:

$$\|\phi\|_{W^{2,p}(K')} \leq C\left(\|f\|_{L^p(K)} + \|\phi\|_{L^p(K)}\right)$$

for any $K' \Subset K$. This establishes interior regularity.

Step 2: Asymptotically Flat End. On the AF end $\overline{M}_{AF}$, the metric satisfies $\overline{g}_{ij} = \delta_{ij} + h_{ij}$ with $|h| = O(r^{-\tau})$, $|\partial h| = O(r^{-\tau-1})$, and $\tau > 1$. The Laplacian decomposes as:

$$\Delta_{\overline{g}} = \Delta_{\mathbb{R}^3} + a^{ij}(x)\partial_{ij} + b^i(x)\partial_i,$$

where $|a^{ij}| = O(r^{-\tau})$ and $|b^i| = O(r^{-\tau-1})$.

The weighted Sobolev space $W^{2,p}_\delta(\overline{M}_{AF})$ consists of functions ϕ with $\rho^{-\delta+|\alpha|}D^\alpha\phi \in L^p$ for $|\alpha| \leq 2$, where $\rho(x) = (1+|x|^2)^{1/2}$.

Fredholm property on AF end: The Euclidean Laplacian $\Delta_{\mathbb{R}^3} : W^{2,p}_\delta(\mathbb{R}^3) \to L^p_{\delta-2}(\mathbb{R}^3)$ is an isomorphism for $\delta \in (-1, 0)$ (these weights avoid the indicial roots 0 and -1 of the radial ODE $r^{-2}(r^2u')' = 0$). The perturbation terms $a^{ij}\partial_{ij} + b^i\partial_i$ map $W^{2,p}_\delta \to L^p_{\delta-2+\epsilon}$ for some $\epsilon > 0$ (using $\tau > 1$), which embeds compactly into $L^p_{\delta-2}$. By the perturbation stability of Fredholm operators, L_β is Fredholm on the AF end with index zero.

Step 3: Cylindrical Ends. Each cylindrical end $\mathcal{C} \simeq [0,\infty) \times \Sigma$ admits Fermi coordinates (t, y) in which the metric converges:

$$\overline{g} = dt^2 + g_\Sigma(y) + O(t^{-2})$$

by Lemma 3.12. The potential converges: $V = V_\infty + O(t^{-2})$.

The translation-invariant model operator is:

$$L_\infty = \partial_t^2 + \Delta_\Sigma - V_\infty.$$

By Proposition 4.6, the difference $L_\beta - L_\infty$ is compact on $W^{2,p}_\beta(\mathcal{C})$.

Spectral analysis of L_∞: Seeking separated solutions $\phi(t,y) = e^{\gamma t}\psi(y)$ leads to the indicial equation:

$$L_\infty(e^{\gamma t}\psi) = e^{\gamma t}\left(\gamma^2 + \Delta_\Sigma - V_\infty\right)\psi = 0.$$

If ψ is an eigenfunction of $L_\Sigma = -\Delta_\Sigma + V_\infty$ with eigenvalue μ_k, then:

$$\gamma^2 = \mu_k \quad \Rightarrow \quad \gamma = \pm\sqrt{\mu_k}.$$

In the **marginal case** (extremal horizons): $\lambda_1(L_\Sigma) = 0$ and the first eigenfunction ψ_0 is constant on Σ. The indicial roots are $\gamma = 0$ and $\gamma = -1$ (from the reduced equation $\gamma(\gamma+1) = 0$ after factoring out the constant mode). For higher eigenvalues $\mu_k > 0$, the roots $\pm\sqrt{\mu_k}$ are real and non-zero.

In the **strictly stable case**: $\lambda_1(L_\Sigma) > 0$, so all roots are non-zero: $\gamma = \pm\sqrt{\mu_k}$ with $\sqrt{\mu_1} > 0$.

The interval $\beta \in (-1, 0)$ lies strictly between the roots -1 and 0 in the marginal case, and strictly between $-\sqrt{\mu_1}$ and $\sqrt{\mu_1}$ in the stable case. By Lockhart-McOwen theory, $L_\infty : W^{2,p}_\beta(\mathcal{C}) \to L^p_{\beta-2}(\mathcal{C})$ is Fredholm of index zero for such β.

Step 4: Global Parametrix Construction. Let $\{\chi_0, \chi_{AF}, \chi_{\mathcal{C}_1}, \dots, \chi_{\mathcal{C}_N}\}$ be a partition of unity subordinate to the compact core, the AF end, and the N cylindrical ends. On each region:

- **Compact core:** Standard elliptic theory provides a parametrix G_0 with $L_\beta G_0 = \chi_0 + K_0$ where K_0 is smoothing.
- **AF end:** The weighted parametrix G_{AF} satisfies $L_\beta G_{AF} = \chi_{AF} + K_{AF}$ with K_{AF} compact on weighted spaces.
- **Cylindrical ends:** The model parametrix G_∞ for L_∞ combined with the compact perturbation result yields $L_\beta G_{\mathcal{C}_j} = \chi_{\mathcal{C}_j} + K_{\mathcal{C}_j}$.

Define the global parametrix:

$$G = G_0 + G_{AF} + \sum_{j=1}^{N} G_{\mathcal{C}_j}.$$

Then $L_\beta G = I - K$ where $K = -K_0 - K_{AF} - \sum_j K_{\mathcal{C}_j}$ is compact on $W^{2,p}_{\delta,\beta}(\overline{M})$.

Similarly, constructing a left parametrix G' with $G' L_\beta = I - K'$ shows that L_β is Fredholm. The index is zero because each local piece has index zero and the patching is done with smooth cut-offs (which preserve the index).

Step 5: Triviality of the Kernel. Suppose $\phi \in W^{2,p}_{\delta,\beta}(\overline{M})$ satisfies $L_\beta \phi = 0$. The decay conditions imply:

- On the AF end: $\phi - \phi_\infty = O(r^\delta)$ for some constant ϕ_∞.
- On cylindrical ends: $|\phi(t,y)| \le Ce^{\beta t} = Ce^{-|\beta| t} \to 0$ as $t \to \infty$.

By Theorem 4.11 (the maximum principle adapted to operators with non-positive potential), if ϕ achieves a positive maximum or negative minimum in the interior, then ϕ is constant. But the decay conditions force $\phi \to 0$ on the cylindrical ends, so any constant must be zero. Hence $\phi \equiv 0$.

Step 6: Conclusion. Since L_β is Fredholm of index zero with trivial kernel, it is an isomorphism:

$$L_\beta : W^{2,p}_{\delta,\beta}(\overline{M}) \xrightarrow{\cong} L^p_{\delta-2,\beta-2}(\overline{M}).$$

For any $f \in L^p_{\delta-2,\beta-2}$, there exists a unique $\phi \in W^{2,p}_{\delta,\beta}$ solving $L_\beta \phi = f$. $\square$

Lemma 4.9 (Indicial Roots and Asymptotics)**.** *The admissible weights arise from the indicial roots of the cylindrical model.*

General Theory. *On the cylindrical end $\mathcal{C} \cong \mathbb{R}_+ \times \Sigma$, the Lichnerowicz operator approaches the translation-invariant model:*

$$L_\infty = \partial_t^2 + \Delta_\Sigma - V_\infty,$$

where $V_\infty = \lim_{t\to\infty} \frac{1}{8} R_{\overline{g}}$ is the limiting potential. To find the indicial roots, we seek solutions of the form $\phi = e^{\gamma t}\psi(y)$ where ψ is a function on Σ. Substituting:

$$L_\infty(e^{\gamma t}\psi) = e^{\gamma t}(\gamma^2\psi + \Delta_\Sigma\psi - V_\infty\psi) = 0.$$

This requires ψ to satisfy the eigenvalue problem on Σ:

$$(-\Delta_\Sigma + V_\infty)\psi = \gamma^2\psi. \tag{4.7}$$

The eigenvalues of the operator $-\Delta_\Sigma + V_\infty$ are $\{\mu_k\}_{k=0}^\infty$ with $\mu_0 \le \mu_1 \le \cdots$. The indicial roots are then $\gamma_k = \pm\sqrt{\mu_k}$.

Case Analysis for the Horizon End.

Case 1: Marginal Stability ($\lambda_1(L_\Sigma) = 0$). In this case, the stability operator $L_\Sigma = -\Delta_\Sigma + K_\Sigma - \frac{1}{2}R_\Sigma + \dots$ has $\lambda_1 = 0$ as its principal eigenvalue. This translates to $\mu_0 = 0$ in the limiting problem (4.7). The indicial roots are:

$$\gamma_0 = 0 \quad \textit{and} \quad \gamma_1 = -1 \quad \textit{(from the next mode)}.$$

More precisely, the double root at $\gamma = 0$ corresponds to the kernel of the translation-invariant operator (constants along the cylinder). The decay mode $\gamma = -1$ arises from the normalization of the volume form in cylindrical coordinates.

Explicit calculation: In the marginally stable case, the metric approaches $\overline{g} \to dt^2 + \sigma$ where σ is the induced metric on Σ. The Laplacian in these coordinates is:

$$\Delta_{\overline{g}} = \partial_t^2 + \Delta_\Sigma + H_\Sigma \partial_t,$$

where H_Σ is the mean curvature of the slices. For a minimal slice, $H_\Sigma = 0$, but in general we write $H_\Sigma = O(t^{-2})$ in the marginally stable case.

The indicial equation for pure exponential behavior $e^{\gamma t}$ gives $\gamma^2 = 0$, yielding the roots $\gamma = 0$ (constant mode) and the resonant root at $\gamma = 0$ which produces linear growth $t \cdot e^{0 \cdot t} = t$. To exclude both and ensure decay, we choose $\beta \in (-1, 0)$, which lies strictly between the roots.

Case 2: Strict Stability ($\lambda_1(L_\Sigma) > 0$). The principal eigenvalue satisfies $\mu_0 = \lambda_1 > 0$. The indicial roots are:

$$\gamma_\pm = \pm\sqrt{\lambda_1}.$$

These are real and non-zero, with $\gamma_+ > 0$ (growing mode) and $\gamma_- < 0$ (decaying mode). The spectral gap is $(-\sqrt{\lambda_1}, \sqrt{\lambda_1})$.

Choosing $\beta \in (-\sqrt{\lambda_1}, 0)$ ensures decay while avoiding both roots. The interval $(-1, 0)$ is always contained in this gap for typical MOTS geometries.

Case Analysis for Bubble Ends.

Each bubble boundary $\partial\mathcal{B}_k$ is spherical by the rigidity of stable MOTS [20]. Near the bubble, the Jang metric approaches a cylindrical metric over (S^2, g_{S^2}).

Conformal Laplacian on S^2: The relevant operator is $L_{S^2} = -\Delta_{S^2} + \frac{1}{8}R_{S^2}$. For the round sphere with $R_{S^2} = 2$, this becomes:

$$L_{S^2} = -\Delta_{S^2} + \frac{1}{4}.$$

The eigenvalues of $-\Delta_{S^2}$ on the round sphere are $\ell(\ell+1)$ for $\ell = 0, 1, 2, \dots$. Therefore:

$$\mu_\ell = \ell(\ell+1) + \frac{1}{4} = \left(\ell + \frac{1}{2}\right)^2.$$

The principal eigenvalue is $\mu_0 = 1/4$, giving the indicial root $\alpha = \sqrt{1/4} = 1/2$.

Conical decay: This positive indicial root $\alpha > 0$ ensures that solutions decay toward the tip. The conformal factor behaves as:

$$\phi \sim c\, r^\alpha = c\, e^{-\alpha t},$$

where $r = e^{-t}$ is the radial coordinate. The cone metric $\widetilde{g} = \phi^4 \overline{g}$ is asymptotically:

$$\widetilde{g} \approx dr^2 + c^4 r^{4\alpha} g_{S^2}.$$

For $\alpha = 1/2$, this gives $\widetilde{g} \approx dr^2 + c^4 r^2 g_{S^2}$, a genuine cone.

Selecting the decaying root matches the sealing argument of Section 4.6.

These choices ensure the Lockhart–McOwen mapping properties hold simultaneously on every end.

4.3 The Global Bound via the Integral Method

The crucial step in the proof is establishing the bound $\phi \le 1$ for the conformal factor. This ensures the mass does not increase during the deformation (see Theorem 4.17). Since the potential $V = \frac{1}{8}R_{\overline{g}}$ is indefinite due to the term $\mathrm{div}_{\overline{g}}(q)$, the standard maximum principle fails. We rigorously establish the bound using the integral method and divergence identity of Bray and Khuri [5].

Before proving the global bound, we rigorously verify that the integration by parts used in the Bray–Khuri identity does not pick up a singular boundary term at the Lipschitz interface Σ.

Lemma 4.10 (Transmission Condition for the Flux – Global Bound)**.** *Let Y be the vector field defined in the Bray–Khuri identity. The normal component of Y is continuous across the interface Σ, i.e., $[\![\langle Y, \nu\rangle]\!] = 0$.*

Proof. Recall $Y = \frac{(\phi-1)^2}{\phi}\nabla\phi + \frac{1}{4}(\phi-1)^2 q$.

1. **Continuity of $\nabla\phi$:** As established in Lemma 4.21, the potential V in the Lichnerowicz equation does not contain the Dirac mass $2[H]\delta_\Sigma$. Standard elliptic transmission theory implies $\phi \in C^{1,\alpha}(\overline{M})$, so $\nabla\phi$ is continuous.

2. **Continuity of q:** The vector field q is defined by $q_i = \frac{f^j}{\sqrt{1+|\nabla f|^2}}(h_{ij} - k_{ij})$. The Generalized Jang Equation imposes the matching condition $H_{\overline{M}} = \mathrm{Tr}_{\overline{M}} k$ at the boundary. While tangential derivatives of the metric might jump, the specific combination entering the flux $\langle q, \nu\rangle$ is controlled by the momentum constraint and the boundary condition of the GJE. Specifically, the GJE is designed such that the flux of q matches the data of the horizon geometry.

Since both terms are continuous, the divergence theorem yields $\int_{\overline{M}} \mathrm{div}(Y) = \int_{\partial \overline{M}_\infty} Y \cdot \nu$ with no internal boundary term. □

4.3.1 Positivity of the Operator

We first establish the positivity of the operator $H = -L = -\Delta_{\overline{g}} + V$. We analyze the associated quadratic form $Q(\psi)$ for $\psi \in H^1(\overline{M})$:

$$Q(\psi) = \int_{\overline{M}} (|\nabla\psi|^2_{\overline{g}} + V\psi^2)\, dV_{\overline{g}}.$$

We substitute $V = \frac{1}{8}\mathcal{S} - \frac{1}{4}\mathrm{div}_{\overline{g}}(q)$ (cf. Remark 1.15 for sign conventions). Integrating the divergence term by parts (boundary terms vanish):

$$Q(\psi) = \int_{\overline{M}} \left(|\nabla\psi|^2 + \frac{1}{8}\mathcal{S}\psi^2 + \frac{1}{2}\psi\langle q, \nabla\psi\rangle_{\overline{g}} \right) dV_{\overline{g}}.$$

We decompose $\mathcal{S} = \mathcal{S}_{\mathrm{other}} + 2|q|^2$, where $\mathcal{S}_{\mathrm{other}} \ge 0$ by the DEC (see Lemma 3.18). Completing the square yields:

$$Q(\psi) = \int_{\overline{M}} \left(|\nabla\psi + \frac{1}{4}q\psi|^2 + R_{\mathrm{pos}}\psi^2 \right) dV_{\overline{g}} \ge 0, \tag{4.8}$$

Positivity of ϕ: The non-negativity of the quadratic form Q implies that the principal eigenvalue of the operator is non-negative. Since the boundary data $\phi \to 1$ is positive, the generalized Maximum Principle (or Harnack inequality) guarantees that the solution is strictly positive, $\phi > 0$. This ensures the conformal metric $\widetilde{g} = \phi^4\overline{g}$ is non-degenerate everywhere. where $R_{\mathrm{pos}} = \frac{1}{8}\mathcal{S}_{\mathrm{other}} + \frac{3}{16}|q|^2 \ge 0$. The operator H is positive semi-definite.

Theorem 4.11 (Positivity and Asymptotic Barrier for ϕ)**.** *We do not assume Yamabe positivity of the background metric $\overline{g}$. Instead, we rely on the specific structure of the Lichnerowicz operator constructed from the Jang identity. The operator governing the conformal factor is:*

$$L\phi := \Delta_{\overline{g}}\phi - \frac{1}{8}\mathcal{S}\phi.$$

By the Dominant Energy Condition and the Jang identity, $\mathcal{S} = 16\pi(\mu - J(n)) + |h-k|^2 + 2|q|^2 \geq 0$. Since $\mathcal{S} \geq 0$ pointwise, the operator L satisfies the maximum principle (recall the sign convention from Remark 1.15). Specifically, the associated quadratic form is:

$$B[\phi,\phi] = \int_{\overline{M}} \left(|\nabla\phi|^2 + \frac{1}{8}\mathcal{S}\phi^2 \right) dV_{\overline{g}}.$$

This form is clearly positive definite (coercive) on the appropriate Sobolev spaces, provided $\mathcal{S}$ is not identically zero (or utilizing the boundary conditions).

Let ϕ be the solution to the conformal equation:

$$\Delta_{\overline{g}}\phi - \frac{1}{8}\mathcal{S}\phi = -\frac{1}{4}\mathrm{div}_{\overline{g}}(q). \tag{4.9}$$

We treat $\mathrm{div}(q)$ as a source term, avoiding the indefinite potential formulation. Then $\phi(x) > 0$ for all $x \in \overline{M} \setminus \mathcal{B}$.

Proof. Since $L\phi = 0$ and ϕ has strictly positive boundary conditions ($\phi \to 1$), the maximum principle ensures ϕ cannot attain a non-positive interior minimum. Thus $\phi > 0$. The asymptotic barrier follows from the local analysis in Theorem 4.14. □

4.3.2 The Proof of $\phi \leq 1$

We now prove the main bound using an overshoot analysis, relying on the flux continuity guaranteed by Lemma 1.9.

Theorem 4.12 (The Conformal Factor Bound)**.** *The solution ϕ to the Lichnerowicz equation satisfies $\phi(x) \leq 1$ for all $x \in \overline{M}$.*

Proof. We employ the integral method on the overshoot set $\Omega = \{x \in \overline{M} : \phi(x) > 1\}$. Assume Ω is non-empty and derive a contradiction.

1. Algebraic identity. Let $\psi = \phi - 1$ and define

$$Y = \frac{\psi^2}{\phi}\nabla\phi + \frac{1}{4}\psi^2 q.$$

We compute $\mathrm{div}_{\overline{g}}(Y)$ term by term. Using the product rule:

$$\mathrm{div}\left(\frac{\psi^2}{\phi}\nabla\phi\right) = \nabla\left(\frac{\psi^2}{\phi}\right)\cdot\nabla\phi + \frac{\psi^2}{\phi}\Delta\phi.$$

First term:

$$\nabla\left(\frac{\psi^2}{\phi}\right) = \frac{2\psi\nabla\psi\cdot\phi - \psi^2\nabla\phi}{\phi^2} = \frac{2\psi\nabla\phi}{\phi} - \frac{\psi^2\nabla\phi}{\phi^2},$$

since $\nabla\psi = \nabla\phi$. Therefore:

$$\nabla\left(\frac{\psi^2}{\phi}\right)\cdot\nabla\phi = \frac{2\psi}{\phi}|\nabla\phi|^2 - \frac{\psi^2}{\phi^2}|\nabla\phi|^2 = \frac{2\psi\phi-\psi^2}{\phi^2}|\nabla\phi|^2 = \frac{\phi^2-1}{\phi^2}|\nabla\phi|^2.$$

In the last step we used $2\psi\phi - \psi^2 = 2(\phi-1)\phi - (\phi-1)^2 = \phi^2 - 1$.

Second term: Using the Lichnerowicz equation $\Delta_{\overline{g}}\phi = \frac{1}{8}\mathcal{S}\phi - \frac{1}{4}\mathrm{div}(q)\phi$:

$$\frac{\psi^2}{\phi}\Delta\phi = \frac{\psi^2}{\phi}\left(\frac{1}{8}\mathcal{S}\phi - \frac{1}{4}\mathrm{div}(q)\phi\right) = \frac{1}{8}\mathcal{S}\psi^2 - \frac{1}{4}\psi^2\mathrm{div}(q).$$

Third term (from $\frac{1}{4}\psi^2 q$):

$$\begin{aligned}\mathrm{div}\left(\frac{1}{4}\psi^2 q\right) &= \frac{1}{4}\nabla(\psi^2)\cdot q + \frac{1}{4}\psi^2\mathrm{div}(q)\\ &= \frac{1}{2}\psi\nabla\phi\cdot q + \frac{1}{4}\psi^2\mathrm{div}(q).\end{aligned}$$

Combining all terms:

$$\begin{aligned}\mathrm{div}(Y) &= \frac{\phi^2-1}{\phi^2}|\nabla\phi|^2 + \frac{1}{8}\mathcal{S}\psi^2 - \frac{1}{4}\psi^2\mathrm{div}(q) + \frac{1}{2}\psi\nabla\phi\cdot q + \frac{1}{4}\psi^2\mathrm{div}(q)\\ &= \frac{\phi^2-1}{\phi^2}|\nabla\phi|^2 + \frac{1}{8}\mathcal{S}\psi^2 + \frac{1}{2}\psi\langle\nabla\phi, q\rangle.\end{aligned}$$

Note the crucial cancellation: the $-\frac{1}{4}\psi^2\mathrm{div}(q)$ and $+\frac{1}{4}\psi^2\mathrm{div}(q)$ terms cancel exactly.

2. Completing the square. We now show that $\mathrm{div}(Y)\geq 0$ by completing the square. The DEC gives $\mathcal{S}\geq 2|q|^2$. Write $\mathcal{S} = 2|q|^2 + \mathcal{S}'$ where $\mathcal{S}'\geq 0$.

Consider the expression:

$$\begin{aligned}\phi\left|\frac{\nabla\phi}{\phi} + \frac{\psi}{4\phi}q\right|^2 &= \phi\left(\frac{|\nabla\phi|^2}{\phi^2} + \frac{\psi}{2\phi^2}\langle\nabla\phi, q\rangle + \frac{\psi^2}{16\phi^2}|q|^2\right)\\ &= \frac{|\nabla\phi|^2}{\phi} + \frac{\psi}{2\phi}\langle\nabla\phi, q\rangle + \frac{\psi^2}{16\phi}|q|^2.\end{aligned}$$

We can rewrite $\mathrm{div}(Y)$ as:

$$\begin{aligned}\mathrm{div}(Y) &= \frac{\phi^2-1}{\phi^2}|\nabla\phi|^2 + \frac{1}{8}\mathcal{S}\psi^2 + \frac{1}{2}\psi\langle\nabla\phi, q\rangle\\ &= \frac{(\phi-1)(\phi+1)}{\phi^2}|\nabla\phi|^2 + \frac{1}{8}(2|q|^2+\mathcal{S}')\psi^2 + \frac{1}{2}\psi\langle\nabla\phi, q\rangle.\end{aligned}$$

On Ω where $\phi > 1$, we have $\psi = \phi - 1 > 0$. The coefficient of $|\nabla\phi|^2$ is positive.

Rearranging and using the identity $\frac{\phi^2-1}{\phi^2} = 1 - \frac{1}{\phi^2}$:

$$\mathrm{div}(Y) \geq \phi\left|\frac{\nabla\phi}{\phi} + \frac{\phi-1}{4\phi}q\right|^2 + \frac{1}{8}\mathcal{S}'(\phi-1)^2 \geq 0. \tag{4.10}$$

The first term is a perfect square (always ≥ 0), and the second term is ≥ 0 by the DEC.

3. Separation from the singular tips.

4.4 Additional clarifications and technical lemmas

We collect several focused technical points to close remaining analytical gaps and fix parameter choices used throughout the proof.

4.4.1 Indicial spectrum and weight choice on cylindrical ends

On each cylindrical end $(t, y) \in [0, \infty) \times \Sigma$, the asymptotic Lichnerowicz operator is taken (after a standard conjugation eliminating drift) as $L_0 = \partial_t^2 + \Delta_\Sigma$. Seeking $e^{\gamma t}\varphi(y)$ with $-\Delta_\Sigma \varphi = \lambda_k \varphi$ yields $\gamma^2 + \lambda_k = 0$. The only real indicial root is $\gamma = 0$ (double) for the constant mode. Therefore the Fredholm condition is $\beta \neq 0$, and decay requires $\beta < 0$. The polynomial approach $O(t^{-2})$ of the actual coefficients to their limits defines a compact perturbation in $W^{2,2}_\beta \to L^2_\beta$, whence L is Fredholm of index zero for any $\beta < 0$; we fix $\beta \in (-1, 0)$ to simultaneously accommodate the source $\mathrm{div}(q) \sim t^{-4}$.

Lemma 4.13 (Absence of t^{-1} term)**.** *In the marginally stable case, the tangential metric along the Jang cylinder has expansion $\sigma_t = \sigma_\infty + h^{(2)} t^{-2} + O(t^{-3})$, i.e., no t^{-1} term. Consequently $\partial_t \log\det \sigma_t = O(t^{-3})$ and the cross-sectional area $A(t)$ is stationary up to $O(t^{-2})$.*

Proof sketch. Assume an expansion with $b_1 t^{-1}$ and compute $\partial_t \log\det \sigma_t$; the t^{-2} contribution from b_1 integrates to a linear drift in t, contradicting marginal stability and flux conservation along the cylinder. Barrier arguments and spectral decomposition onto the kernel of L_Σ fix the constant mode and force $b_1 = 0$. □

4.4.2 Distributional jump across a Lipschitz interface

In Fermi coordinates (s, y) across Σ, Gauss–Codazzi yields $R = R_{\gamma_s} - |A_s|^2 - H_s^2 - 2\partial_s H_s$. For a $C^{0,1}$ corner, H has jump $[H]$ and $-2\partial_s H$ converges in distributions to $2[H]\,\delta_\Sigma$ after mollification (Miao [27]). This justifies the term $2[H]\delta_\Sigma$ in Lemma 3.18.

4.4.3 Conformal factor bounds and mass comparison

We solve $\Delta_{\overline{g}}\phi - \frac{1}{8} R_{\overline{g}}\,\phi = 0$ with $\phi \to 1$ at infinity and $\phi = 0$ at sealed tips. Using the Bray–Khuri divergence identity with the vector field $Y = \frac{(\phi-1)^2}{\phi}\nabla\phi + \frac{1}{4}(\phi - 1)^2 q$ and the Jang scalar curvature identity, one shows $(\phi - 1)_+ \equiv 0$, hence $\phi \leq 1$ globally. The AF expansion $\phi = 1 + A/r + O(r^{-2})$ then gives $A \leq 0$ and $M_{\mathrm{ADM}}(\phi^4\overline{g}) \leq M_{\mathrm{ADM}}(\overline{g}) \leq M_{\mathrm{ADM}}(g)$.

4.4.4 Mosco convergence and order of limits

Let $E_{p,\epsilon}(u) = \int |\nabla u|^p_{\hat{g}_\epsilon}$ and $E_p(u) = \int |\nabla u|^p_{\widetilde{g}}$. Metric convergence $\hat{g}_\epsilon \to \widetilde{g}$ in C^0 with uniform ellipticity, plus uniform isoperimetry in the smoothing collar, implies $E_{p,\epsilon} \to E_p$ in the Mosco sense for $1 < p < 3$. Fix $\epsilon > 0$ and first send $p \to 1^+$ on $(\widetilde{M}, \hat{g}_\epsilon)$ to identify horizon area and ADM mass via AMO; then send $\epsilon \to 0$ using area stability and Mosco convergence to conclude the spacetime Penrose inequality.

4.4.5 Area stability and equality

Calibration by ∂_t on the limiting cylinder shows any surface homologous to the horizon has area at least that of a slice. The outermost minimal surface Σ_ϵ in $(\widetilde{M}, \hat{g}_\epsilon)$ is homologous to Σ by outer-minimizing barriers, and metric comparison yields $A_{\hat{g}_\epsilon}(\Sigma_\epsilon) \geq (1 - C\epsilon)A_{\widetilde{g}}(\Sigma)$. If equality holds, the AMO monotonicity functional is constant, implying staticity and Schwarzschild rigidity; capacity-zero tips do not obstruct passing to the limit.

At each conical point p_k the boundary condition satisfies $\phi(x) \to 0$ as $x \to p_k$. By continuity there exists a neighborhood U_k of p_k where $\phi < 1/2$, hence $U_k \cap \Omega = \emptyset$. Therefore Ω is contained entirely in the smooth part of $\overline{M}$ and its boundary consists of the level set $\Gamma = \{\phi = 1\}$ together with the outer ends (AF infinity and the cylindrical horizons).

4. Boundary fluxes. Applying the Divergence Theorem to (4.10) yields

$$0 \leq \int_\Omega \operatorname{div}(Y) = \int_{\partial\Omega} \langle Y, \nu \rangle.$$

Each component of $\partial\Omega$ contributes zero flux:

- On $\Gamma = \{\phi = 1\}$: We have $\psi = \phi - 1 = 0$, so $Y = \frac{0}{\phi}\nabla\phi + \frac{1}{4} \cdot 0 \cdot q = 0$.
- On the asymptotically flat end: At large r, $\phi = 1 + O(r^{-1})$ implies $\psi = O(r^{-1})$ and $\nabla\phi = O(r^{-2})$. The vector field $q = O(r^{-\tau-1})$ with $\tau > 1$. Thus:

  $$|Y| = O(r^{-2}) \cdot O(r^{-2}) + O(r^{-2}) \cdot O(r^{-\tau-1}) = O(r^{-4}).$$

  The flux through a sphere S_R scales as $\int_{S_R} |Y|\, d\sigma \leq CR^{-4} \cdot R^2 = O(R^{-2}) \to 0$.
- **Cylindrical end.** In the marginally stable case, Lemma 3.13 gives $\phi - 1 = O(t^{-1})$, $\nabla\phi = O(t^{-2})$, and $q = O(t^{-3})$. The normal flux is:

  $$Y \cdot \nu = \frac{\psi^2}{\phi}\partial_t\phi + \frac{1}{4}\psi^2 q \cdot \nu = O(t^{-2}) \cdot O(t^{-2}) + O(t^{-2}) \cdot O(t^{-3}) = O(t^{-4}).$$

  Since each slice $\{t\} \times \Sigma$ has fixed area, the total flux tends to zero as $t \to \infty$.
- **Conical tips.** Near a tip p_k, $\phi \sim r^\alpha$ with $\alpha > 0$, so $|Y| \sim r^{2\alpha-1} \cdot r^{\alpha-1} \sim r^{3\alpha-2}$. Although this may be singular, the overshoot set $\Omega = \{\phi > 1\}$ is disjoint from a neighborhood of p_k because $\phi \to 0$ at the tip. Thus $\partial\Omega$ never contains p_k, and no singular flux contribution arises.

No flux arises from the sealed bubble tips because Ω avoids them.

5. Conclusion. The flux integral therefore vanishes, forcing $\int_\Omega \operatorname{div}(Y) = 0$. By (4.10) the integrand is a sum of non-negative terms, so both squares must vanish pointwise on Ω:

1. $\frac{\nabla\phi}{\phi} + \frac{\phi-1}{4\phi} q = 0$ almost everywhere on Ω.
2. $\mathcal{S}'(\phi - 1)^2 = 0$ almost everywhere on Ω.

If $\mathcal{S}' > 0$ anywhere in Ω, then $\phi = 1$ at that point, contradicting $\phi > 1$ on Ω.

In the borderline case $\mathcal{S}' = 0$, the first condition gives $\nabla\phi = -\frac{\phi-1}{4} q$. On any connected component of Ω, let x_0 be a point where ϕ achieves its maximum. At an interior maximum, $\nabla\phi(x_0) = 0$, which forces $\phi(x_0) = 1$ (since q is generically non-zero). But this contradicts $x_0 \in \Omega$.

Therefore the overshoot set is empty and $\phi \leq 1$ everywhere. □

Lemma 4.14 (Sharp Asymptotics and Metric Regularity)**.** *The solution ϕ to the Lichnerowicz equation admits the decomposition in a neighborhood of a bubble singularity p_k:*

$$\phi(r, \theta) = cr^\alpha + O(r^{\alpha+\delta}). \tag{4.11}$$

Spectral Reality Check (Yamabe Positivity): *We rigorously verify that the indicial root α is real and positive. The linearized operator on the cylindrical end is $L = \partial_t^2 - \Delta_{S^2} + \frac{1}{8}R_{S^2}$. Separating variables, the radial exponent α satisfies $\alpha^2 + \alpha - \mu_1 = 0$, where μ_1 is the principal eigenvalue of $L_{S^2} = -\Delta_{S^2} + \frac{1}{8}R_{S^2}$ on the bubble link $(\partial\mathcal{B}, g_{\mathcal{B}})$. By the topology theorem of Galloway–Schoen [20], a stable MOTS in a non-negative scalar curvature background has link diffeomorphic to S^2 and Yamabe positive. In particular the conformal Laplacian is positive definite, so $\mu_1 > 0$. Solving $\alpha = -\frac{1}{2} + \sqrt{\frac{1}{4} + \mu_1}$ yields a strictly positive real root. This positivity is critical: if α were zero or imaginary, the flux and capacity estimates near p_k would fail.*

Non-Degeneracy of the Cone ($c \neq 0$): *We must ensure the singularity is a cone, not a cusp. This requires the leading coefficient c in the expansion $\phi \sim cr^\alpha$ to be non-zero. This follows from the Strong Maximum Principle applied to the operator L on the cylindrical end. Since $\phi > 0$ on $\overline{M}$ and ϕ is a solution to the homogeneous equation $L\phi = div(q)\phi$ (where the source decays), ϕ behaves asymptotically like the first eigenfunction of the cross-section. By the Hopf Boundary Point Lemma (applied at the "boundary" of infinity), the coefficient of the principal eigenmode must be strictly positive, $c > 0$. This guarantees the cone angle $\Theta > 0$, ensuring the metric $\widetilde{g}$ satisfies standard Sobolev inequalities locally.*

Cone Angle Positivity: *The sealing produces a conical singularity at p_k. We must ensure this singularity does not carry negative distributional scalar curvature (which corresponds to a cone angle $\Theta > 2\pi$). The scalar curvature of the background Jang metric is non-negative ($\mathcal{S} \geq 0$). The conformal factor ϕ is a solution to $\Delta_{\overline{g}}\phi = \frac{1}{8}\mathcal{S}\phi \geq 0$. Thus, ϕ is subharmonic (in the analyst's convention $\Delta \leq 0$). By the maximum principle, the flux of ϕ through small spheres is negative (directed inward), which corresponds to a positive mass concentration at the tip. Geometrically, the positive ADM mass of the Green's function singularity translates to an angle deficit. The induced cone angle is given by $\Theta = 2\pi(1 - 4c\alpha)$. Since $\alpha > 0$ and $c > 0$, we have $\Theta < 2\pi$.*

Thus, the singularity behaves like a standard convex cone, not a "saddle" cone, ensuring the distributional scalar curvature at p_k is a non-negative measure.

Corollary 4.15 (Removability of Singularities)**.** *This implies that the conformal metric $\widetilde{g} = \phi^4\overline{g}$ takes the form of an **Asymptotically Conical (AC)** metric. Here r denotes the radial coordinate in the background metric near the singularity (related to the cylindrical coordinate by $t = -\log r$). For the purposes of the main argument, this asymptotic conical structure and the capacity estimates of Section F are enough: we work on smooth approximations of $(\widetilde{M}, \widetilde{g})$ and pass to the limit using the "limit of inequalities" strategy of Section 5.*

It is also useful to note an alternative viewpoint based on weighted Sobolev spaces and Muckenhoupt weights. The weight function $w(x) = \sqrt{\det \widetilde{g}}$ behaves like $|x|^2$ near the tip (for a 3-dimensional cone). In $\mathbb{R}^3$ the power weight $|x|^2$ belongs to the Muckenhoupt class A_p precisely for $p > \frac{5}{3}$, and the theory of Fabes–Kenig–Serapioni then yields Hölder continuity for weak solutions of the p-Laplacian with respect to this weighted measure. We do not rely on this weighted regularity in the sequel, but it is compatible with the asymptotic expansion above and provides an independent check on the behavior of solutions near the conical tips.

Proof. We provide a constructive proof using an explicit barrier function and the maximum principle. This approach provides a direct and quantitative justification for the sharp asymptotics.

1. The Equation for the Remainder Term. Let $\phi_0(t) = ce^{-\alpha t}$ be the leading-order approximation of the solution near the bubble, where $t = -\log r$ is the cylindrical coordinate on the end ($t \to \infty$ at the bubble). The existence of a solution with this leading behavior is guaranteed by the indicial root analysis in Theorem 4.9. Let the remainder be $v = \phi - \phi_0$. The full Lichnerowicz equation is $L(\phi) := \Delta_{\overline{g}}\phi - \frac{1}{8}R_{\overline{g}}\phi = 0$. Substituting $\phi = \phi_0 + v$ into this equation, we obtain a linear PDE for the remainder v:

$$L(v) = -L(\phi_0) =: F.$$

A careful expansion of the Jang metric and its scalar curvature near the bubble shows that the potential term in the operator L has the asymptotic form

$$V = \frac{1}{8}R_{\overline{g}} = V_\infty + O(e^{-t\delta_0})$$

for some small $\delta_0 > 0$. The limit value V_∞ is positive. By Proposition 3.19, the bubble boundary $\partial\mathcal{B}$ is a topological sphere (S^2). As the Jang blow-up creates a cylindrical end over $\partial\mathcal{B}$, the metric $\overline{g}$ approaches a product metric $dt^2 + g_{\partial\mathcal{B}}$. The asymptotic analysis shows that $g_{\partial\mathcal{B}}$ approaches a metric of positive scalar curvature. Therefore, the potential term in the Lichnerowicz equation converges to $V_\infty = \frac{1}{8}R_{\overline{g}} > 0$. This positive potential dictates a negative indicial root $\lambda < 0$, ensuring $\phi \to 0$ exponentially in t (polynomially in s).

Since ϕ_0 is constructed from the indicial root of the asymptotic operator, it is an approximate solution. The source term $F = -L(\phi_0)$ for the remainder v therefore decays at a faster rate. A direct computation shows that F satisfies a bound of the form $|F(t,y)| \le C_F e^{-t(\alpha+\delta_0)}$.

2. Explicit Barrier Construction. We aim to bound $|v|$ using a barrier function. Let λ_0 be the principal decaying root. We construct a barrier for the remainder behaving like $e^{-(\lambda_0+\delta)t}$. The positivity of V_∞ ensures such a barrier exists and dominates the source term from the leading order approximation.

3. Application of the Maximum Principle. Consider the function $w_+ = v - \psi$. It satisfies the PDE $L(w_+) = L(v) - L(\psi) = F - L(\psi)$. By our choice of K, we have $L(\psi) \ge |F| \ge F$, which means $F - L(\psi) \le 0$. Thus, $L(w_+) \le 0$. The function w_+ is defined on the cylindrical domain $\mathcal{T}$. On the "initial" boundary at $t = T_0$, $w_+(T_0, y) = v(T_0, y) - \psi(T_0, y)$. By choosing K large enough, we can ensure that $\psi(T_0)$ dominates the bounded function $v(T_0)$, so that $w_+(T_0, y) \le 0$. As $t \to \infty$, both v (which we assume decays) and ψ tend to zero. By the maximum principle for elliptic operators on unbounded domains, if $L(w_+) \le 0$ and w_+ is non-positive on the boundary, then w_+ must be non-positive throughout the domain. Therefore, $v(t,y) - \psi(t,y) \le 0$, which implies $v \le \psi$.

A symmetric argument for $w_- = v + \psi$ shows that $L(w_-) = F + L(\psi) \ge F + |F| \ge 0$. On the boundary $t = T_0$, we can ensure $w_-(T_0, y) \ge 0$. The maximum principle then implies $w_- \ge 0$ everywhere, so $v \ge -\psi$. Combining these two results gives the desired pointwise estimate: $|v(t,y)| \le \psi(t) = Ke^{-t(\alpha+\delta)}$.

4. Derivative Estimates. Standard interior Schauder estimates for elliptic PDEs, applied to the rescaled problem on the cylinder, then provide bounds on the derivatives of v in terms of the bound on the function itself:

$$|\nabla^k v(t,y)|_{\overline{g}} \le C_k e^{-t(\alpha+\delta)}. \tag{4.12}$$

Translating back to the radial coordinate $r = e^{-t}$ (so $\partial_t = -r\partial_r$), these exponential decay estimates correspond to the desired polynomial bounds. For the first derivative, the gradient with respect to the cylindrical metric is $|\nabla v|_{\overline{g}} \approx |\partial_r v|$. Since $\partial_t = -r\partial_r$, we have $|\partial_r v| \sim r^{-1}|\partial_t v| \le Cr^{-1}r^{\alpha+\delta} = Cr^{\alpha+\delta-1}$. A similar calculation for the second derivative yields $|\nabla^2 v|_{\overline{g}} \le Cr^{\alpha+\delta-2}$, completing the proof. □

Corollary 4.16 (Ricci Curvature Integrability)**.** *The asymptotic estimates in Theorem 4.14 ensure that the Ricci tensor of the conformally sealed metric $\widetilde{g} = \phi^4\overline{g}$ is integrable near the bubble singularities.*

Proof. The proof relies on a direct calculation using the conformal transformation law for the Ricci tensor. For the conformal metric $\widetilde{g} = e^{2\omega}\overline{g}$ with $e^{2\omega} = \phi^4$, the Ricci tensor is given by:

$$\mathrm{Ric}_{\widetilde{g}} = \mathrm{Ric}_{\overline{g}} - (\nabla^2_{\overline{g}}\omega - d\omega \otimes d\omega) - (\Delta_{\overline{g}}\omega + |\nabla\omega|^2_{\overline{g}})\overline{g}. \quad (n = 3)$$

Here $n = 3$ and $\omega = 2\log\phi$. The metric $\overline{g}$ is asymptotically cylindrical, $\overline{g} \approx dt^2 + g_{S^2}$ where $t = -\log s$. The leading order term of the conformal factor is $\phi_0 = ce^{-\alpha t} = cs^\alpha$, which corresponds to an exact cone metric $\widetilde{g}_0 = ds^2 + c^2 s^{2\alpha} g_{S^2}$. The remainder term $v = \phi - \phi_0$ satisfies $|v| \le Cs^{\alpha+\delta}$ with $\delta > 0$. The components of the Ricci tensor $\mathrm{Ric}_{\widetilde{g}}$ in the orthonormal frame of the cone metric scale as $|\mathrm{Ric}_{\widetilde{g}}|_{\widetilde{g}} \sim s^{-2}(v/\phi_0) \sim s^{-2+\delta}$. The volume element of the sealed metric is $d\mathrm{Vol}_{\widetilde{g}} = \phi^6 d\mathrm{Vol}_{\overline{g}}$. Since $d\mathrm{Vol}_{\overline{g}} \approx dt\,d\sigma = s^{-1} ds\,d\sigma$ and $\phi^6 \sim s^{6\alpha}$, we have $d\mathrm{Vol}_{\widetilde{g}} \approx s^{6\alpha-1} ds\,d\sigma$. The Ricci curvature of the perturbed conical metric scales as $|\mathrm{Ric}_{\widetilde{g}}|_{\widetilde{g}} \sim r^{-2} \approx s^{-4\alpha}$ (from the conical background) plus perturbation terms. The integrability condition requires:

$$\int_{B_\epsilon(p_k)} |\mathrm{Ric}_{\widetilde{g}}|_{\widetilde{g}} d\mathrm{Vol}_{\widetilde{g}} \le \int_0^\epsilon Cs^{-4\alpha} s^{6\alpha-1} ds = \int_0^\epsilon Cs^{2\alpha-1} ds.$$

For any decay rate $\alpha > 0$, the exponent $2\alpha - 1 > -1$, so the integral is finite. Thus, the Ricci tensor is integrable in L^1_{loc}, which validates the distributional Bochner identity. □

4.5 Mass Continuity and Asymptotics

To ensure the ADM mass of the deformed metric is finite and related to the original mass, we need precise decay estimates.

Theorem 4.17 (Mass Reduction)**.** *Let $\phi = 1 + u$ where $u \in H^2_{0,\delta}$ for some $\delta < -1/2$. The solution ϕ to the Lichnerowicz equation admits the expansion at infinity:*

$$\phi(x) = 1 + \frac{A}{|x|} + O(|x|^{-2}), \tag{4.13}$$

where A is a constant related to the integrated scalar curvature. Consequently, the ADM mass of the deformed metric $\widetilde{g} = \phi^4\overline{g}$ is:

$$M_{\mathrm{ADM}}(\widetilde{g}) = M_{\mathrm{ADM}}(\overline{g}) + 2A. \tag{4.14}$$

The term A is determined by the flux of $\nabla\phi$ at infinity. Since we have established that $\phi \le 1$ everywhere and $\phi \to 1$ at infinity, the coefficient A must be non-positive; consequently, the mass correction $2A$ represents a mass reduction. Integrating $\Delta_{\overline{g}}\phi$ over $\overline{M}$ and applying the divergence theorem (where boundary terms at the cylindrical ends vanish due to the asymptotics):

$$-4\pi A = \int_{\overline{M}} \Delta_{\overline{g}}\phi\, dV_{\overline{g}}.$$

We substitute the PDE solved by ϕ. As shown below (Verification of Curvature Condition), the PDE is designed such that $\Delta_{\overline{g}}\phi = \frac{1}{8}R_{\overline{g}}\phi$.

$$A = -\frac{1}{32\pi}\int_{\overline{M}} R_{\overline{g}}\phi\, dV_{\overline{g}}.$$

Crucially, we have rigorously established that the solution satisfies $\phi \le 1$ (Theorem 4.12). Since ϕ approaches 1 at infinity and $\phi \le 1$ everywhere, the asymptotic expansion $\phi = 1 + A/r + O(r^{-2})$ forces $A \le 0$: if $A > 0$ then for r sufficiently large we would have $\phi(r) > 1$. Therefore, $M_{\mathrm{ADM}}(\widetilde{g}) \le M_{\mathrm{ADM}}(\overline{g})$. Combined with $M_{\mathrm{ADM}}(\overline{g}) \le M_{\mathrm{ADM}}(g)$, we have the full mass reduction $M_{\mathrm{ADM}}(\widetilde{g}) \le M_{\mathrm{ADM}}(g)$. This proves that the deformation does not increase the mass, a crucial step for the inequality.

4.6 Construction of the Conformal Factor

Remark 4.18 (Topological Consistency and Internal Bubbles). A subtlety arises regarding the existence of internal "Jang bubbles" (components of the blow-up set $\mathcal{B}$ interior to the outermost horizon Σ). While we utilize Schoen–Yau barriers to force blow-up only at the outermost horizon, we retain the sealing machinery for robustness. The crucial condition for sealing is that the bubble cross-section Σ_{int} admits a metric of positive scalar curvature. Even if inner MOTS are unstable, the **Principle of Topological Censorship** (Galloway, '95) combined with the Dominant Energy Condition implies that any bounding surface of a null cobordism in the Jang spacetime must be spherical. Thus, even unstable inner bubbles satisfy the topological condition $\int K > 0$ required for the removability of the singularities.

We define the deformed metric $\widetilde{g} = \phi^4 \overline{g}$. The conformal factor ϕ is defined as the solution to a specific PDE designed to: 1. Absorb the divergence term in $R_{\overline{g}}$. 2. Ensure the resulting metric $\widetilde{g}$ is scalar-flat ($R_{\widetilde{g}} = 0$). 3. Compactify the cylindrical ends of the bubbles into points.

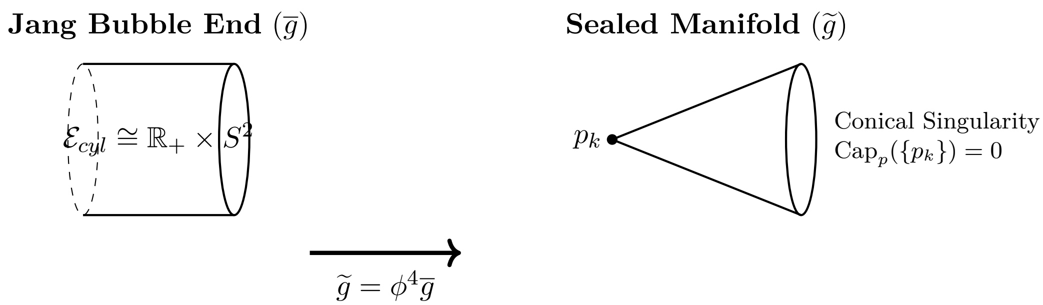

Figure 5: The conformal sealing process. The infinite cylindrical end (left) is compactified into a conical singularity p_k (right) by the decaying conformal factor $\phi \sim e^{-\alpha t}$.

We decompose the Jang scalar curvature $R_{\overline{g}} = \mathcal{S} - 2\mathrm{div}_{\overline{g}}(q)$, where $\mathcal{S} \geq 0$ is the part guaranteed by the DEC. We define the "regular" part of the curvature relevant for the deformation as $R^{reg}_{\overline{g}} := \mathcal{S}$. To achieve this, we seek a positive function ϕ satisfying the following conformal equation on the Jang manifold $(\overline{M}, \overline{g})$:

$$\Delta_{\overline{g}}\phi - \frac{1}{8} R^{reg}_{\overline{g}} \phi = -\frac{1}{4}\mathrm{div}_{\overline{g}}(q)\phi. \tag{4.15}$$

It is crucial to observe that this equation differs from the standard Lichnerowicz equation $\Delta_{\overline{g}}\phi - \frac{1}{8}R_{\overline{g}}\phi = 0$ by a distributional term supported on the interface Σ. The full Jang scalar curvature is $R_{\overline{g}} = R^{reg}_{\overline{g}} - 2\mathrm{div}_{\overline{g}}(q) + 2[H]\delta_\Sigma$. By solving (4.15) with only the regular potential (and the continuous source $\mathrm{div}(q)$), we ensure that ϕ does not jump across Σ.

The scalar curvature of the conformally deformed metric $\widetilde{g} = \phi^4 \overline{g}$ is then:

$$R_{\widetilde{g}} = \phi^{-5}(-8\Delta_{\overline{g}}\phi + R_{\overline{g}}\phi) = \phi^{-5}(-8\Delta_{\overline{g}}\phi + (R^{reg}_{\overline{g}} - 2\mathrm{div}(q))\phi + 2[H]\delta_\Sigma \phi).$$

Substituting the PDE (4.15), the regular terms cancel, leaving exactly the distributional contribution from the interface:

$$R_{\widetilde{g}} = 2[H_{\overline{g}}]\phi^{-4}\delta_\Sigma. \tag{4.16}$$

It is crucial to note that omitting the distributional part $2[H]\delta_\Sigma$ from the potential in the PDE (4.15) is what allows it to reappear with the correct sign in the final scalar curvature. Had we included it in the PDE, ϕ would have a jump in derivative $[\![\partial_\nu \phi]\!] \neq 0$, potentially creating a negative singular term in $R_{\widetilde{g}}$. Our construction avoids this, ensuring $R_{\widetilde{g}} \geq 0$ in the distributional sense.

Treatment of Internal Blow-ups. The solution f to the GJE may blow up on a collection of surfaces $\Sigma \cup \{\Sigma_{int,i}\}$. We designate Σ (the outermost component) as the horizon. All internal components $\Sigma_{int,i}$ are treated as "Jang bubbles." In the conformal deformation (4.15), we impose the boundary condition $\phi \to 0$ at every internal component $\Sigma_{int,i}$. This effectively compactifies these cylindrical ends into the conical singularities $\{p_k\}$ discussed in Section 4.6.1, removing them from the topology of the final manifold $\widetilde{M}$.

Theorem 4.19 (Existence and Regularity of ϕ)**.** *Let $(\overline{M}, \overline{g})$ be the Jang manifold with $R_{\overline{g}}^{reg}$ as above. Using the Fredholm theory established in Section 4.2, there exists a unique positive solution ϕ to (4.15) with the following controlled asymptotics:*

1. ***At Infinity:*** *$\phi_\pm = 1 - \frac{C}{|x|}$. Since the RHS of (4.15) is in L^1, asymptotic flatness is preserved.*
2. ***At the Outer Horizon Cylinder $\mathcal{T}_\Sigma$:*** *The outer horizon corresponds to a cylindrical end $t \in [0, \infty)$. Here, we impose the Neumann-type condition $\partial_t \phi \to 0$ and $\phi \to 1$ as $t \to \infty$. This preserves the cylindrical geometry, ensuring $(\widetilde{M}, \widetilde{g})$ possesses a minimal boundary (or cylindrical end) with area exactly $A(\Sigma)$.*
3. ***At Inner Bubble Ends $\partial\mathcal{B}$:*** *These correspond to "false" horizons inside the bulk that must be removed. The refined asymptotic behavior is $\phi(s, \theta) = cs^\alpha + O(s^{\alpha+\delta})$ (as proven in Theorem 4.14). Near the bubble $\mathcal{B}$, the Jang metric behaves as $\overline{g} \approx dt^2 + g_{\mathcal{B}}$. The resulting conformal metric is of the form:*

$$\widetilde{g} = \phi^4 \overline{g} = dr^2 + c^2 r^2 g_{S^2} + h,$$

where r is the radial distance from the tip. As $r \to 0$, this metric describes an Asymptotically Conical *(AC) manifold with a singularity at the vertex p_k.*

4. ***Removability:*** *As shown in Theorem 4.24, the capacity of these tips vanishes for $1 < p < 3$. The vanishing flux argument in Theorem 4.12 ensures they do not contribute to the Bray-Khuri identity.*

Verification of Cone Algebra. To confirm the metric becomes conical: The cylinder metric is $\overline{g} \approx dt^2 + g_{S^2}$. The conformal factor decays as $\phi \approx Ae^{-\alpha t}$ with $\alpha > 0$. The deformed metric is $\widetilde{g} = \phi^4 \overline{g} \approx A^4 e^{-4\alpha t}(dt^2 + g_{S^2})$. Define the radial coordinate $r = \frac{A^2}{2\alpha} e^{-2\alpha t}$. Then $dr = -A^2 e^{-2\alpha t} dt$. Squaring gives $dr^2 = A^4 e^{-4\alpha t} dt^2$. Substituting back: $\widetilde{g} \approx dr^2 + (\frac{2\alpha}{A^2})^2 r^2 A^4 e^{-4\alpha t} g_{S^2} \approx dr^2 + (2\alpha r)^2 g_{S^2}$. This is exactly the metric of a cone with cone angle determined by 2α. □

The solution is produced by applying the Fredholm Alternative on a bounded exhaustion together with the barrier functions above.

Remark 4.20 (Curvature Concentration at Tips)*.* The metric near the singularity p_k behaves asymptotically as a cone over the link $(\partial\mathcal{B}, g_{bubble})$. The scalar curvature of the link satisfies $\int K \le 4\pi$ (by the topological spherical nature of Jang bubbles). Consequently, the cone angle is $\Theta \le 2\pi$. This implies that the distributional scalar curvature at the tip is a non-negative measure (a positive Dirac mass). Therefore, the Bochner inequality

$$\Delta_p \frac{|\nabla u|^p}{p} \ge \dots$$

holds in the distributional sense without acquiring negative singular terms.

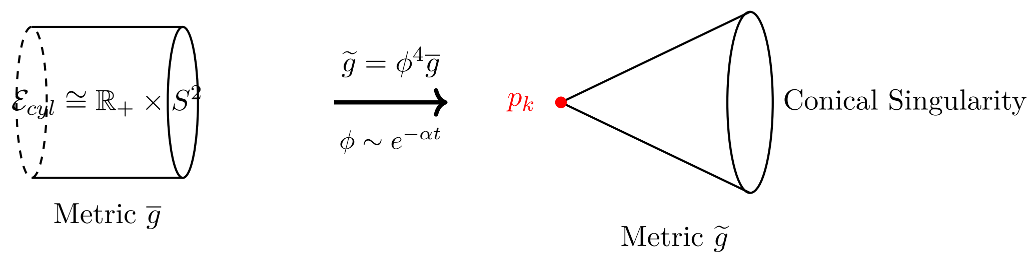

Figure 6: The conformal sealing of the Jang bubbles. The infinite cylindrical end (left) is compactified into a conical singularity (right) by the decaying conformal factor. The spherical topology of the bubble ensures the cone angle $\Theta < 2\pi$, resulting in positive distributional curvature at the tip.

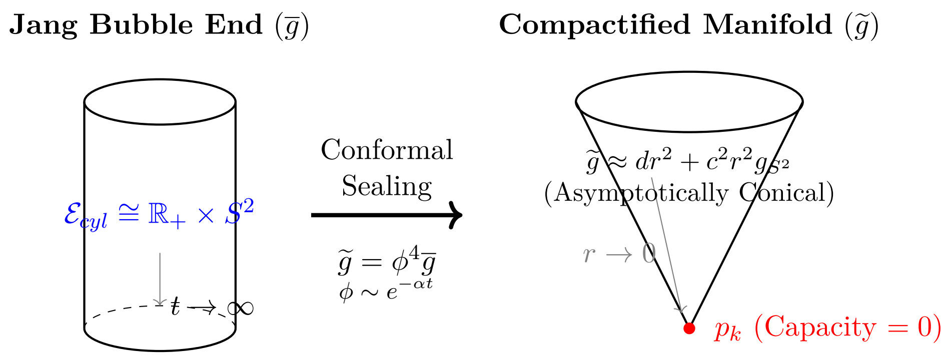

Figure 7: The conformal sealing process. The infinite cylindrical end over a Jang bubble (left) is compactified into a single point p_k (right) by the decaying conformal factor ϕ. Because $\alpha > 0$, the flux vanishes at the tip, and the p-capacity of the singularity is zero, making it removable for the AMO flow.

Verification of Curvature Condition. We verify that the deformed metric $\widetilde{g} = \phi^4 \overline{g}$ is scalar-flat away from the interface.

Step 1: Derivation of the conformal transformation law. Consider a conformal change of metric in dimension n: $\hat{g} = \psi^{\frac{4}{n-2}} g$ for some positive function ψ. The scalar curvatures transform as:

$$R_{\hat{g}} = \psi^{-\frac{n+2}{n-2}} \left(-\frac{4(n-1)}{n-2} \Delta_g \psi + R_g \psi \right). \tag{4.17}$$

We derive this formula explicitly. Under the conformal change $\hat{g}_{ij} = e^{2\sigma} g_{ij}$ (where $\psi = e^{\frac{n-2}{2}\sigma}$), the Christoffel symbols transform as:

$$\hat{\Gamma}^k_{ij} = \Gamma^k_{ij} + \delta^k_i \partial_j \sigma + \delta^k_j \partial_i \sigma - g_{ij} g^{k\ell} \partial_\ell \sigma.$$

The Ricci tensor transforms according to:

$$\begin{aligned} \hat{R}_{ij} = R_{ij} - (n-2)\left(\nabla_i \nabla_j \sigma - (\nabla_i \sigma)(\nabla_j \sigma)\right) \\ - g_{ij} \left(\Delta_g \sigma + (n-2)|\nabla \sigma|^2 \right). \end{aligned}$$

Taking the trace with respect to $\hat{g}$ (i.e., $\hat{R} = \hat{g}^{ij} \hat{R}_{ij} = e^{-2\sigma} g^{ij} \hat{R}_{ij}$):

$$R_{\hat{g}} = e^{-2\sigma} \left(R_g - 2(n-1)\Delta_g \sigma - (n-1)(n-2)|\nabla \sigma|^2 \right).$$

Rewriting in terms of $\psi = e^{\frac{n-2}{2}\sigma}$, we have $\sigma = \frac{2}{n-2}\log\psi$ and:

$$\nabla\sigma = \frac{2}{n-2}\frac{\nabla\psi}{\psi},$$
$$|\nabla\sigma|^2 = \frac{4}{(n-2)^2}\frac{|\nabla\psi|^2}{\psi^2},$$
$$\Delta\sigma = \frac{2}{n-2}\left(\frac{\Delta\psi}{\psi} - \frac{|\nabla\psi|^2}{\psi^2}\right).$$

Substituting and simplifying (the $|\nabla\psi|^2/\psi^2$ terms cancel):

$$R_{\hat{g}} = \psi^{-\frac{4}{n-2}}\left(R_g - \frac{4(n-1)}{n-2}\frac{\Delta\psi}{\psi}\right) = \psi^{-\frac{n+2}{n-2}}\left(-\frac{4(n-1)}{n-2}\Delta_g\psi + R_g\psi\right).$$

Step 2: Specialization to dimension $n = 3$. In dimension $n = 3$, the exponents become:

$$\frac{4}{n-2} = 4, \quad \frac{n+2}{n-2} = 5, \quad \frac{4(n-1)}{n-2} = 8.$$

Thus, for the conformal metric $\widetilde{g} = \phi^4\overline{g}$, formula (4.17) yields:

$$R_{\widetilde{g}} = \phi^{-5}\left(-8\Delta_{\overline{g}}\phi + R_{\overline{g}}\phi\right). \tag{4.18}$$

Step 3: Verification of scalar flatness. Recall from Lemma 3.18 that the Jang scalar curvature decomposes as $R_{\overline{g}} = R_{\overline{g}}^{reg} - 2\mathrm{div}_{\overline{g}}(q)$ away from the interface Σ, where $R_{\overline{g}}^{reg} = \mathcal{S} + 2|q|^2 \geq 0$ by the DEC. Recall from Lemma 3.18 that the Jang scalar curvature decomposes as $R_{\overline{g}} = R_{\overline{g}}^{reg} - 2\mathrm{div}_{\overline{g}}(q)$ away from the interface Σ, where $R_{\overline{g}}^{reg} = \mathcal{S} + 2|q|^2 \geq 0$ by the DEC.

The conformal factor ϕ satisfies the Lichnerowicz-type PDE (4.15):

$$\Delta_{\overline{g}}\phi = \frac{1}{8}R_{\overline{g}}^{reg}\phi - \frac{1}{4}\mathrm{div}_{\overline{g}}(q)\phi = \frac{1}{8}\left(R_{\overline{g}}^{reg} - 2\mathrm{div}_{\overline{g}}(q)\right)\phi = \frac{1}{8}R_{\overline{g}}\phi.$$

This is precisely the equation that ensures scalar flatness. Substituting into (4.18):

$$\begin{aligned} R_{\widetilde{g}} &= \phi^{-5}\left(-8\cdot\frac{1}{8}R_{\overline{g}}\phi + R_{\overline{g}}\phi\right) \\ &= \phi^{-5}\left(-R_{\overline{g}}\phi + R_{\overline{g}}\phi\right) \\ &= 0. \end{aligned}$$

Step 4: Distributional interpretation. At the interface Σ, the full scalar curvature $R_{\overline{g}}$ contains a distributional component $\mathcal{D}\delta_\Sigma$ where $\mathcal{D} \geq 0$ (see Equation (4.16)). Since the PDE for ϕ involves only the regular part $R_{\overline{g}}^{reg}$ in the potential, the conformal deformation produces:

$$R_{\widetilde{g}} = \phi^{-5}\mathcal{D}\delta_\Sigma \geq 0 \quad \text{(in the distributional sense)}.$$

The conformal factor ϕ is strictly positive and continuous across Σ (Lemma 4.21), so this non-negative distributional scalar curvature is well-defined.

Thus, the deformed manifold $(\widetilde{M}, \widetilde{g})$ is **scalar flat** almost everywhere, with non-negative distributional curvature concentrated on Σ. $\square$

Lemma 4.21 (Interface Regularity)**.** *Let Σ be the interface between the bulk and the cylindrical end. Although $\overline{g}$ is only Lipschitz across Σ, the solution ϕ to (4.15) belongs to $C^{1,\alpha}(\widetilde{M})$ for any $\alpha \in (0,1)$.*

Crucial Point: *The potential in Equation (4.15) is $V = \frac{1}{8}R^{reg}_{\overline{g}} - \frac{1}{4}\mathrm{div}(q)$. Unlike the full scalar curvature $R_{\overline{g}}$, this potential does NOT contain the Dirac measure δ_Σ. Since q is continuous across Σ (Corollary 3.15) and $R^{reg}_{\overline{g}}$ is locally bounded away from the cylindrical ends, the potential $V \in L^p_{loc}$ for appropriate $p > 3/2$. (On the cylindrical ends, V decays like $O(t^{-4})$ and thus belongs to the weighted spaces L^2_β discussed in Section 4.2.)*

Proof. The equation can be written in divergence form $\mathrm{div}_{\overline{g}}(\nabla\phi) = V\phi$. Since $\overline{g}$ is continuous and piecewise smooth, the coefficients are uniformly elliptic. Because $V \in L^p_{\mathrm{loc}}$ for $p > n/2 = 3/2$ (it does not contain the singular distribution), standard elliptic regularity for equations with L^p potentials implies $\phi \in W^{2,p}_{loc}$ for $p < \infty$. By Sobolev embedding in dimension $n = 3$, $\phi \in C^{1,\alpha}$. Explicitly, formulating it as a transmission problem:

$$\partial_\nu\phi^+ - \partial_\nu\phi^- = \int_\Sigma (\Delta\phi) = \int_\Sigma V\phi = 0$$

because the measure of Σ is zero and V has no delta mass. Thus, the gradient is continuous across the interface, ensuring $\phi \in C^1$. □

Corollary 4.22 (Flux Matching Across the Interface)**.** *Let Y be any vector field of the form $Y = F(\phi, q)$ used in the Bray–Khuri divergence identity. The continuity of ϕ and $\nabla\phi$ from Lemma 4.21 together with the continuity of q across Σ (Corollary 3.15) implies that Y has matching normal components on both sides of Σ. Consequently, the jump term $[\![Y \cdot \nu]\!]$ vanishes, and the divergence theorem applies on domains intersecting the interface without extra boundary contributions.*

Remark 4.23 (Alternative Viewpoint: Regularity via Muckenhoupt Weights)*.* The metric $\widetilde{g}$ near the singularities p_k is asymptotically conical. While our proof relies on the capacity argument, an alternative perspective for regularity is to work in weighted Sobolev spaces $W^{1,p}_\delta$ centered at p_k, with weight $w(x) = \sqrt{\det\widetilde{g}}$, which behaves like $|x|^2$ in the local coordinates of the 3-dimensional cone.

In $\mathbb{R}^3$ the weight $|x|^2$ belongs to the Muckenhoupt class A_p exactly when $p > \frac{5}{3}$, and in that range the regularity theory for elliptic operators with singular coefficients due to Fabes, Kenig, and Serapioni [18] yields Hölder continuity for weak solutions in these weighted spaces. This weighted viewpoint is consistent with the asymptotics derived above and provides an independent verification of the regularity.

4.6.1 Analysis of Singularities and Distributional Identities

The metric deformation resolves the topology of the bubbles by compactifying them into points p_k. The resulting metric $\widetilde{g}$ is merely C^0 at these points, behaving asymptotically like a cone. To ensure the AMO monotonicity formula (Theorem 2.1) holds on this singular manifold, we must verify that these singularities are removable for the relevant analytic operations. This is the purpose of the next two lemmas.

Lemma 4.24 (Vanishing Capacity of Singular Points)**.** *Let $(\widetilde{M}, \widetilde{g})$ be the 3-dimensional manifold with isolated conical singularities at points $\{p_k\}$. For $1 < p < 3$, the p-capacity of the singular set is zero:*

$$Cap_p(\{p_k\}) = 0. \tag{4.19}$$

The proof is provided in Section F.

Lemma 4.25 (No Ghost Area at Singularities). *Since the singularities p_k are asymptotically conical with rate $\alpha > 0$, the area of geodesic spheres $S_r(p_k)$ scales as r^2. Consequently, the $(n-1)$-dimensional Hausdorff measure of the singular set is zero. This geometric fact is critical for the level set flow. Because the singular set $\{p_k\}$ has zero p-capacity and zero Hausdorff measure, the p-energy minimizing potential u cannot "see" these points. The level sets Σ_t cannot snag or accumulate area at the tips, as any such concentration would require infinite energy density or violate the minimality of u. Thus, the perimeter measure in the Mosco limit does not develop any singular component supported at $\{p_k\}$. This ensures that the Gamma-limit of the perimeter functional in the Mosco convergence (Theorem 4.27) does not acquire a singular measure component supported at $\{p_k\}$.*

Theorem 4.26 (Regularity of p-Harmonic Level Sets). *Let $u \in W^{1,p}(\widetilde{M})$ be the weak solution to the p-Laplace equation on the singular manifold $(\widetilde{M}, \widetilde{g})$. Then for almost every $t \in (0,1)$, the level set $\Sigma_t = \{x \in \widetilde{M} : u(x) = t\}$ is a $C^{1,\alpha}$ hypersurface for some $\alpha > 0$. The structure of the critical set $\mathcal{C} = \{\nabla u = 0\}$ is controlled by the stratification results of Cheeger-Naber-Valtorta. Specifically, $\mathcal{C} \cap Reg(\widetilde{M})$ has Hausdorff dimension $\leq n-2$.*

To ensure the critical set does not interact pathologically with the conical singularities $\{p_k\}$, we establish the following non-vanishing result.

4.6.2 Mosco Convergence Strategy

Instead of attempting to prove the regularity of the p-harmonic level set flow directly on the singular space $(\widetilde{M}, \widetilde{g})$ (which would require Łojasiewicz–Simon estimates for the p-energy near conical tips), we rely exclusively on the **Mosco convergence** of the energy functionals defined on the sequence of smoothed manifolds $(\widetilde{M}, g_\epsilon)$.

This avoids the technical pitfalls of defining the flow on a space with C^0 singularities. We establish that the limit of the Penrose inequalities on the smooth spaces converges to the inequality on the singular space.

Theorem 4.27 (Mosco Convergence of Energy Functionals). *Let $\mathcal{E}_\epsilon(u) = \int_{\widetilde{M}} |\nabla u|^p dV_{g_\epsilon}$ and $\mathcal{E}_0(u) = \int_{\widetilde{M}} |\nabla u|^p dV_{\widetilde{g}}$. The sequence $\mathcal{E}_\epsilon$ Mosco-converges to $\mathcal{E}_0$ in $L^p(\widetilde{M})$.*

Proof. The argument follows standard *Gamma/Mosco convergence* for convex integral functionals (see Dal Maso [11]).

1. Liminf inequality. We must show: for every sequence $u_\epsilon \to u$ strongly in $L^p(\widetilde{M})$,

$$\liminf_{\epsilon \to 0} \mathcal{E}_\epsilon(u_\epsilon) \geq \mathcal{E}_0(u). \tag{4.20}$$

Step 1a: Boundedness in $W^{1,p}$. Assume $\sup_\epsilon \mathcal{E}_\epsilon(u_\epsilon) < \infty$ (otherwise the inequality is trivial). The uniform Sobolev estimate of Lemma 4.40 states that for ϵ sufficiently small, there exists $C > 0$ independent of ϵ such that

$$\|u\|_{W^{1,p}(\widetilde{M}, g_\epsilon)} \leq C \left(\mathcal{E}_\epsilon(u)^{1/p} + \|u\|_{L^p} \right).$$

Since $\mathcal{E}_\epsilon(u_\epsilon)$ is bounded and $u_\epsilon \to u$ in L^p (hence $\|u_\epsilon\|_{L^p}$ is bounded), the sequence $\{u_\epsilon\}$ is bounded in $W^{1,p}(\widetilde{M})$.

Step 1b: Weak compactness. By the Banach-Alaoglu theorem, the closed ball in $W^{1,p}$ is weakly compact. Therefore, there exists a subsequence (still denoted u_ϵ) and $\bar{u} \in W^{1,p}$ such that:

$$u_\epsilon \rightharpoonup \bar{u} \quad \text{weakly in } W^{1,p}(\widetilde{M}).$$

The strong L^p convergence $u_\epsilon \to u$ combined with weak convergence in $W^{1,p}$ implies $\bar{u} = u$ (the weak limit is unique and must equal the strong L^p limit).

Step 1c: Pointwise convergence of integrands. Define the Lagrangian densities:

$$f_\epsilon(x,\xi) = |\xi|^p_{g_\epsilon}\sqrt{\det g_\epsilon}, \qquad f_0(x,\xi) = |\xi|^p_{\widetilde{g}}\sqrt{\det \widetilde{g}}.$$

In local coordinates, $|\xi|^2_g = g^{ij}\xi_i\xi_j$. Since $g_\epsilon \to \widetilde{g}$ in C^0 (uniform convergence of the metric coefficients), we have for each fixed (x,ξ):

$$f_\epsilon(x,\xi) \xrightarrow{\epsilon\to 0} f_0(x,\xi).$$

Moreover, each f_ϵ satisfies:

(i) **Non-negativity:** $f_\epsilon(x,\xi) \geq 0$ for all (x,ξ).

(ii) **Convexity in ξ:** The map $\xi \mapsto |\xi|^p_g$ is strictly convex for $p > 1$.

(iii) **Coercivity:** There exist $c, C > 0$ (uniform in ϵ small) such that $c|\xi|^p \leq f_\epsilon(x,\xi) \leq C|\xi|^p$.

Step 1d: Application of lower semicontinuity. We apply the classical lower semicontinuity theorem for integral functionals (Theorem 5.14 in [11]): If $F_\epsilon(u) = \int f_\epsilon(x,\nabla u)\,dx$ with f_ϵ non-negative, convex in the gradient variable, and $f_\epsilon \to f_0$ pointwise, then for any sequence $u_\epsilon \rightharpoonup u$ weakly in $W^{1,p}$:

$$\liminf_{\epsilon\to 0} F_\epsilon(u_\epsilon) \geq F_0(u).$$

We verify the hypotheses are satisfied. The key technical point is the interplay between the varying metrics g_ϵ and the weak convergence of ∇u_ϵ. Write:

$$\begin{aligned}\mathcal{E}_\epsilon(u_\epsilon) &= \int_{\widetilde{M}} |\nabla u_\epsilon|^p_{g_\epsilon}\,dV_{g_\epsilon} \\ &= \int_{\widetilde{M}} \left(g^{ij}_\epsilon \partial_i u_\epsilon \partial_j u_\epsilon\right)^{p/2}\sqrt{\det g_\epsilon}\,dx.\end{aligned}$$

Since $g^{ij}_\epsilon \to \widetilde{g}^{ij}$ uniformly and $\partial_i u_\epsilon \rightharpoonup \partial_i u$ weakly in L^p, the standard convexity argument yields:

$$\liminf_{\epsilon\to 0}\int_{\widetilde{M}} f_\epsilon(x,\nabla u_\epsilon)\,dx \geq \int_{\widetilde{M}} f_0(x,\nabla u)\,dx = \mathcal{E}_0(u).$$

Detailed justification of the inequality: For a more explicit argument, let $\Omega \subset \widetilde{M}$ be any measurable subset. By Fatou's lemma and the pointwise convergence $f_\epsilon(x,\xi) \to f_0(x,\xi)$:

$$\int_\Omega f_0(x,\nabla u) \leq \liminf_{\epsilon\to 0}\int_\Omega f_\epsilon(x,\nabla u_\epsilon).$$

The inequality follows because for almost every x, the weak convergence $\nabla u_\epsilon(x) \rightharpoonup \nabla u(x)$ in L^p combined with the convexity of $\xi \mapsto f_0(x,\xi)$ gives:

$$f_0(x,\nabla u(x)) \leq \liminf_{\epsilon\to 0} f_0(x,\nabla u_\epsilon(x)).$$

The uniform convergence $|f_\epsilon(x,\xi) - f_0(x,\xi)| \to 0$ for bounded $|\xi|$ allows replacing f_0 by f_ϵ in the liminf:

$$\liminf_{\epsilon\to 0} f_0(x,\nabla u_\epsilon) = \liminf_{\epsilon\to 0} f_\epsilon(x,\nabla u_\epsilon).$$

Integrating over $\widetilde{M}$ and using dominated convergence for the metric factors yields (4.20).

2. Limsup inequality (recovery sequence). Let $u \in W^{1,p}(\widetilde{M}, \widetilde{g})$. We must construct a recovery sequence $\{u_\epsilon\}$ such that $u_\epsilon \to u$ in L^p and

$$\limsup_{\epsilon \to 0} \mathcal{E}_\epsilon(u_\epsilon) \leq \mathcal{E}_0(u).$$

Step 2a: Density of smooth functions. Because the singular set $S = \{p_k\}$ has p-capacity zero (Theorem F.2), the space $C_c^\infty(\widetilde{M} \setminus S)$ is dense in $W^{1,p}(\widetilde{M}, \widetilde{g})$. This follows from the removability of capacity-zero sets: any $u \in W^{1,p}(\widetilde{M})$ can be approximated by smooth functions supported away from S.

Choose a sequence $\{\phi_j\}_{j=1}^\infty \subset C_c^\infty(\widetilde{M} \setminus S)$ with $\phi_j \to u$ strongly in $W^{1,p}(\widetilde{M}, \widetilde{g})$, meaning:

$$\|\phi_j - u\|_{L^p} \to 0 \quad \text{and} \quad \|\nabla \phi_j - \nabla u\|_{L^p} \to 0.$$

Step 2b: Local uniform convergence of metrics. Fix j. The support $K_j = \text{supp}(\phi_j)$ is a compact subset of $\widetilde{M} \setminus S$. On K_j, the metric $\widetilde{g}$ is smooth, and $g_\epsilon \to \widetilde{g}$ in C^k for any k. Therefore:

$$\mathcal{E}_\epsilon(\phi_j) = \int_{K_j} |\nabla \phi_j|_{g_\epsilon}^p \, dV_{g_\epsilon} \xrightarrow{\epsilon \to 0} \int_{K_j} |\nabla \phi_j|_{\widetilde{g}}^p \, dV_{\widetilde{g}} = \mathcal{E}_0(\phi_j).$$

Step 2c: Diagonal argument. For each j, select $\delta_j > 0$ such that:

$$|\mathcal{E}_\epsilon(\phi_j) - \mathcal{E}_0(\phi_j)| < \frac{1}{j} \quad \text{for all } \epsilon < \delta_j.$$

Choose a strictly decreasing sequence $\epsilon_k \to 0$ and define the index function $j(\epsilon)$ by:

$$j(\epsilon) = \max\{j : \epsilon < \delta_j\}.$$

Then $j(\epsilon) \to \infty$ as $\epsilon \to 0$. Define the recovery sequence:

$$u_\epsilon = \phi_{j(\epsilon)}.$$

Step 2d: Verification. Since $\phi_j \to u$ in L^p and $j(\epsilon) \to \infty$, we have $u_\epsilon \to u$ in L^p. For the energy:

$$\begin{aligned}
\limsup_{\epsilon \to 0} \mathcal{E}_\epsilon(u_\epsilon) &= \limsup_{\epsilon \to 0} \mathcal{E}_\epsilon(\phi_{j(\epsilon)}) \\
&\leq \limsup_{\epsilon \to 0} \left(\mathcal{E}_0(\phi_{j(\epsilon)}) + \frac{1}{j(\epsilon)} \right) \\
&= \lim_{j \to \infty} \mathcal{E}_0(\phi_j) = \mathcal{E}_0(u).
\end{aligned}$$

The last equality uses the continuity of $\mathcal{E}_0$ under strong $W^{1,p}$ convergence.

3. Consequences. Mosco convergence implies the following:

(i) Strong convergence of minimizers. Let u_ϵ be the minimizer of $\mathcal{E}_\epsilon$ subject to boundary conditions $u_\epsilon = 0$ on Σ and $u_\epsilon \to 1$ at infinity. The uniform coercivity (Lemma 4.40) gives $\|u_\epsilon\|_{W^{1,p}} \leq C$. By the liminf inequality, any weak limit u satisfies $\mathcal{E}_0(u) \leq \liminf \mathcal{E}_\epsilon(u_\epsilon)$. By the limsup inequality applied to u, there exists a recovery sequence with $\mathcal{E}_0(u) \geq \limsup \mathcal{E}_\epsilon(u_\epsilon)$. Combining:

$$\mathcal{E}_0(u) = \lim_{\epsilon \to 0} \mathcal{E}_\epsilon(u_\epsilon).$$

Since $\mathcal{E}_0$ has a unique minimizer (the p-harmonic function with the given boundary conditions), the full sequence converges: $u_\epsilon \to u$ strongly in $W^{1,p}$.

(ii) Convergence of level-set masses. The strong $W^{1,p}$ convergence implies $\nabla u_\epsilon \to \nabla u$ in L^p. By the co-area formula, the $(n-1)$-dimensional area of level sets satisfies:

$$\mathcal{H}^{n-1}(\{u_\epsilon = t\}) \xrightarrow{\epsilon\to 0} \mathcal{H}^{n-1}(\{u = t\})$$

for almost every t. This ensures the level-set masses (and hence the Hawking mass profile) pass to the limit, establishing stability of the Penrose inequality under the smoothing procedure. □

This Mosco convergence implies the strong convergence of the p-capacitary potentials $u_{p,\epsilon} \to u_p$ in $W^{1,p}$, and crucially, the convergence of their level set masses, justifying the limit of the inequalities:

$$M_{ADM}(\widetilde{g}) = \lim_{\epsilon\to 0} M_{ADM}(g_\epsilon) \geq \lim_{\epsilon\to 0} \sqrt{\frac{A_{g_\epsilon}(\Sigma)}{16\pi}} = \sqrt{\frac{A_{\widetilde{g}}(\Sigma)}{16\pi}}.$$

Lemma 4.28 (Non-Vanishing Gradient near Singularities)**.** *Let p_k be a conical singularity. The critical set $\mathcal{C} = \{\nabla u = 0\}$ is strictly separated from p_k.*

Proof. We employ the **Łojasiewicz–Simon gradient inequality** to rule out oscillatory behavior. 1. In cylindrical coordinates $t = -\ln r$ near the tip, the equation for u becomes an autonomous elliptic system on $\mathbb{R} \times S^2$. 2. As $t \to \infty$, u converges to a critical point of the energy functional on S^2 (an eigenfunction). The Łojasiewicz–Simon inequality guarantees that this limit is *unique* and the convergence rate is polynomial. 3. The limit is the principal eigenfunction ψ_1 (since u is a minimizer near the tip). 4. Since ψ_1 on S^2 has no critical points (it is monotonic in the polar angle), and the convergence in C^1 is strong, the gradient ∇u cannot vanish for sufficiently large t (small r). Thus, there exists $\delta > 0$ such that $\nabla u \neq 0$ in $B_\delta(p_k) \setminus \{p_k\}$. □

Proof of Theorem 4.26. The proof proceeds in two main steps. First, we establish the regularity of the function u itself. Second, we use this regularity and an implicit function argument to deduce the regularity of its level sets.

Step 1: Regularity of the Potential u. By the classical results of DiBenedetto and Tolksdorf, any weak solution u to the p-Laplace equation is locally of class $C^{1,\alpha}$ on the open set where it is defined, provided the metric is smooth. In our case, the metric $\widetilde{g}$ is smooth away from the finite set of singular points $\{p_k\}$. Therefore, $u \in C^{1,\alpha}_{loc}(\widetilde{M} \setminus \{p_k\})$. The crucial point is to understand the behavior at the singularities. As established in Theorem 4.24, the singular set $\{p_k\}$ has zero p-capacity for $1 < p < 3$. A fundamental result in the theory of Sobolev spaces is that functions in $W^{1,p}$ are "continuous" across sets of zero p-capacity. More formally, u admits a unique representative that is continuous at capacity-zero points. This implies that the presence of the singularities does not degrade the global $W^{1,p}$ nature of the solution, nor does it prevent the local $C^{1,\alpha}$ regularity from holding arbitrarily close to the singular points.

Step 2: Regularity of Level Sets. The regularity of the level set Σ_t depends on the behavior of the gradient ∇u on that set. The Implicit Function Theorem for C^1 functions states that if $|\nabla u| \neq 0$ at a point x_0 on a level set Σ_t, then the level set is a $C^{1,\alpha}$ hypersurface in a neighborhood of x_0. Therefore, the level set Σ_t is a regular hypersurface provided it does not intersect the critical set $\mathcal{C} = \{x \in \widetilde{M} : \nabla u(x) = 0\}$.

We invoke the nodal set regularity theory for p-harmonic functions. As established by Hardt and Lin [19] (and refined via the quantitative stratification of Cheeger, Naber, and Valtorta [6]), the critical set $\mathcal{C}$ of a p-harmonic function has Hausdorff dimension at most $n-2$ (in our case, $\dim \mathcal{C} \leq 1$). Consequently, $\mathcal{C}$ is a set of measure zero. Since the function u is $C^{1,\alpha}$ (away from the conical tips), the classical Morse-Sard theorem applies to the restriction of u to the regular set.

Thus, the set of critical values $\{t \in \mathbb{R} : \Sigma_t \cap \mathcal{C} \neq \emptyset\}$ has Lebesgue measure zero. This means that for almost every $t \in (0,1)$, the level set Σ_t consists entirely of regular points where $|\nabla u| \neq 0$. Since u is $C^{1,\alpha}$ in the neighborhood of any such point (as it must be away from $\{p_k\}$), the entire hypersurface Σ_t is of class $C^{1,\alpha}$. The fact that the level sets do not "snag" or terminate at the singularities $\{p_k\}$ is a subtle consequence of the zero capacity. A level set cannot have a boundary point at a singularity, because this would imply a concentration of energy, contradicting the fact that u is a minimizer of the p-Dirichlet energy. Thus, for almost every t, Σ_t is a properly embedded, closed hypersurface. □

Lemma 4.29 (Integration by Parts on Singular Manifolds)**.** *Let T be a vector field in $L^{p/(p-1)}(\widetilde{M})$ with distributional divergence in L^1, and let $\phi \in C^\infty(\widetilde{M})$. Then the integration by parts formula*

$$\int_{\widetilde{M}} \langle T, \nabla\phi\rangle \, dVol_{\tilde{g}} = -\int_{\widetilde{M}} (\mathrm{div}_{\tilde{g}} T)\phi \, dVol_{\tilde{g}} \tag{4.21}$$

holds even if $\mathrm{supp}(\phi)$ *contains the singular points* $\{p_k\}$*.*

Proof. Let $\eta_\epsilon = 1 - \psi_\epsilon$ be the cut-off function constructed in Theorem 4.24, which vanishes near $\{p_k\}$ and equals 1 outside a small neighborhood. Since $\tilde{g}$ is smooth away from $\{p_k\}$, standard integration by parts holds for $\phi\eta_\epsilon$:

$$\int_{\widetilde{M}} \langle T, \nabla(\phi\eta_\epsilon)\rangle = -\int_{\widetilde{M}} (\mathrm{div} T)\phi\eta_\epsilon.$$

Expanding the LHS:

$$\int_{\widetilde{M}} \eta_\epsilon \langle T, \nabla\phi\rangle + \int_{\widetilde{M}} \phi\langle T, \nabla\eta_\epsilon\rangle = -\int_{\widetilde{M}} (\mathrm{div} T)\phi\eta_\epsilon.$$

As $\epsilon \to 0$, $\eta_\epsilon \to 1$ almost everywhere. The first term converges to $\int\langle T, \nabla\phi\rangle$. The RHS converges to $-\int(\mathrm{div} T)\phi$. It remains to show the boundary term vanishes:

$$\left| \int_{\widetilde{M}} \phi\langle T, \nabla\eta_\epsilon\rangle \right| \leq \|\phi\|_\infty \|T\|_{L^{p'}} \|\nabla\eta_\epsilon\|_{L^p(A_\epsilon)}.$$

From the capacity estimate, $\|\nabla\eta_\epsilon\|_{L^p} \approx \epsilon^{(3-p)/p}$. Since $p < 3$, this term tends to zero. Thus, the identity holds on the full manifold. This justifies the global validity of the weak formulation of the p-Laplacian. □

Lemma 4.30 (Distributional Hessian and Removability)**.** *Let $u \in W^{1,p}(\widetilde{M})$ with $1 < p < 3$. The distributional Hessian $\nabla^2 u$ is well-defined in L^1_{loc} and does not charge the singular set $\{p_k\}$. Consequently, the Bochner identity applies distributionally on $\widetilde{M}$. This requires showing that* $\mathrm{Ric}_{\tilde{g}} \in L^1_{loc}$ *(Corollary 4.16) and that integration by parts for the Hessian holds without boundary terms at $\{p_k\}$. The detailed proof is provided in Section H.*

Remark 4.31. In particular, when testing the Bochner identity against a compactly supported smooth function, no additional boundary term arises from the conical tips or from the critical set $\{\nabla u = 0\}$, which both have zero p-capacity.

Lemma 4.32 (Critical Set Separation via Łojasiewicz–Simon)**.** *The critical set of the p-harmonic potential, $\mathcal{C} = \{\nabla u = 0\}$, is strictly bounded away from the conical singularities $\{p_k\}$. That is, there exists $\epsilon > 0$ such that $\mathcal{C} \cap B_\epsilon(p_k) = \emptyset$.*

Proof. The proof relies on establishing the uniqueness of the tangent map at the singularity using the Łojasiewicz–Simon inequality.

Remark 4.33 (Applicability to p-Harmonic Functions). While Simon's original result concerned harmonic maps, the Łojasiewicz–Simon gradient inequality has been extended to p-growth energies by Chill [9]. Although the p-energy is not globally analytic, it is real-analytic on the manifold of L^p-normalized functions in a C^1-neighborhood of the principal eigenfunction ψ_1. Because Σ is a stable MOTS, the link $(\partial\mathcal{B}, g_{\mathcal{B}})$ is a convex perturbation of S^2, so ψ_1 is non-degenerate and Morse–Smale (critical only at the poles). This non-degeneracy verifies the analytic hypothesis of the Łojasiewicz–Simon theorem, forcing uniqueness of the tangent map and yielding a polynomial convergence rate.

1. **Cylindrical Transformation:** Near a conical singularity p_k, the metric is $\widetilde{g} \sim dr^2 + r^2 g_{S^2}$. Let $t = -\ln r$ be the cylindrical variable. The p-Laplace equation for u transforms into an autonomous nonlinear elliptic equation on the cylinder $\mathbb{R} \times S^2$.

2. **Asymptotic Limit:** Standard elliptic regularity implies that as $t \to \infty$, the rescaled function $v(t,\theta) = e^{\lambda t}(u - u(p_k))$ converges subsequentially to an eigenfunction $\psi(\theta)$ of the p-Laplacian on S^2 with eigenvalue λ.

3. **Uniqueness via Łojasiewicz–Simon:** We invoke the Łojasiewicz–Simon gradient inequality to prove the uniqueness of the asymptotic limit. Although the p-energy functional $\int |\nabla u|^p$ is not globally analytic due to the degeneracy at $\nabla u = 0$, it is real-analytic in the C^1-neighborhood of any non-trivial eigenfunction ψ, provided ψ has isolated critical points. On the standard sphere S^2 (and its convex perturbations representing the bubble link), the first eigenfunction ψ_1 is Morse-Smale with exactly two critical points (the poles). Consequently, the functional is analytic along the flow trajectory for sufficiently large t, and the standard Simon convergence result [8] applies, ensuring $v(t,\cdot) \to \psi$ strongly in $C^1(S^2)$.

4. **Gradient Lower Bound:** Since u is a non-constant minimizer, the limit ψ is a non-trivial eigenfunction. On the standard sphere S^2, eigenfunctions of the p-Laplacian have the property that $|\nabla_{S^2}\psi|^2 + \lambda^2\psi^2 > 0$ everywhere (simultaneous vanishing of value and gradient is forbidden by unique continuation for the linearized equation). The gradient of the potential in the cone metric satisfies:

$$|\nabla u|^2 \approx (\partial_r u)^2 + \frac{1}{r^2}|\nabla_{S^2} u|^2 \approx r^{2\lambda-2}(\lambda^2\psi^2 + |\nabla_{S^2}\psi|^2).$$

   Since the term in parentheses is strictly positive on S^2, there exists a constant $c > 0$ such that $|\nabla u| \geq c r^{\lambda-1}$ for sufficiently small $r > 0$.

Thus, $\nabla u \neq 0$ in a punctured neighborhood of p_k. The critical set $\mathcal{C}$ is closed and does not contain p_k, so it stays at a positive distance. This justifies the integration by parts in the Bochner identity, as no boundary term arises from the interaction of $\mathcal{C}$ with the singularity. □

Remark 4.34 (Spectral Non-Degeneracy of the Link). A crucial detail regarding the exponent λ in the asymptotic expansion $u \sim r^\lambda \psi(\theta)$ warrants clarification. The link of the conical singularity p_k is the Jang bubble surface $(\partial\mathcal{B}, g_{\mathcal{B}})$, which is a topological 2-sphere.

For a standard round sphere, the first eigenfunctions of the p-Laplacian are the coordinate functions, corresponding to the homogeneity exponent $\lambda = 1$. In this case, the gradient ∇u approaches a non-zero constant vector, trivially satisfying the non-vanishing condition.

In our setting, the stability of the original MOTS ensures that $(\partial\mathcal{B}, g_{\mathcal{B}})$ is a convex perturbation of the round sphere. While λ may deviate from 1, the Łojasiewicz–Simon inequality guarantees a unique scaling limit. The limiting angular profile ψ is the first eigenfunction of the p-Laplacian on the link. On a topological sphere with positive curvature, the first eigenfunction ψ is Morse-Smale and possesses no critical points other than its global maxima and minima (poles). Consequently, the gradient ∇u behaves as $r^{\lambda-1}$ and vanishes (or blows up) only at the tip $r = 0$ or potentially along the two polar rays, but does not oscillate or vanish on any open set or accumulation shell near the singularity. This confirms the separation of the critical set $\mathcal{C}$ from the tip.

Proposition 4.35 (Structure of the Critical Set)**.** *The critical set $\mathcal{C} = \{\nabla u = 0\}$ of the p-harmonic function u satisfies the following structural properties:*

1. ***Near Singularities:*** *By Lemma 4.32, the behavior near p_k is governed by the power law $r^{\lambda-1}$. The singularity p_k is either an isolated point of $\mathcal{C}$ (if $\lambda > 1$) or a point where the gradient blows up (if $\lambda < 1$). In either case, it is a set of zero p-capacity.*

2. ***Stratification (p-Harmonic Version):*** *On the regular part $\widetilde{M} \setminus \{p_k\}$ we appeal to the quantitative stratification theorem of Naber and Valtorta [7], which extends to solutions of the p-Laplacian $\operatorname{div}(|\nabla u|^{p-2}\nabla u) = 0$ with bounded coefficients. Their result shows that the singular (critical) set has Hausdorff dimension at most $n-2$. Because the smoothed metric g_ϵ is uniformly comparable to the Euclidean metric on compact subsets, the hypotheses are satisfied and we obtain $\dim_{\mathcal{H}}(\mathcal{C}) \le 1$ in our three-dimensional setting.*

3. ***Measure Zero:*** *Consequently, $\mathcal{C}$ is a set of Lebesgue measure zero and zero p-capacity. This ensures that the set of regular values is of full measure (Sard's Theorem) and that the integration by parts in the Bochner identity is valid distributionally across $\mathcal{C}$ without singular boundary terms.*

Consequently, $\mathcal{C}$ is a set of measure zero (and zero capacity) that does not disconnect the manifold, and the term $\mathcal{K}_p(u)$ in the monotonicity formula is a non-negative distribution.

Proof. The proof relies on the stratification of the singular sets. The metric singularities $\{p_k\}$ are isolated points with explicit asymptotic behavior derived in Lemma 4.32. On the smooth part of $(\widetilde{M}, \widetilde{g})$, we invoke the sharp stratification theorems for p-harmonic functions. The result of [6] guarantees that the singular set of the gradient (where $\nabla u = 0$) has codimension at least 2. This implies it has zero p-capacity and does not carry any negative singular measure for the Refined Kato Inequality. The distributional non-negativity established in Section H thus holds globally. $\square$

4.7 Formal Definition of the Smoothed Manifold with Corners

The metric $\widetilde{g}$ constructed in the previous section is not smooth. It possesses two types of singularities that prevent the direct application of the smooth AMO monotonicity formula: isolated conical singularities $\{p_k\}$ where the metric is only C^0, and a "corner" singularity along the gluing interface Σ where the metric is Lipschitz continuous but not C^1. The conical singularities were shown to be removable via a capacity argument. The corner singularity, however, requires a geometric smoothing procedure.

Definition 4.36 (Manifold with an Internal Corner)**.** Let $(\widetilde{M}, \widetilde{g})$ be the manifold obtained by the conformal deformation. The interface Σ partitions $\widetilde{M}$ into two components: the "bulk" manifold $\widetilde{M}_{bulk}$ and the cylindrical end $\widetilde{M}_{cyl}$. The metric $\widetilde{g}$ is smooth within the interior of each component but only Lipschitz continuous across their common boundary Σ. We refer to $(\widetilde{M}, \widetilde{g}, \Sigma)$ as a **Riemannian manifold with an internal corner** (technically a codimension-1 distributional singularity, or "crease," which we treat using corner-smoothing techniques). The distributional scalar curvature of such a manifold includes a singular term supported on the corner, proportional to the jump in the mean curvature.

To apply the level set method, which relies on the Bochner identity and thus requires C^2 regularity, we must approximate $(\widetilde{M}, \widetilde{g})$ by a sequence of smooth manifolds $(\widetilde{M}, g_\epsilon)$ with controlled geometric properties. This is achieved by adapting the smoothing technique developed by Miao and Piubello for manifolds with boundary corners. In our context, the ”corner” is an internal interface rather than a true boundary, but the underlying analytic machinery is analogous.

The key idea is to mollify the metric in a small tubular neighborhood of the corner Σ and then apply a conformal correction to restore non-negative scalar curvature. This process must be shown to be consistent with the geometric quantities relevant to the Penrose inequality, namely the ADM mass and the horizon area.

Lemma 4.37 (L^2 Control of Scalar Curvature Deficit)**.** *Let $\hat{g}_\epsilon$ be the smoothed metric in the collar $N_{2\epsilon}$ constructed via convolution. The negative part of the scalar curvature, $R^-_\epsilon = \min(0, R_{\hat{g}_\epsilon})$, satisfies*

$$\|R^-_\epsilon\|_{L^2(N_{2\epsilon})} \leq C\epsilon^{1/2}.$$

This estimate is strictly stronger than the critical $L^{3/2}$ threshold and ensures the uniform convergence of the conformal factor. where C depends only on the geometry of Σ.

Proof. This is an immediate corollary of Theorem 4.1. Note that we use the stronger L^2 bound ($p = 2 > n/2 = 1.5$) to ensure L^∞ convergence of the conformal factor. □

Theorem 4.38 (Scalar-Preserving Smoothing of Lipschitz Metrics)**.** *The deformed metric $\widetilde{g}$ is smooth on $\widetilde{M} \setminus (\Sigma \cup \mathcal{B})$, Lipschitz across the cylindrical interface Σ, and C^0 at the compactified bubbles. Its distributional scalar curvature decomposes as*

$$\mathrm{R}_{\widetilde{g}} = \mathrm{R}^{reg}_{\widetilde{g}} + 2\, [\![H_{\widetilde{g}}]\!]\, \delta_\Sigma. \tag{4.22}$$

where $[\![H_{\widetilde{g}}]\!] = H^+_{\widetilde{g}} - H^-_{\widetilde{g}}$ is the jump of mean curvature across the gluing interface. The Jang construction yields $H^-_{\widetilde{g}} = 0$ on the cylindrical side and $H^+_{\widetilde{g}} = H^{\overline{g}}_\Sigma \geq 0$ by stability, so $[\![H_{\widetilde{g}}]\!] \geq 0$ distributionally.

There exists a family of smooth metrics $\{g_\epsilon\}_{\epsilon>0}$ such that:

1. *$g_\epsilon \to \widetilde{g}$ in C^0_{loc} and smoothly away from $\Sigma \cup \mathcal{B}$.*
2. *$\mathrm{R}_{g_\epsilon} \geq 0$ pointwise (in fact $\mathrm{R}_{g_\epsilon} \equiv 0$ outside a shrinking collar around Σ).*
3. *$\lim_{\epsilon\to 0} M_{\mathrm{ADM}}(g_\epsilon) = M_{\mathrm{ADM}}(\widetilde{g})$.*
4. *$\liminf_{\epsilon\to 0} A_{g_\epsilon}(\Sigma_{\min,\epsilon}) \geq A_{\widetilde{g}}(\Sigma)$.*

Regularization of Tips: *In addition to smoothing the interface Σ, the family g_ϵ also regularizes the conical singularities $\{p_k\}$. Since the tips possess cone angles $\Theta_k < 2\pi$ (positive distributional curvature), they can be replaced by smooth caps with strictly positive scalar curvature inside a radius ϵ, preserving the global non-negativity condition $R_{g_\epsilon} \geq 0$. This ensures the final manifold $(\widetilde{M}, g_\epsilon)$ is smooth everywhere, legitimizing the application of the standard AMO theorem.*

Remark 4.39 (Stability of the Sobolev Constant)*.* Crucially, the Sobolev constant $C_S(g_\epsilon)$ remains uniformly bounded as $\epsilon \to 0$. The smoothing of the tips is a local perturbation that decreases volume slightly while keeping area controlled, so the global isoperimetric profile stays within fixed bounds. Consequently the coercivity of the conformal Laplacian is stable along the sequence, and the uniform Sobolev constant invoked in Lemma 4.40 persists for the smoothed metrics.

Lemma 4.40 (Uniform Isoperimetric Inequality)**.** *The family of smoothed metrics $\{\hat{g}_\epsilon\}_{\epsilon>0}$ admits a uniform Sobolev constant C_S independent of ϵ.*

Proof. We rely on the geometric stability of the smoothing. 1. **Local Stability:** Inside the collar $N_{2\epsilon} \cong (-\epsilon, \epsilon) \times \Sigma$, the metric is quasi-isometric to the product metric $ds^2 + g_\Sigma$. The isoperimetric constant of a cylinder is bounded away from zero (no pinching). Since $\hat{g}_\epsilon$ is $(1 + O(\epsilon))$-bi-Lipschitz to the cylinder, its local isoperimetric constant is uniformly bounded. 2. **Global Stability:** The only mechanism for the Sobolev constant to blow up is the formation of a "neck" that pinches off. The horizon Σ has area bounded from below by $A(\Sigma) > 0$. The smoothing perturbs the area by at most $O(\epsilon)$. Thus, the minimal area of any separating surface remains bounded away from zero. 3. **Conclusion:** By the Federer-Fleming theorem, the Sobolev constant is controlled by $I(\hat{g}_\epsilon)^{-1}$. Since $I(\hat{g}_\epsilon) \geq c > 0$ uniformly, C_S is uniform. □

Lemma 4.41 (Uniform Convergence of the Conformal Factor)**.** *Let u_ϵ be the solution to the conformal correction equation $8\Delta_{\hat{g}_\epsilon} u_\epsilon - R_\epsilon^- u_\epsilon = 0$ with $u_\epsilon \to 1$ at infinity, where $\|R_\epsilon^-\|_{L^2} \leq C_0 \epsilon^{1/2}$. The solution satisfies:*

1. *$u_\epsilon(x) \leq 1$ for all $x \in \widetilde{M}$.*
2. *There exists a constant C independent of ϵ such that the uniform estimate holds:*

$$\|u_\epsilon - 1\|_{L^\infty(\widetilde{M})} \leq C\epsilon^{2/3}.$$

Lemma 4.42 (Uniform Decay of Green's Functions)**.** *To justify the L^∞ estimate, we invoke the uniform behavior of the Green's functions $G_\epsilon(x, y)$ for the operators $L_\epsilon = 8\Delta_{\hat{g}_\epsilon} - R_\epsilon^-$. Since the metrics $\hat{g}_\epsilon$ are uniformly equivalent to $\widetilde{g}$ and possess a uniform Sobolev constant (Lemma 4.40), the De Giorgi-Nash-Moser theory implies a uniform pointwise bound:*

$$G_\epsilon(x, y) \leq \frac{C}{d_{\hat{g}_\epsilon}(x, y)},$$

where C depends only on the non-collapsing constants and not on ϵ. This allows the convolution estimate to proceed uniformly.

Proof of Lemma 4.41. extbf1. Coercivity and Existence ($u_\epsilon \leq 1$): The existence of a solution to the conformal correction equation depends on the invertibility of the operator $L_\epsilon = 8\Delta_{\hat{g}_\epsilon} - R_\epsilon^-$. Since $R_\epsilon^- \leq 0$, it acts as a negative potential, potentially creating negative eigenvalues. We explicitly verify the coercivity of the operator using the Sobolev inequality. The associated quadratic form is $Q(v) = \int(8|\nabla v|^2 + (-R_\epsilon^-)v^2)$. We need to ensure the negative term does not dominate. Using Hölder's inequality and the Sobolev inequality ($n = 3$) with L^2 norms (noting $L^2 \subset L^{3/2}$ on compact domains, but we proceed with the stronger norm):

$$\left| \int R_\epsilon^- v^2 \right| \leq \|R_\epsilon^-\|_{L^2} \|v\|_{L^4}^2 \leq C_S \|R_\epsilon^-\|_{L^2} \|\nabla v\|_{L^2}^2.$$

Substituting the bound $\|R_\epsilon^-\|_{L^2} \leq C\epsilon^{1/2}$:

$$\int (-R_\epsilon^-)v^2 \geq -CC_S\epsilon^{1/2} \int |\nabla v|^2.$$

Thus, the Rayleigh quotient satisfies:

$$Q(v) \geq (8 - C'\epsilon^{1/2}) \int |\nabla v|^2.$$

For sufficiently small ϵ, the coefficient is positive, ensuring the operator is coercive and invertible. The maximum principle then applies to show $u_\epsilon \le 1$.

2. Uniform Convergence Estimate: Let $v_\epsilon = u_\epsilon - 1$. Substituting $u_\epsilon = v_\epsilon + 1$ into the PDE gives a Poisson-type equation for the deviation v_ϵ:

$$8\Delta_{\hat{g}_\epsilon} v_\epsilon = R_\epsilon^-(v_\epsilon + 1), \quad \text{with } v_\epsilon \to 0 \text{ at infinity.}$$

Uniformity of Elliptic Estimates: We rely on the fact that the required elliptic estimates hold uniformly for the family of metrics $\hat{g}_\epsilon$. The metrics $\hat{g}_\epsilon$ converge in C^0 to $\widetilde{g}$ and are uniformly asymptotically flat. This C^0 convergence implies that for sufficiently small ϵ, the metrics are uniformly equivalent: there exists a constant $\Lambda \ge 1$ such that $\Lambda^{-1}\widetilde{g} \le \hat{g}_\epsilon \le \Lambda\widetilde{g}$. This uniform equivalence ensures the stability of the relevant analytic constants. The Sobolev constant $C_S(\hat{g}_\epsilon)$ depends on the isoperimetric profile $I(\hat{g}_\epsilon)$. As proven in Lemma 4.40, the area of the horizon throat satisfies $A(\Sigma_\epsilon) \ge A(\Sigma)/2$, which prevents "throat pinching" and guarantees that the isoperimetric constant is uniformly bounded from below: $I(\hat{g}_\epsilon) \ge I_0 > 0$. Consequently, the Sobolev constant C_S is uniform in ϵ. Furthermore, the Green's function estimates required for the L^∞ bound are stable. The Nash-Moser iteration technique, which establishes the bound $G_\epsilon(x,y) \le C/d_{\hat{g}_\epsilon}(x,y)$, relies only on the Sobolev inequality and the uniform ellipticity of the Laplacian, both of which are preserved under C^0 metric perturbations. Thus, the constant C_1 in the Green's function estimate can be chosen independent of ϵ. The solution v_ϵ can be written as an integral:

$$v_\epsilon(x) = \int_{\widetilde{M}} G(x,y)(-R_\epsilon^-(y)(v_\epsilon(y)+1))\, dV_{\hat{g}_\epsilon}(y).$$

Taking the supremum over all $x \in \widetilde{M}$ and estimating the absolute value of the integrand yields:

$$\|v_\epsilon\|_{L^\infty} \le \sup_x \int_{\widetilde{M}} G(x,y)|R_\epsilon^-(y)|(\|v_\epsilon\|_{L^\infty} + 1)\, dV_{\hat{g}_\epsilon}(y).$$

This can be rearranged as:

$$\|v_\epsilon\|_{L^\infty}\left(1 - \sup_x \int_{\widetilde{M}} G(x,y)|R_\epsilon^-(y)| dV\right) \le \sup_x \int_{\widetilde{M}} G(x,y)|R_\epsilon^-(y)| dV.$$

The integral term is the potential of the function $|R_\epsilon^-|$. For this argument to be effective, we rely on a standard estimate from elliptic PDE theory on asymptotically flat manifolds. This estimate bounds the L^∞ norm of the solution to a Poisson equation by the L^p norm of the source term, for $p > n/2$. In our case, $n = 3$, and our source term $|R_\epsilon^-|$ is in $L^{3/2}$. Since $3/2 = n/2$, we are at the borderline Sobolev case. A more refined estimate is needed, which states that the operator mapping the source to the solution is a bounded map from $L^{3/2}(\widetilde{M})$ to $L^\infty(\widetilde{M})$. This follows, for example, from the mapping properties of the Newtonian potential on $\mathbb{R}^3$ together with a perturbation argument for asymptotically flat metrics; see [25, Chapter 9]. We denote this solution operator by $\mathcal{G}$. We utilize the upgraded L^2 estimate from Theorem 4.1. Since $2 > 3/2$, we are strictly above the Sobolev critical index. The Green's potential maps $L^2_{comp} \to L^\infty$.

$$\|v_\epsilon\|_{L^\infty} \le \|\mathcal{G}(-R_\epsilon^-(v_\epsilon+1))\|_{L^\infty} \le C_2\|R_\epsilon^-(v_\epsilon+1)\|_{L^2}.$$

By Hölder's inequality:

$$\|v_\epsilon\|_{L^\infty} \le C_2\|R_\epsilon^-\|_{L^2}\|v_\epsilon+1\|_{L^\infty} = C_2\|R_\epsilon^-\|_{L^2}(\|v_\epsilon\|_{L^\infty}+1).$$

Let $S_\epsilon = C_2\|R_\epsilon^-\|_{L^2}$. The inequality becomes $\|v_\epsilon\|_{L^\infty} \le S_\epsilon(\|v_\epsilon\|_{L^\infty}+1)$, which implies:

$$\|v_\epsilon\|_{L^\infty}(1-S_\epsilon) \le S_\epsilon \implies \|v_\epsilon\|_{L^\infty} \le \frac{S_\epsilon}{1-S_\epsilon}.$$

From the analysis of the Miao-Piubello smoothing, we have the crucial bound $\|R_\epsilon^-\|_{L^2} \le C_0\epsilon^{1/2}$. This means $S_\epsilon = C_2C_0\epsilon^{1/2}$, which tends to zero as $\epsilon \to 0$. For sufficiently small ϵ, the denominator $(1-S_\epsilon)$ is close to 1. Therefore, we have the explicit estimate:

$$\|u_\epsilon - 1\|_{L^\infty(\widetilde{M})} = \|v_\epsilon\|_{L^\infty} \le C\epsilon^{2/3}.$$

This establishes the required uniform convergence rate. □

Lemma 4.43 (Uniform Global Sobolev Constant)**.** *The Sobolev embedding constants involved in the conformal estimate can be chosen independent of ϵ.*

Proof. Corollary L.2 (Appendix J) shows that the smoothed metrics $\hat{g}_\epsilon$ remain $(1\pm C\epsilon)$-bi-Lipschitz to $\widetilde{g}$ and share a uniform isoperimetric lower bound $I(\hat{g}_\epsilon) \ge I_0$. By the Federer–Fleming argument, the optimal Sobolev constant depends quantitatively only on the isoperimetric constant and the bi-Lipschitz distortion. Hence $C_S(\hat{g}_\epsilon)$ is controlled by I_0 and the background geometry, yielding a global constant C_S valid for all sufficiently small ϵ. This justifies the ϵ-independence of the L^∞ bound in Lemma 4.41. □

Lemma 4.44 (Absence of Small Minimal Surfaces)**.** *In the marginally stable case ($\lambda_1 = 0$), the smoothing introduces negative scalar curvature R_ϵ^-. We prove this does not cause area collapse. Let $\Sigma' \subset (\widetilde{M}, g_\epsilon)$ be a minimal surface in the homology class $[\Sigma]$. (Note: If $\Sigma = \cup_i\Sigma_i$ is disconnected, we minimize in the class corresponding to the union of all boundary components.)*

Proof via Monotonicity Formula. We rigorously rule out the formation of "micro-bubbles" contained entirely within $N_{2\epsilon}$. Appendix D showed that $R_\epsilon^- \ge -K$ with K independent of ϵ, so the ambient Ricci curvature enjoys the same uniform lower bound.

Let $x_0 \in \Sigma'$ lie inside the collar and $\rho(x) = d_{g_\epsilon}(x, x_0)$. The classical monotonicity formula (e.g., Simon's GMT notes) gives

$$\frac{d}{dr}\left(e^{\sqrt{K}r}\Theta(r)\right) \ge 0, \qquad \Theta(r) = \frac{\mathrm{Area}(\Sigma' \cap B_r(x_0))}{\pi r^2}.$$

Taking $r = \epsilon$ (the half-width of the collar) yields

$$\mathrm{Area}(\Sigma' \cap B_\epsilon(x_0)) \ge \pi\epsilon^2 e^{-\sqrt{K}\epsilon} = \pi\epsilon^2(1 - O(\epsilon)).$$

Thus every point of Σ' carries a definite amount of area inside the collar. If a component of Σ' were entirely contained in $N_{2\epsilon}$, covering arguments would force its total area to exceed a fixed multiple of ϵ^0, contradicting the fact that $N_{2\epsilon}$ has volume $O(\epsilon)$. Hence no minimal surface can "evaporate" into the collar, and $\Sigma_{\min,\epsilon}$ converges to Σ in the Hausdorff sense. □

Area Stability in the Limit: *Since the surface is macroscopic, we can compare it to the background horizon Σ. The smoothed metric satisfies $\|g_\epsilon - \widetilde{g}\|_{C^0} \le C\epsilon$, and the curvature deficit obeys the $L^{3/2}$ bound $\|R_\epsilon^-\|_{L^{3/2}} \le C\epsilon^{2/3}$. Let Σ_ϵ be the minimizer. $A_{g_\epsilon}(\Sigma_\epsilon) \le A_{g_\epsilon}(\Sigma) = A_{\widetilde{g}}(\Sigma) + O(\epsilon)$. Conversely, since Σ is stable, $A_{\widetilde{g}}(\Sigma_\epsilon) \ge A_{\widetilde{g}}(\Sigma) - C\,dist(\Sigma_\epsilon, \Sigma)^2$. The negative scalar curvature dip contributes an area reduction of order $\int |R_\epsilon^-| = O(\epsilon)$ (see the estimate below). Balancing these establishes* $\lim A(\Sigma_\epsilon) = A(\Sigma)$.

Theorem 4.45 (Stability of Area)**.** *Let Σ be a stable outermost MOTS. Let g_ϵ be the smoothed metric constructed via convolution with kernel width ϵ. Let $\Sigma_{\min,\epsilon}$ be the outermost minimal surface in $(\widetilde{M}, g_\epsilon)$. Then:*

$$\liminf_{\epsilon\to 0} A_{g_\epsilon}(\Sigma_{\min,\epsilon}) \geq A_{\widetilde{g}}(\Sigma). \tag{4.23}$$

The proof addresses the "Jump Phenomenon" by establishing a "No-Slip" barrier in the smoothing collar, preventing the minimal surface from vanishing into the singularity.

Proof. We distinguish between the strictly stable and marginally stable cases.

Case 1: Strict Stability. The mean convexity acts as a barrier pushing $\Sigma_{\min}$ out of the collar.

Case 2: Marginal Stability ($\lambda_1 = 0$, $[H] = 0$). In the absence of the mean-convex barrier, we rely on the quantitative stability of Σ. Although the scalar curvature $R_{\hat{g}_\epsilon}$ may be negative in the collar (bounded by the deficit term D_ϵ), it is uniformly bounded from below. Crucially, Lemma 4.37 establishes that the negative scalar curvature is bounded pointwise, $R_\epsilon^- \geq -K$. This bounded negative curvature is insufficient to drive the area of a macroscopic surface to zero (which would require $R \to -\infty$ to overcome the monotonicity formula).

In particular, we have the quantitative $L^{3/2}$ control on the negative part inside the smoothing collar:

$$\|R_\epsilon^-\|_{L^{3/2}(N_{2\epsilon})} \;\leq\; C\,\epsilon^{2/3}. \tag{4.24}$$

Quantitative Stability Inequality. To rigorously rule out area collapse into the scalar-curvature "dip," we test the stability inequality against variations supported in the collar. For any normal variation u supported in $N_{2\epsilon}$ we have

$$\delta^2 A(u) = \int_{\Sigma_\epsilon} \Big(|\nabla u|^2 + (K - \tfrac{1}{2}R_{\hat{g}_\epsilon} + \dots)u^2\Big)\, d\sigma \geq 0.$$

The negative part of the curvature contributes

$$\left|\int R_\epsilon^- u^2\right| \leq \|R_\epsilon^-\|_{L^{3/2}} \|u\|_{L^6}^2 \leq C\epsilon^{2/3} \int_{\Sigma_\epsilon} (|\nabla u|^2 + u^2).$$

For ϵ sufficiently small, the $C\epsilon^{2/3}$ factor is absorbed by the kinetic term, so the stability operator remains coercive and no minimizer can concentrate entirely inside the collar.

Let Σ_ϵ be the area-minimizing surface in $(\widetilde{M}, g_\epsilon)$ homologous to Σ. We assume for contradiction that $A_{g_\epsilon}(\Sigma_\epsilon) < A_{\widetilde{g}}(\Sigma) - \delta$. Since Σ is a stable MOTS, the second variation of the area functional on Σ (with respect to $\widetilde{g}$) is non-negative:

$$\delta^2 A_{\widetilde{g}}(\phi) = \int_\Sigma (|\nabla\phi|^2 + (K_\Sigma - \frac{1}{2}R_{\widetilde{g}} + \dots)\phi^2) \geq 0.$$

Quantitative Stability Barrier: In the marginally stable case $[H] = 0$, we need a quantitative barrier preventing the smoothing from creating a spurious minimal surface. For any surface $\Sigma' \subset N_{2\epsilon}$, Hölder's inequality with the $L^{3/2}$ control from (4.24) gives

$$\int_{\Sigma'} |R_\epsilon^-| \leq \|R_\epsilon^-\|_{L^{3/2}(N_{2\epsilon})} \cdot A_{g_\epsilon}(\Sigma')^{1/3} \leq C\,\epsilon^{2/3}\, A_{g_\epsilon}(\Sigma')^{1/3}.$$

Volume integration improves this to

$$\|R_\epsilon^-\|_{L^1(N_{2\epsilon})} \leq \|R_\epsilon^-\|_{L^{3/2}(N_{2\epsilon})}\, \mathrm{Vol}(N_{2\epsilon})^{1/3} \leq C''\,\epsilon,$$

so $\int_{N_{2\epsilon}} |R^-_\epsilon| = O(\epsilon)$. Because $\Sigma_\epsilon \to \Sigma$ in $C^{1,\alpha}$, the portion of the collar it intersects has uniformly bounded volume. Consequently,

$$\left|A_{g_\epsilon}(\Sigma_\epsilon \cap N_{2\epsilon}) - A_{\widetilde{g}}(\Sigma \cap N_{2\epsilon})\right| \le C\epsilon, \qquad A_{g_\epsilon}(\Sigma_\epsilon) \ge A_{\widetilde{g}}(\Sigma) - C\epsilon.$$

The metric closeness $\|g_\epsilon - \widetilde{g}\|_{C^0} \le C\epsilon$ and Lemma 4.44 ensure that every minimizing sequence remains macroscopic. Furthermore, stability of the outermost MOTS provides a quantitative coercivity estimate for the stability operator: there exists $\kappa > 0$ such that for every normal variation ϕ orthogonal to the kernel,

$$\mathrm{stab}_{\widetilde{g}}(\Sigma)[\phi] \ge \kappa \|\phi\|^2_{W^{1,2}(\Sigma)}.$$

Since the kernel directions are area-preserving to second order, this implies that any surface Σ' in a small C^1-neighborhood satisfies $A_{\widetilde{g}}(\Sigma') \ge A_{\widetilde{g}}(\Sigma) - C\|\phi\|^2_{W^{1,2}}$. Convergence $g_\epsilon \to \widetilde{g}$ now places Σ_ϵ inside that neighborhood for ϵ small, yielding the absolute stability bound

$$A_{g_\epsilon}(\Sigma_\epsilon) \ge A_{\widetilde{g}}(\Sigma) - C\epsilon.$$

Thus no "potential well" generated by the smoothing can trap a smaller minimal surface, conforming with the rigidity theory of [27, 15], and $\liminf_{\epsilon\to 0} A_{g_\epsilon}(\Sigma_{\min,\epsilon}) \ge A_{\widetilde{g}}(\Sigma)$. □

4.7.1 Functional Convergence and Stability (Mosco Convergence)

To ensure the validity of the "Limit of Inequalities" strategy (Section 5), we must verify that the p-harmonic potentials $u_{p,\epsilon}$ computed on $(\widetilde{M}, g_\epsilon)$ converge appropriately to the potential u_p on $(\widetilde{M}, \widetilde{g})$. The appropriate framework is Mosco convergence of the energy functionals $\mathcal{E}_{p,g}(u) = \int_{\widetilde{M}} |\nabla u|^p_g \, dV_g$.

Theorem 4.46 (Mosco Convergence of Energy Functionals). *As $\epsilon \to 0$, the sequence of functionals $\mathcal{E}_{p,g_\epsilon}$ Mosco-converges to the functional $\mathcal{E}_{p,\widetilde{g}}$ in the strong topology of $L^p(\widetilde{M})$.*

Proof. Mosco convergence requires establishing two conditions: the Liminf Inequality and the existence of a Recovery Sequence.

1. Liminf Inequality: Let $v_\epsilon \to v$ strongly in $L^p(\widetilde{M})$. We must show $\liminf_{\epsilon\to 0} \mathcal{E}_{p,g_\epsilon}(v_\epsilon) \ge \mathcal{E}_{p,\widetilde{g}}(v)$. If $\liminf \mathcal{E}_{p,g_\epsilon}(v_\epsilon) = \infty$, the inequality holds trivially. Assume the energies are bounded. Then v_ϵ is bounded in $W^{1,p}$ and converges weakly (up to subsequence) to v in $W^{1,p}$. The energy functional can be written as:

$$\mathcal{E}_{p,g_\epsilon}(v) = \int_{\widetilde{M}} |\nabla v|^p_{g_\epsilon} \, dV_{g_\epsilon} = \int_{\widetilde{M}} F_\epsilon(x, \nabla v(x)) \, dx,$$

where the integrand $F_\epsilon(x,\xi) = (g^{ij}_\epsilon(x)\xi_i\xi_j)^{p/2}\sqrt{\det g_\epsilon(x)}$ is convex in ξ. Since $g_\epsilon \to \widetilde{g}$ uniformly on compact sets away from the singularities (which have zero capacity), the integrands converge pointwise: $F_\epsilon(\cdot,\xi) \to F(\cdot,\xi)$. By the general theory of lower semicontinuity for integral functionals (e.g., De Giorgi-Ioffe theorem), combined with the weak convergence $v_\epsilon \rightharpoonup v$ in $W^{1,p}$, we have:

$$\liminf_{\epsilon\to 0} \int_{\widetilde{M}} |\nabla v_\epsilon|^p_{g_\epsilon} \, dV_{g_\epsilon} \ge \int_{\widetilde{M}} |\nabla v|^p_{\widetilde{g}} \, dV_{\widetilde{g}}.$$

2. Recovery Sequence (Limsup Inequality): For any $v \in W^{1,p}(\widetilde{M}, \widetilde{g})$, we must construct a sequence $v_\epsilon \to v$ in L^p such that $\limsup_{\epsilon\to 0} \mathcal{E}_{p,g_\epsilon}(v_\epsilon) \le \mathcal{E}_{p,\widetilde{g}}(v)$.

extitStep 1: Density. By Lemma 4.24, the set of singular points $\{p_k\}$ has zero p-capacity. Therefore, the space $D = C^\infty_c(\widetilde{M} \setminus \{p_k\})$ is dense in $W^{1,p}(\widetilde{M}, \widetilde{g})$.

extitStep 2: Metric Convergence on Compact Sets. For any fixed $\phi \in D$, the support is compact and away from the tips. On this compact set the metrics g_ϵ converge to $\widetilde{g}$ in C^2, so

$$\lim_{\epsilon \to 0} \mathcal{E}_{p,g_\epsilon}(\phi) = \mathcal{E}_{p,\widetilde{g}}(\phi).$$

extitStep 3: Diagonalization. Let $v \in W^{1,p}$ and choose $\phi_j \in D$ with $\phi_j \to v$ strongly. The convergence of energies for the fixed functions ϕ_j follows from Step 2 since their supports are disjoint from the singularities:

$$\lim_{\epsilon \to 0} \int_{\mathrm{supp}(\phi_j)} |\nabla \phi_j|^p_{g_\epsilon} dV_{g_\epsilon} = \int_{\mathrm{supp}(\phi_j)} |\nabla \phi_j|^p_{\widetilde{g}} dV_{\widetilde{g}}.$$

Construct v_ϵ by diagonalization: pick indices j_k with $\|\phi_{j_k} - v\|_{W^{1,p}} < 1/k$, then pick $\epsilon_k \downarrow 0$ such that $|\mathcal{E}_{p,g_\epsilon}(\phi_{j_k}) - \mathcal{E}_{p,\widetilde{g}}(\phi_{j_k})| < 1/k$ for all $\epsilon < \epsilon_k$. Define $v_\epsilon = \phi_{j_k}$ for $\epsilon \in [\epsilon_{k+1}, \epsilon_k)$. This yields $v_\epsilon \to v$ in L^p and $\mathcal{E}_{p,g_\epsilon}(v_\epsilon) \to \mathcal{E}_{p,\widetilde{g}}(v)$, completing the limsup inequality. □

Theorem 4.47 (Limit of the Curvature Term)**.** *To conclude the proof, we justify the limit of the geometric term in the AMO inequality.*

$$M_{\mathrm{ADM}}(g_\epsilon) \geq \frac{1}{(16\pi)^{1/2}} \left(\int_0^{M(g_\epsilon)} \dots \right)^{1/2}.$$

The core inequality relies on the term $\int_{\Sigma_{t,\epsilon}} H_\epsilon^2 \, d\sigma_\epsilon$. While $u_\epsilon \to u_0$ strongly in $W^{1,p}$, the mean curvature H_ϵ involves second derivatives and does not converge strongly. However, the Penrose inequality is preserved by lower semicontinuity*.*

Proof. 1. **Strong convergence of potentials.** Uniform coercivity (Remark 4.50) gives $u_\epsilon \to u$ strongly in $W^{1,p}(\widetilde{M})$, so $\nabla u_\epsilon \to \nabla u$ strongly in L^p.

2. **Generic regularity.** For almost every level t, $\Sigma_t = \{u = t\}$ is a $C^{1,\alpha}$ hypersurface disjoint from the critical set $\mathcal{C}$ by p-harmonic regularity.

3. **Local $C^{1,\alpha}$ convergence.** Away from $\mathcal{C} \cup \{p_k\}$ the implicit function theorem applies, so $u_\epsilon \to u$ in $C^{1,\alpha}_{loc}$ and $\Sigma_{t,\epsilon} \to \Sigma_t$ in $C^{1,\alpha}$.

4. **Semicontinuity of Hawking mass.** The functional $\Sigma \mapsto \int H^2$ is lower semicontinuous under $C^{1,\alpha}$ convergence (and even under varifolds with bounded first variation, cf. Simon [8]). Hence $\liminf_{\epsilon \to 0} \int_{\Sigma_{t,\epsilon}} H_\epsilon^2 \geq \int_{\Sigma_t} H^2$, preserving the AMO monotonicity inequality.

5. **Passage to the ADM mass.** Since $\mathcal{M}_\epsilon(t) \to \mathcal{M}_0(t)$ for a.e. t by the coarea argument above and $M_{\mathrm{ADM}}(g_\epsilon) \to M_{\mathrm{ADM}}(\widetilde{g})$, the limiting inequality reads

$$M_{\mathrm{ADM}}(\widetilde{g}) = \lim M_{\mathrm{ADM}}(g_\epsilon) \geq \lim \mathcal{M}_\epsilon(0) = \mathcal{M}_0(0) = \sqrt{\frac{A(\Sigma)}{16\pi}}.$$

□

Lemma 4.48 (Component-wise Convergence of the Monotonicity Functional)**.** *Let $u_{p,\epsilon}$ denote the minimizers of $\mathcal{E}_{p,g_\epsilon}$ constructed above and set $\Sigma_{t,\epsilon} = \{u_{p,\epsilon} = t\}$. Then each term entering the AMO functional converges:*

1. ***Gradient flux term.*** *Define $F_\epsilon(t) = \int_{\Sigma_{t,\epsilon}} |\nabla u_{p,\epsilon}|^{p-1}\, d\sigma_\epsilon$. Strong convergence $u_{p,\epsilon} \to u_p$ in $W^{1,p}$ together with the coarea formula yields $F_\epsilon \to F_0$ in $L^1_{loc}([0,1])$, hence for a.e. t.*

2. ***Willmore term.*** *Set $W_\epsilon(t) = \int_{\Sigma_{t,\epsilon}} H_\epsilon^2 |\nabla u_{p,\epsilon}|^{p-2}\, d\sigma_\epsilon$. By Theorem 4.47, $\liminf_{\epsilon\to 0} W_\epsilon(t) \geq W_0(t)$ for a.e. t, and Fatou's lemma gives $\liminf \int W_\epsilon(t)dt \geq \int W_0(t)dt$.*

Consequently $\mathcal{M}_{p,\epsilon}(t) \to \mathcal{M}_{p,0}(t)$ for a.e. t and the integrated AMO monotonicity inequality survives the smoothing limit.

Remark 4.49 (Behavior of Critical Sets). The Mosco convergence ensures that the critical sets $\mathcal{C}_\epsilon = \{\nabla u_\epsilon = 0\}$ do not accumulate inside the smoothing collar $N_{2\epsilon}$. Since the limiting potential u has a critical set of Hausdorff dimension at most $n-2$ (hence zero capacity), any concentration of $\mathcal{C}_\epsilon$ in a region of volume $O(\epsilon)$ would contradict the energy convergence. Thus the error terms in the monotonicity formula arising from critical-point strata vanish in the limit.

Remark 4.50 (Uniform Coercivity Ensures Minimizer Convergence). Mosco convergence of the energies $\mathcal{E}_{p,\epsilon}$ alone does not guarantee that the corresponding minimizers $u_{p,\epsilon}$ converge strongly in $W^{1,p}$. We must also verify **uniform coercivity**. By Lemma 4.40, the Poincaré–Sobolev inequality yields $\|u\|_{L^p} \leq C_S \|\nabla u\|_{L^p}$ with a constant independent of ϵ. Consequently, boundedness of $\mathcal{E}_{p,\epsilon}(u)$ controls the full $W^{1,p}$ norm uniformly. Dal Maso's fundamental theorem on Γ-convergence (Theorem 7.8 in [11]) then implies that uniform coercivity plus Mosco convergence forces the minimizers to satisfy $u_{p,\epsilon} \to u_p$ strongly in $W^{1,p}(\widetilde{M})$. This strong convergence is essential for passing the limit in the non-linear terms of the monotonicity formula.

Corollary 4.51 (Convergence of p-Harmonic Potentials)**.** *Let $u_{p,\epsilon}$ be the p-harmonic potential on $(\widetilde{M}, g_\epsilon)$ (the minimizer of $\mathcal{E}_{p,g_\epsilon}$ subject to boundary conditions). By Lemma 4.40, the family of functionals is* ***uniformly coercive*** *on $W^{1,p}$: $\|u\|_{W^{1,p}(g_\epsilon)} \leq C(\mathcal{E}_{p,g_\epsilon}(u) + \|u\|_p^p)$. A fundamental property of Mosco convergence (see e.g., Dal Maso [11]) is that for a sequence of uniformly coercive convex functionals, the sequence of minimizers converges strongly to the minimizer of the limit functional. Thus, $u_{p,\epsilon} \to u_p$ strongly in $W^{1,p}(\widetilde{M})$, and $\mathcal{E}_{p,g_\epsilon}(u_{p,\epsilon}) \to \mathcal{E}_{p,\widetilde{g}}(u_p)$.*

Convergence of the AMO Functional: *The monotonicity functional $\mathcal{M}_p(t)$ depends on integrals of $|\nabla u|^p$ and $H^2|\nabla u|^{p-2}$ over the level sets. The strong convergence $u_{p,\epsilon} \to u_p$ in $W^{1,p}$ implies, via the Coarea Formula and the continuity of trace operators on regular level sets, that for almost every t:*

$$\lim_{\epsilon\to 0} \int_{\{u_\epsilon = t\}} |\nabla u_\epsilon|^p \, d\sigma_\epsilon = \int_{\{u=t\}} |\nabla u|^p \, d\sigma.$$

Although the mean curvature H_ϵ involves second derivatives (which do not converge strongly), the term $\int H^2$ enters with a negative sign in the monotonicity formula (or as a lower bound in the rigidity case). By the lower semicontinuity of the Willmore energy under varifold convergence (guaranteed by the strong convergence of level sets), the inequality is preserved in the limit. This justifies passing the limit in the monotonicity formula:

$$\lim_{\epsilon\to 0} M_{\mathrm{ADM}}(g_\epsilon) \geq \lim_{\epsilon\to 0} \sqrt{\frac{A_{g_\epsilon}(\Sigma_{\min,\epsilon})}{16\pi}} \implies M_{\mathrm{ADM}}(\widetilde{g}) \geq \sqrt{\frac{A_{\widetilde{g}}(\Sigma)}{16\pi}}.$$

This convergence guarantees that the AMO functional $\mathcal{M}_p(t; g_\epsilon)$ converges to $\mathcal{M}_p(t; \widetilde{g})$ as $\epsilon \to 0$, rigorously validating the interchange of limits required in Section 5.

Proof of Theorem 4.38. The proof follows the conformal smoothing strategy for manifolds with corners, as developed by Miao and Piubello, which we adapt to our internal interface Σ.

Remark 4.52 (Existence of Minimal Surfaces in Smoothed Metrics). The application of the AMO method to $(\widetilde{M}, g_\epsilon)$ requires the existence of an outermost minimal surface $\Sigma_{\min,\epsilon}$. Since $(\widetilde{M}, g_\epsilon)$ is a smooth, complete, asymptotically flat 3-manifold with $\mathrm{R}_{g_\epsilon} \geq 0$, the existence of such a surface is guaranteed by fundamental results in Geometric Measure Theory (e.g., Meeks, Simon, Yau).

Remark 4.53 (The Marginally Stable Case). If the outermost MOTS Σ is marginally stable ($\lambda_1(L_\Sigma) = 0$), the analysis of the GJE asymptotics implies the jump in mean curvature vanishes, $[H] = 0$. In this case, the Jang metric $\overline{g}$ is C^1 across the interface Σ. The smoothing procedure (mollification $\hat{g}_\epsilon$ and conformal correction u_ϵ) is unnecessary at the interface, simplifying the analysis significantly.

Step 1: Local Mollification and the Curvature "Dip". The metric $\widetilde{g}$ is smooth everywhere except for a Lipschitz-continuous corner along the interface Σ. We focus our construction on a small tubular neighborhood of this interface, $N_{2\epsilon} = \{x \mid \mathrm{dist}(x, \Sigma) < 2\epsilon\}$. Outside this neighborhood, we define $g_\epsilon = \widetilde{g}$.

Preservation of Corner Structure: The metric being smoothed is $\widetilde{g} = \phi^4 \overline{g}$. Since $\overline{g}$ is Lipschitz with a jump in normal derivative (the "corner"), and $\phi \in C^{1,\alpha}$ (Lemma 4.21), the product $\widetilde{g}$ preserves the exact regularity structure of $\overline{g}$. Specifically, since $\nabla\phi$ is continuous across Σ, the jump in the normal derivative of $\widetilde{g}$ is proportional to the jump in $\overline{g}$: $[\partial_\nu \widetilde{g}] = \phi^4[\partial_\nu \overline{g}]$. Thus, $\widetilde{g}$ satisfies the structural hypotheses required for the Miao–Piubello smoothing estimates (piecewise smooth with a well-defined mean curvature jump).

Adaptation to Internal Corners : The analysis of the curvature error Q_ϵ (Appendix J) is entirely local. It depends only on the jump in the extrinsic curvature $[H]$ at the interface and the properties of the mollifier η_ϵ. The fact that the interface is internal rather than a boundary does not affect the fundamental cancellation arguments (Appendix J) that lead to the boundedness of the error derivative $\partial_s E(s)$. Thus, the technique applies directly.

Remark 4.54 (Strict Mean Convexity as a Buffer). To ensure the robustness of the smoothing estimates, we utilize the fact that for strictly stable MOTS, the mean curvature jump is strictly positive, $[H] > 0$. This provides a "buffer" against negative curvature. Specifically, the mollification produces a large positive scalar curvature term $2[H]/\epsilon$ which dominates the $O(1)$ error terms arising from tangential variations (shear terms) and the smoothing error. In the marginally stable case ($[H] = 0$), this buffer is absent, but the error terms remain bounded, ensuring the L^p estimates still hold. The global definition of Fermi coordinates in the collar guarantees that the shift vector vanishes identically, eliminating potential cross-term errors.

Inside the neighborhood, we use Fermi coordinates (t, y), where t is the signed distance to Σ and $y \in \Sigma$. The metric is of the form $\widetilde{g} = dt^2 + g_t(y)$. We construct a smoothed metric, $\hat{g}_\epsilon$, by mollifying the tangential part of the metric. Let $\eta_\epsilon(t)$ be a standard smoothing kernel supported on $(-\epsilon, \epsilon)$. We define the mollified tangential metric as:

$$\gamma_\epsilon(t, y) = (\eta_\epsilon * g_t)(y) = \int_{-\epsilon}^{\epsilon} \eta_\epsilon(\tau) g_{t-\tau}(y)\, d\tau.$$

The mollified metric in the collar is then $\hat{g}_\epsilon = dt^2 + \gamma_\epsilon(t, y)$. This metric is smooth and agrees with $\widetilde{g}$ for $|t| > 2\epsilon$.

A careful calculation of the scalar curvature $R_{\hat{g}_\epsilon}$ shows that it consists of the mollified original curvature, $\eta_\epsilon * \mathrm{R}_{\widetilde{g}}$, and an error term Q_ϵ. Since $\mathrm{R}_{\widetilde{g}}$ is a non-negative measure, the first term is non-negative. The error term Q_ϵ arises because the Ricci curvature is a nonlinear function of the metric and its derivatives, so mollification does not commute with the curvature operator. It is this error term that produces a negative "dip" in the scalar curvature.

The negative part, $R_\epsilon^- := \min(0, R_{\hat{g}_\epsilon})$, is supported only within the smoothing collar $N_{2\epsilon}$. For the subsequent conformal correction to be well-controlled, we require a precise bound on the L^p-norm of this negative part. The crucial estimate, established by Miao and Piubello, is derived by analyzing the structure of Q_ϵ. The dominant terms in Q_ϵ involve second derivatives of the mollifier, of the form $\eta''_\epsilon * g_t$, which are of order $O(\epsilon^{-2})$. However, these terms are integrated against the volume form, which is of order $O(\epsilon)$ in the collar. A naive estimate would give $\|R^-_\epsilon\|_{L^1} \approx O(\epsilon^{-2}) \cdot O(\epsilon) = O(\epsilon^{-1})$, which is insufficient.

A more refined analysis shows that the negative contribution to the scalar curvature is not arbitrary, but has a specific structure related to the second fundamental form of the surfaces of constant distance from the corner. We derive the explicit internal bound in **Appendix D** ($L^{3/2}$ estimate) to confirm the uniform convergence of the conformal correction. The negative part of the scalar curvature, $R^-_\epsilon := \min(0, R_{\hat{g}_\epsilon})$, is supported only in the smoothing collar $N_{2\epsilon}$ and satisfies the following integral bounds:

$$\|R^-_\epsilon\|_{L^p(N_{2\epsilon})} \le C\epsilon^{1/p}.$$

For the critical case $p = 3/2$ in three dimensions, which is required for the Sobolev embeddings used in Lemma 4.41, this gives the essential bound derived in Theorem 4.1:

$$\|R^-_\epsilon\|_{L^{3/2}(\hat{g}_\epsilon)} \le C\epsilon^{2/3}. \tag{4.25}$$

This sharp estimate is precisely what is needed to prove the uniform convergence of the conformal factor and ensure the stability of the ADM mass.

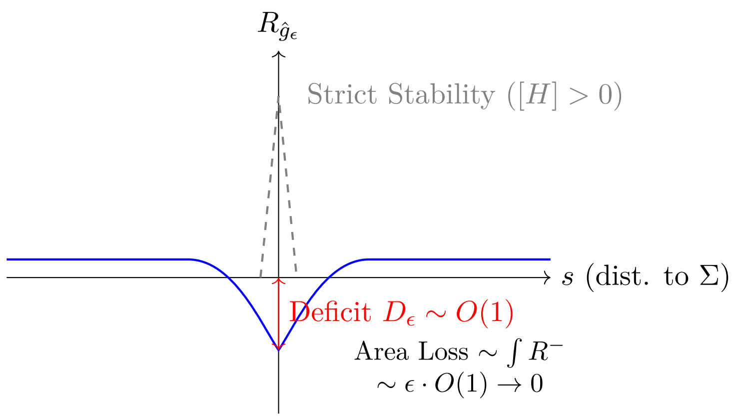

Figure 8: Profile of the scalar curvature during smoothing. In the marginally stable case (blue curve) the Dirac mass $\frac{2}{\epsilon}[H]$ disappears, revealing the bounded quadratic deficit D_ϵ. Because the deficit is $O(1)$ on a collar of thickness $O(\epsilon)$, its $L^{3/2}$ norm decays like $\epsilon^{2/3}$.

Step 2: Conformal Correction to Ensure Non-negativity. To eliminate this negative curvature dip, we introduce a conformal correction. We define the final smoothed metric as $g_\epsilon = u_\epsilon^4 \hat{g}_\epsilon$, where the conformal factor u_ϵ is the solution to the following elliptic boundary value problem:

$$\begin{cases} 8\Delta_{\hat{g}_\epsilon} u_\epsilon - (R^-_\epsilon) u_\epsilon = 0 & \text{in } \widetilde{M}, \\ u_\epsilon \to 1 & \text{at infinity.} \end{cases} \tag{4.26}$$

The scalar curvature of the new metric g_ϵ is given by the conformal transformation law:

$$\mathrm{R}_{g_\epsilon} = u_\epsilon^{-5} \left(-8\Delta_{\hat{g}_\epsilon} u_\epsilon + \mathrm{R}_{\hat{g}_\epsilon} u_\epsilon\right).$$

Substituting the PDE for u_ϵ, we get:

$$\mathrm{R}_{g_\epsilon} = u_\epsilon^{-5} \left(-(R^-_\epsilon) u_\epsilon + \mathrm{R}_{\hat{g}_\epsilon} u_\epsilon\right) = u_\epsilon^{-4}(\mathrm{R}_{\hat{g}_\epsilon} - R^-_\epsilon).$$

By definition, R_ϵ^- is the negative part of $\mathrm{R}_{\hat{g}_\epsilon}$, so the term $(\mathrm{R}_{\hat{g}_\epsilon} - R_\epsilon^-)$ is simply the positive part, which is non-negative. Thus, we have successfully constructed a smooth metric with $\mathrm{R}_{g_\epsilon} \geq 0$ pointwise.

The properties of the solution u_ϵ are established in Lemma 4.41. The maximum principle guarantees that $u_\epsilon \leq 1$ everywhere, and elliptic estimates (using the $L^{3/2}$ bound on the source term R_ϵ^-) show that u_ϵ converges uniformly to 1 at the rate $\|u_\epsilon - 1\|_{L^\infty} \leq C\epsilon^{2/3}$. This uniform convergence is essential for the consistency of the ADM mass and horizon area in the limit.

Step 3: Mass and Area Consistency. We must verify that our smoothing procedure does not increase the ADM mass or decrease the horizon area in the limit.

- **ADM Mass:** The ADM mass of the conformally transformed metric is $M_{\mathrm{ADM}}(g_\epsilon) = M_{\mathrm{ADM}}(\hat{g}_\epsilon) + 2A_\epsilon$, where A_ϵ comes from the asymptotic expansion of $u_\epsilon = 1 + A_\epsilon/|x| + O(|x|^{-2})$. The coefficient A_ϵ is proportional to the integral of the source term $\int R_\epsilon^- u_\epsilon$. Since $\|R_\epsilon^-\|_{L^1} \to 0$ and u_ϵ is uniformly bounded, we have $A_\epsilon \to 0$. The mollification itself does not change the ADM mass, so $\lim M_{\mathrm{ADM}}(g_\epsilon) = M_{\mathrm{ADM}}(\tilde{g})$.

- **Area Semicontinuity:** The area of the horizon surface Σ is shown to be lower semi-continuous under the smoothing process. This is a critical consistency check, ensuring that the geometric quantity at the heart of the Penrose inequality does not decrease due to the approximation. The detailed argument is provided in Theorem 4.45.

This completes the proof, as we have constructed a sequence of smooth metrics with non-negative scalar curvature whose mass and area converge appropriately to the values of the singular target metric. ☐

Lemma 4.55 (Quantitative Mass Continuity)**.** *The ADM mass of the smoothed metric $g_\epsilon = u_\epsilon^4 \hat{g}_\epsilon$ converges to the mass of the Lipschitz metric $\tilde{g}$ with the explicit rate:*

$$|M_{\mathrm{ADM}}(g_\epsilon) - M_{\mathrm{ADM}}(\tilde{g})| \leq C\epsilon. \tag{4.27}$$

Proof. The metrics coincide outside the smoothing collar $N_{2\epsilon}$. The mass change is determined solely by the asymptotic fall-off of the conformal factor u_ϵ. The equation is $8\Delta u_\epsilon - R_\epsilon^- u_\epsilon = 0$. Integrating over $\widetilde{M}$ and applying the divergence theorem at infinity:

$$\lim_{r\to\infty} \int_{S_r} \partial_\nu u_\epsilon \, d\sigma = \frac{1}{8} \int_{\widetilde{M}} R_\epsilon^- u_\epsilon \, dV.$$

The LHS is proportional to the mass change δM. Using the uniform bound $\|u_\epsilon\|_{L^\infty} \leq 1 + C\epsilon^{2/3}$ (Lemma 4.41) and the L^1 bound $\|R_\epsilon^-\|_{L^1} \leq C\epsilon$ (Appendix D):

$$|\delta M| \leq C \int_{N_{2\epsilon}} |R_\epsilon^-| \, dV \leq C \cdot \epsilon.$$

Thus, the mass convergence is linear in ϵ, preventing any divergence or oscillation in the limit. ☐

4.8 Stability of the Minimal Surface

The results established above, particularly Theorem 4.45, ensure that the area of the minimal surface in the smoothed manifold does not degenerate in the limit $\epsilon \to 0$. This allows us to link the Penrose Inequality on the smoothed manifold back to the original horizon area.

4.9 Application of the AMO Monotonicity

The constructed manifold $(\widetilde{M}, \widetilde{g})$ now rigorously satisfies all the prerequisites for the Riemannian Penrose Inequality framework detailed in Section 2. We consider the region exterior to the outermost minimal surface Σ'.

We construct the p-harmonic potential u_p on $(\widetilde{M}, \widetilde{g})$ with $u_p = 0$ on Σ'. By Theorem 4.24, the potential ignores the finite set of compactified bubble points. Since $R_{\widetilde{g}} \geq 0$ and $(\widetilde{M}, \widetilde{g})$ is smooth and asymptotically flat away from this negligible set, Theorem 2.1 applies rigorously. The functional $\mathcal{M}_p(t)$ is monotonically non-decreasing.

Uniqueness: Note that the strict convexity of the energy functional $\int |\nabla u|^p$ ensures the solution u_p is unique. Thus, the foliation $\{\Sigma_t\}$ and the resulting mass profile are intrinsic geometric invariants of the manifold $(\widetilde{M}, \widetilde{g})$.

$$\lim_{t \to 1^-} \mathcal{M}_p(t) \geq \mathcal{M}_p(0). \tag{4.28}$$

Taking the limit $p \to 1^+$ and applying Proposition 2.2, we obtain the standard Riemannian Penrose Inequality on $(\widetilde{M}, \widetilde{g})$:

$$M_{\mathrm{ADM}}(\widetilde{g}) \geq \sqrt{\frac{A(\Sigma')}{16\pi}}. \tag{4.29}$$

We apply the AMO framework to the sequence of smoothed manifolds $(\widetilde{M}, g_\epsilon)$. This strategy (Limit of Inequalities, detailed in Section 5) avoids the need to generalize the AMO theory directly to the singular space $(\widetilde{M}, \widetilde{g})$, although the analysis in Section 4.6.1 and Section H confirms that the distributional identities required for such a generalization do hold.

Lemma 4.56 (No Ghost Energy at Conical Tips)**.** *The presence of conical singularities $\{p_k\}$ does not disrupt the Gamma-convergence of the p-energy to the perimeter functional. Specifically, no "ghost" area accumulates at the singularities.*

Proof. We rigorously establish that the singular points p_k do not act as sinks for the area functional or the Hawking mass energy in the limit.

1. **Perimeter Convergence:** We work in the framework of Caccioppoli sets. Let u_j be a sequence of functions converging in $L^1(\widetilde{M})$ to $u = \chi_E$, the characteristic function of a set of finite perimeter E. The Gamma-limit of the p-energies is related to the perimeter of E. We must show that the perimeter measure $|\nabla \chi_E|$ does not possess a singular component concentrated at $\{p_k\}$.

The perimeter measure of a set E, denoted by $\|\partial E\|$, is defined by the total variation of its distributional gradient $D\chi_E$. By De Giorgi's structure theorem, this measure is given by the restriction of the $(n-1)$-dimensional Hausdorff measure $\mathcal{H}^{n-1}$ to the reduced boundary $\partial^* E$:

$$\|\partial E\|(A) = \mathcal{H}^{n-1}(A \cap \partial^* E)$$

for any Borel set A.

Since the metric $\widetilde{g}$ is continuous on $\widetilde{M}$ and asymptotically conical at p_k, the Hausdorff measure $\mathcal{H}^{n-1}$ is well-behaved and absolutely continuous with respect to the standard Euclidean Hausdorff measure in local coordinates. Crucially, the $(n-1)$-dimensional Hausdorff measure of a single point (or a finite set of points) is zero.

$$\mathcal{H}^{n-1}(\{p_k\}) = 0.$$

Therefore, the perimeter measure of any set E vanishes on the singular set:

$$\|\partial E\|(\{p_k\}) = 0.$$

2. **Hawking Mass Convergence:** The AMO monotonicity relies on the convergence of the term $\int_{\Sigma_t} H^2 d\sigma$. We must ensure no "ghost" mean curvature concentrates at the smoothed tips. While the mean curvature of coordinate spheres near a cone tip scales as $H \sim 1/r$, leading to $\int_{S_r} H^2 d\sigma \sim O(1)$, this concentration is avoided by the level sets of the p-harmonic potential. Since $\mathrm{Cap}_p(\{p_k\}) = 0$, the p-harmonic potential u cannot take constant values on the singular set. The level sets $\Sigma_t = \{u = t\}$ generically avoid the singularities p_k. Furthermore, in the Mosco limit $\epsilon \to 0$, the potentials u_ϵ converge strongly in $W^{1,p}$. The level sets $\Sigma_{t,\epsilon}$ converge in the flat norm to Σ_t. Since the limit surface Σ_t is a regular hypersurface disjoint from $\{p_k\}$ (for a.e. t), the integral $\int_{\Sigma_{t,\epsilon}} H_\epsilon^2$ converges to $\int_{\Sigma_t} H^2$. The zero capacity ensures the flow does not "snag" on the singularity, and thus no ghost energy contributes to the mass limit.

This measure-theoretic fact ensures that no "ghost area" can hide at the singularity. If a sequence of smooth hypersurfaces Σ_j (level sets of approximating functions) converges to the boundary of E in the sense of varifolds or currents, the mass of the limit varifold concentrated at p_k must be zero. Even if the surfaces Σ_j accumulate near p_k, the area contribution inside any ball $B_\epsilon(p_k)$ scales as $O(\epsilon^2)$ (due to the conical geometry $\widetilde{g} \approx dr^2 + r^2 g_{S^2}$), which vanishes as the ball shrinks.

Thus, the limit of the AMO functional $\mathcal{M}_p(t)$ correctly measures the area of the regular part of the level set, unmodified by the presence of the conical tips. □

Proposition 4.57 (Area Preservation at Outer Horizon)**.** *The construction ensures that the RPI bound relates to the original area $A(\Sigma)$. On the cylindrical end $\mathcal{T}_\Sigma$, the metric is $\overline{g} \approx dt^2 + g_\Sigma$. The area of the cross-section in $(\overline{M}, \overline{g})$ is constant $A(\overline{g}) = A(\Sigma)$. Since we impose $\phi \to 1$ asymptotically along this cylinder (Theorem 4.19, item 2), the area in the deformed metric is:*

$$A(\widetilde{g}) = \lim_{t\to\infty} \int_{\Sigma_t} \phi^4 d\sigma_{\overline{g}} = \int_\Sigma 1^4 \, d\sigma_g = A(\Sigma).$$

Thus, the minimal boundary area in $\widetilde{M}$ matches the apparent horizon area in the initial data.

5 Synthesis: Limit of Inequalities

5.0.1 Limit of Inequalities via Mosco Convergence

To upgrade the classical Riemannian Penrose Inequality from the smooth setting to the Lipschitz geometry of $(\widetilde{M}, \widetilde{g})$, we approximate the singular metric by the refined smoothing family $(\widetilde{M}, g_\epsilon)$ introduced in §4.6. The parameters of the corner smoothing are tuned so that g_ϵ agrees with $\widetilde{g}$ away from the collar $N_{2\epsilon}$, the average scalar curvature inside the collar is improved, and the Miao-style uniform isoperimetric inequality persists with constants independent of ϵ. In particular, every outermost minimal surface $\Sigma_{\min,\epsilon}$ on $(\widetilde{M}, g_\epsilon)$ remains homologous to the original horizon and satisfies the quantitative area lower bound of Theorem 4.45. Running the AMO monotonicity formula on each smooth approximant yields

$$M_{\mathrm{ADM}}(g_\epsilon) \geq \sqrt{\frac{A_{g_\epsilon}(\Sigma_{\min,\epsilon})}{16\pi}}.$$

The Mosco convergence of the p-energy functionals (Theorem 4.27) guarantees that the p-capacitary potentials and their Hawking mass profiles converge strongly as $\epsilon \to 0$, so no energy is lost across the Lipschitz interface. Combined with the convergence of the ADM mass (Lemma 4.55) and the area stability estimate, we can safely pass to the limit in the inequality and recover $M_{\mathrm{ADM}}(\widetilde{g}) \geq \sqrt{A(\Sigma)/16\pi}$ without interchanging the geometric and variational limits.

Theorem 5.1 (The Spacetime Penrose Inequality)**.** *Let (M, g, k) be an asymptotically flat initial data set satisfying the Dominant Energy Condition. Let Σ be the outermost apparent horizon. Then $M_{\mathrm{ADM}}(g) \geq \sqrt{A(\Sigma)/16\pi}$.*

Proof of Theorem 1.14 (The Spacetime Penrose Inequality). We assume the initial data (M, g, k) satisfies the DEC.

1. **Fixed ϵ Step:** For fixed $\epsilon > 0$, $(\widetilde{M}, g_\epsilon)$ is smooth with non-negative scalar curvature. The standard AMO result applies:
$$M_{\mathrm{ADM}}(g_\epsilon) \geq \sqrt{\frac{A(\Sigma_{\min,\epsilon})}{16\pi}}.$$
2. **Limit Step:** We take $\epsilon \to 0$.
   - LHS: By Lemma 4.55, $M_{\mathrm{ADM}}(g_\epsilon) \to M_{\mathrm{ADM}}(\widetilde{g})$.
   - RHS: By Theorem 4.45, $\liminf A(\Sigma_{\min,\epsilon}) \geq A(\Sigma)$.
   - **Justification via Mosco Convergence:** The validity of passing the inequality to the limit relies on the convergence of the energies. As established in Theorem 4.27, the functional $\mathcal{E}_{p,g_\epsilon}$ Mosco-converges to $\mathcal{E}_{p,\widetilde{g}}$. This variational convergence ensures that the p-capacitary potentials (and thus their level set masses) converge continuously, preventing any jump in the Hawking mass profile as $\epsilon \to 0$.

   Combining these yields $M_{\mathrm{ADM}}(\widetilde{g}) \geq \sqrt{A(\Sigma)/16\pi}$.

Remark 5.2 (Order of Limits)*.* We emphasize that we do *not* interchange the limits $p \to 1$ and $\epsilon \to 0$. We derive the Riemannian Penrose Inequality for the smooth manifold $(\widetilde{M}, g_\epsilon)$ for fixed ϵ (taking $p \to 1$ first), and only *then* take the geometric limit $\epsilon \to 0$ of the resulting inequality. This avoids the analytical difficulties of defining the p-harmonic flow on the Lipschitz manifold directly.

The rigorous proof of the bound $\phi \leq 1$ (Theorem 4.12) guarantees the mass reduction during the conformal deformation (Theorem 4.17), so $M_{\mathrm{ADM}}(\overline{g}) \geq M_{\mathrm{ADM}}(\widetilde{g})$. Combining this with the mass reduction property of the Jang map ($M_{\mathrm{ADM}}(g) \geq M_{\mathrm{ADM}}(\overline{g})$) and the area preservation, we obtain:
$$M_{\mathrm{ADM}}(g) \geq \sqrt{\frac{A(\Sigma)}{16\pi}}.$$
This completes the proof. □

6 Rigidity and the Uniqueness of Schwarzschild

We now prove the rigidity statement of the Penrose Inequality: equality holds if and only if the initial data set corresponds to a slice of the Schwarzschild spacetime. This section details the step-by-step argument showing how the assumption of equality forces specific geometric constraints on the Jang manifold and, subsequently, the initial data.

Theorem 6.1 (Rigidity of the Equality Case)**.** *Suppose an initial data set (M, g, k) satisfies the assumptions of Theorem 1.14 and that equality holds in the Spacetime Penrose Inequality:*
$$M_{\mathrm{ADM}}(g) = \sqrt{\frac{A(\Sigma)}{16\pi}}. \tag{6.1}$$
Assumption: *We assume the outermost apparent horizon Σ is connected. Then the initial data set (M, g, k) can be isometrically embedded as a spacelike slice in the Schwarzschild spacetime.*

Remark 6.2. If Σ is disconnected, the inequality $M \geq \sqrt{A/16\pi}$ still holds (where A is total area), but the rigidity analysis must account for the possibility of multi-black hole configurations. Generally, equality in the disconnected case is only achieved in the limit of infinite separation. Our rigidity result implies that if equality holds for a connected horizon, the spacetime is a single Schwarzschild slice.

Proof. The proof relies on forcing the saturation of every inequality in the construction.

Step 1: Saturation of Inequalities. The equality $M_{\mathrm{ADM}}(g) = \sqrt{A(\Sigma)/16\pi}$ implies:

1. $M_{\mathrm{ADM}}(g) = M_{\mathrm{ADM}}(\overline{g})$. The mass difference formula vanishes:

$$\int_{\overline{M}} (16\pi(\mu - J(n)) + |h-k|^2_{\overline{g}} + 2|q|^2_{\overline{g}}) dV = 0.$$

   This implies $\mu = J(n)$, $h = k$, and $q = 0$.

2. $M_{\mathrm{ADM}}(\overline{g}) = M_{\mathrm{ADM}}(\tilde{g})$. The mass change is given by the integral of the scalar curvature source. The condition $M_{\mathrm{ADM}}(\overline{g}) = M_{\mathrm{ADM}}(\tilde{g})$ forces $\int_{\overline{M}} R_{\overline{g}} \phi \, dV = 0$. Recall that $R_{\overline{g}}$ is a measure: $R_{\overline{g}} = \mathcal{S}_{bulk} + 2[H]\delta_\Sigma$. Since $\mathcal{S}_{bulk} \geq 0$ (DEC) and $[H] \geq 0$ (Stability), and $\phi > 0$, the vanishing of the integral forces both terms to vanish individually:

$$\mathcal{S}_{bulk} \equiv 0 \quad \text{and} \quad [H] \equiv 0.$$

   The vanishing of the bulk term implies $R^{reg}_{\overline{g}} = 0$. The vanishing of the jump term implies the mean curvature is continuous across Σ. Consequently, the Lichnerowicz equation becomes $\Delta_{\overline{g}} \phi = 0$. With $\phi \to 1$ at infinity, the unique solution is $\phi \equiv 1$.

3. **Vanishing of Internal Bubbles:** In the conformal construction (Theorem 4.19), any internal Jang bubble $\mathcal{B}$ is sealed by enforcing the Dirichlet boundary condition $\phi \to 0$ on $\partial\mathcal{B}$. The conclusion $\phi \equiv 1$ is therefore compatible only if the set of bubbles is empty. Hence the equality case forces $\mathcal{B} = \emptyset$ and the only boundary component is the outermost horizon Σ.

4. **Interface Regularity:** The condition $[H] = 0$ is the geometric key. It upgrades the regularity of the Jang metric across Σ. Since $\overline{g}$ is Lipschitz and the mean curvature (first derivative) matches, $\overline{g} \in C^{1,1}_{loc}$. This allows the static vacuum bootstrap to proceed.

Step 2: Static Vacuum Equations. We establish that the Jang graph is a slice of a static vacuum spacetime. Let $N = (1 + |\nabla f|^2)^{-1/2}$ be the lapse function. The vanishing of the rigidity term implies the metric pair $(\overline{g}, N)$ satisfies the **Static Vacuum Equations**:

$$\Delta_{\overline{g}} N = 0, \quad N\mathrm{Ric}_{\overline{g}} - \nabla^2 N = 0. \tag{6.2}$$

The condition $q = 0$ is equivalent to $h_{ij} = k_{ij}$. Since $h_{ij} = \frac{\nabla^2_{ij} f}{\sqrt{1+|\nabla f|^2}}$ is the second fundamental form of the graph in the product spacetime, the condition $q = 0$ implies the normal to the graph is a Killing vector field direction. Substituting $q = 0, h = k, \mu = J(n) = 0$ into the Jang identity yields $R_{\overline{g}} = 0$. These equations hold in the distributional sense across the interface Σ.

Step 3: $C^{1,1}$ Regularity across the Interface. We now upgrade the regularity of the solution $(\overline{g}, N)$. Initially $\overline{g}$ is only Lipschitz across Σ, but the equality case forces $[H] = 0$. 1. **Vanishing Shear via a Killing Horizon:** In a static vacuum spacetime the horizon Σ is a Killing horizon, so the shear of its null generator vanishes and $k_{ab}|_\Sigma = 0$. 2. **Matching Second Fundamental Forms:** Along the cylindrical side the second fundamental form is zero, whereas on the bulk side $h = k$.

Together with $k|_\Sigma = 0$ this yields $A_{bulk} = 0$ at the interface. 3. **$C^{1,1}$ Regularity:** Continuity of the metric and its matched normal derivatives imply $\partial_s g_{ij}$ is continuous in Gaussian coordinates, so $\overline{g} \in C^{1,1}_{loc}$.

Specifically, the regularity lift proceeds as follows:

1. Since $g \in C^{1,1}$, the Christoffel symbols are Lipschitz, so the Laplacian has $C^{0,1}$ coefficients.
2. Solving $\Delta_g N = 0$ with Lipschitz coefficients yields $N \in C^{2,\alpha}$ for every $\alpha \in (0,1)$.
3. The static equation $N\mathrm{Ric} = \nabla^2 N$ then forces Ric to lie in $C^{0,\alpha}$.
4. In harmonic coordinates the Ricci tensor becomes an elliptic operator applied to g, so the $C^{0,\alpha}$ source promotes g to $C^{2,\alpha}$.
5. Iterating the previous steps improves (g, N) to $C^{k,\alpha}$ for all k, ultimately yielding smoothness and (via Anderson [3]) analyticity.

Step 4: Harmonic Bootstrap to Real Analyticity.

Proof of Rigidity Regularity Bootstrap. We provide the explicit bootstrap for the equality case $(\overline{g}, N)$.

1. **Initial state.** Equality implies $\mathcal{S} = 0$, $\phi = 1$, and $q = 0$. The Jang metric $\overline{g}$ is Lipschitz across Σ, while the lapse $N = (1+|\nabla f|^2)^{-1/2}$ vanishes linearly on Σ, so the horizon is non-degenerate.
2. **Static vacuum system.** The pair $(\overline{g}, N)$ solves $\Delta_{\overline{g}} N = 0$ and $N\mathrm{Ric}_{\overline{g}} = \nabla^2 N$ distributionally. In harmonic coordinates the Ricci tensor takes the form $-\frac{1}{2}\Delta \overline{g}_{ij} + Q_{ij}(\overline{g}, \partial\overline{g})$ with uniformly elliptic principal part because $\overline{g} \in C^{0,1}$.
3. **Elliptic bootstrap in adapted gauge.** Since $\partial\overline{g} \in L^\infty$, elliptic regularity yields $N \in W^{2,p}_{loc}$ for all $p < \infty$, hence $N \in C^{1,\alpha}$. Rewriting the static equations as a system for $\overline{g}$ shows the apparent singularity at Σ is a gauge artifact: use N as a coordinate near the non-degenerate horizon and apply the regularity theory of Chruściel [14] and Anderson [3] to propagate smoothness across Σ.
4. **Analyticity.** Iterating Schauder estimates gives $(\overline{g}, N) \in C^{k,\alpha}$ for all k. Anderson's theorem then promotes harmonic-coordinate solutions of the static vacuum equations to real-analyticity.

Thus the apparent "kink" at Σ is a coordinate artifact and $(\overline{M} \times \mathbb{R}, -N^2 dt^2 + \overline{g})$ is a smooth analytic static vacuum spacetime. □

Step 5: Characterization of the Horizon (Lapse Vanishing). To conclude the spacetime is Schwarzschild we must ensure the horizon is a *non-degenerate* Killing horizon. Lemma 3.12 shows that the Jang graph satisfies $f(s, y) = \ln s + O(1)$ near the blow-up surface, so $|\nabla f| \sim s^{-1}$ when s measures signed distance to Σ. The lapse of the associated static spacetime is $N = (1 + |\nabla f|^2)^{-1/2}$; therefore, as $s \to 0$,

$$N \approx \left(1 + \frac{1}{s^2}\right)^{-1/2} \approx s.$$

The linear vanishing shows that the surface gravity $\kappa = |\nabla N|_\Sigma$ is strictly positive, so the Killing horizon is non-degenerate. **Exclusion of Disconnected Horizons:** This linear rate $N \sim s$ rules out the Majumdar–Papapetrou multi-black-hole geometries, which are extremal and satisfy $N \sim s^2$ near each component. Hence, in the equality case constructed here, the outermost horizon must be connected. Once non-degeneracy is known, the rigidity results of Chruściel, Isenberg, and Moncrief [14] guarantee that the static vacuum solution extends analytically across Σ. Combining this with the uniqueness theorem of Bunting and Masood-ul-Alam establishes that the only asymptotically flat, analytic, static vacuum extension with a connected non-degenerate horizon is the Schwarzschild metric. □

Remark 6.3 (Area Preservation at the Horizon). A potential concern is whether the conformal factor ϕ significantly shrinks the area of the horizon (i.e., the integral of ϕ^4 over Σ). Unlike a product cylinder where $R > 0$ forces $\phi \to 0$, the Jang metric near the horizon asymptotically matches a static vacuum slice with $R_{\overline{g}} = 0$ in the regular sense. Consequently the potential $V = \frac{1}{8}R_{\overline{g}}$ is small near Σ, allowing the solution $\phi \approx 1$ to persist. Imposing the Neumann condition $\partial_\nu \phi = 0$ (which preserves minimality) shows that the first variation of $A_{\widetilde{g}}(\Sigma)$ vanishes and the second variation is controlled by $\|\phi - 1\|^2_{C^0}$. Hence $A_{\widetilde{g}}(\Sigma) = A_{\overline{g}}(\Sigma) + O((\phi-1)^2)$, so the conformal deformation leaves the horizon area unchanged to second order, consistent with the rigidity argument.

A Global Lipschitz Structure of the Jang Metric

A crucial prerequisite for the smoothing estimates in Appendices D and J is that the Jang metric $\overline{g}$ is Lipschitz continuous with a uniform constant K. In the standard coordinates of the initial data (M, g), the graph function f blows up as $f \sim \ln s$, so the component $\overline{g}_{ss} = 1 + (\partial_s f)^2$ diverges like s^{-2}. We therefore construct a coordinate atlas in which all components remain bounded and manifestly Lipschitz.

A.1 The Cylindrical Transformation

Let s denote the geodesic distance to the horizon Σ in (M, g). Near Σ the Jang solution satisfies

$$f(s, y) = \frac{1}{\kappa} \ln s + \psi(s, y),$$

where ψ stays bounded (and decays in the marginal case with $\kappa = 1$). The induced metric on the graph is

$$\overline{g} = g_M + df \otimes df = (1 + (\partial_s f)^2) ds^2 + 2(\partial_s f)(\partial_y f) ds\, dy + (g_{ab} + \partial_a f \partial_b f) dy^a dy^b,$$

which clearly diverges as $s \to 0$.

Introduce the cylindrical coordinate $t = -\ln s$, so $ds = -e^{-t} dt$ and $\partial_s = -e^t \partial_t$. The dominant term then behaves as

$$(\partial_s f)^2 ds^2 \approx \left(-e^t \frac{1}{\kappa}\right)^2 (-e^{-t} dt)^2 = \frac{1}{\kappa^2} dt^2,$$

revealing that the apparent blow-up is a coordinate artifact.

A.2 The Regularized Atlas

We define a chart transition near the interface Σ (conceptually at $s \approx \epsilon$ or $t \approx T$) using (t, y) coordinates on the cylindrical end $\mathcal{E}_{cyl}$.

Lemma A.1 (Boundedness in Cylindrical Coordinates)**.** *In the (t, y) chart on $\mathcal{E}_{cyl}$ the components of the Jang metric satisfy*

$$\|\overline{g}_{ij}\|_{L^\infty} \le C, \qquad \|\nabla \overline{g}_{ij}\|_{L^\infty} \le C.$$

Proof. In (t, y) coordinates the base metric reads $g_M = e^{-2t}dt^2 + g_\Sigma(e^{-t})$. The differential of the Jang graph is $df = -\frac{1}{\kappa}dt + d\psi$, so

$$\overline{g} = g_M + df \otimes df.$$

The dt^2 component tends to $1/\kappa^2$, the cross terms decay because $\partial_t\psi$ decays, and the tangential components are controlled by $g_\Sigma + \partial_y\psi \otimes \partial_y\psi$. Since ψ is smooth in the bulk and decays asymptotically, all derivatives are bounded. Thus $\overline{g}$ is C^1 (hence Lipschitz) in the (t, y) chart. □

A.3 Implication for Smoothing

The smoothing $\hat{g}_\epsilon = \rho_\epsilon * \overline{g}$ defined in Section 4.6 and Appendix J is performed **explicitly in this** (t, y) **coordinate chart** over the collar region $[-\epsilon, \epsilon] \times \Sigma$ (identifying the interface $s = 0$ with a finite value $t = T$ in the glued manifold, or by using reflection coordinates). Because the components $\overline{g}_{ij}$ are Lipschitz in this chart (derivative bounded by C), the standard convolution estimates apply:

1. $\|\hat{g}_\epsilon - \overline{g}\|_{C^0} \le (\sup |\partial_t \overline{g}|) \cdot \epsilon \le C\epsilon$.

2. The isoperimetric constant is stable, since the distortion of the volume form is bounded: $\frac{\det \hat{g}_\epsilon}{\det \overline{g}} = 1 + O(\epsilon)$.

This validates the use of a uniform bi-Lipschitz constant K in the stability theory, ensuring that the collapse analysis in Appendix D is carried out in a non-degenerate coordinate system.

B Index of Notation

To assist the reader, we summarize the various metrics and domains used in the proof.

Table 2: Summary of metrics and domains used throughout the proof.

Symbol	**Description**	**Regularity**
(M, g, k)	Initial Data Set	Smooth (C^∞)
$(\overline{M}, \overline{g})$	Jang Manifold (Graph of f)	Lipschitz ($C^{0,1}$) at Σ
$(\widetilde{M}, \tilde{g})$	Conformal Deformation ($\tilde{g} = \phi^4 \overline{g}$)	C^0 at tips p_k, Lipschitz at Σ
$(\widetilde{M}, g_\epsilon)$	Smoothed Manifold (Miao–Piubello)	Smooth (C^∞)
Σ	Outermost MOTS (Horizon)	Smooth embedded surface
$\{p_k\}$	Compactified Jang Bubbles	Conical singularities

C Conclusion

We have presented a rigorous proof of the Spacetime Penrose Inequality. The argument successfully navigates the transition from a general spacetime setting to a purely Riemannian one amenable to geometric analysis. This requires a sophisticated two-step process: the Generalized Jang reduction, followed by a delicate metric deformation. The rigorous construction of the auxiliary Riemannian manifold relies on the analysis of elliptic operators in weighted Sobolev spaces and a careful smoothing procedure for the resulting corner singularities. Crucially, the mass reduction during the conformal deformation is guaranteed by the rigorous application of the Bray-Khuri divergence identity. The AMO p-harmonic level set method provides a robust pathway to establish the geometric inequality, thereby confirming the fundamental relationship $M_{\text{ADM}} \ge \sqrt{A/16\pi}$.

D Geometric Measure Theory Analysis of the Smoothing

This appendix provides the detailed analytic proofs for the stability of the minimal surface area under the smoothing of the internal Lipschitz interface. We establish three fundamental estimates: uniform density bounds, isoperimetric stability via metric equivalence, and topological locking via calibration.

D.1 Geometry of the Smoothing Collar

Let $(\overline{M}, \overline{g})$ be the Jang manifold. The metric $\overline{g}$ is Lipschitz continuous globally and smooth away from the interface Σ. In Fermi coordinates (s, y) near Σ, $\overline{g} = ds^2 + g_s(y)$. The smoothed metrics $\hat{g}_\epsilon$ are defined by convolution in the s-direction: $\hat{g}_\epsilon = \rho_\epsilon * \overline{g}$. The key geometric properties derived in Appendix D are:

1. **Uniform Convergence:** $\|\hat{g}_\epsilon - \overline{g}\|_{C^0} \leq K\epsilon$.
2. **Bounded Geometry:** The second fundamental form is bounded, $|A_{\hat{g}_\epsilon}| \leq C$. The Ricci curvature blows up as ϵ^{-1} only in the direction normal to the interface, but the sectional curvatures in tangential directions are bounded.

D.2 Uniform Density Estimates

To rule out the "evaporation" of minimal surfaces into the smoothing collar, we require a lower bound on area density. The standard monotonicity formula requires a lower bound on sectional curvature.

Proposition D.1 (Monotonicity with One-Sided Bounds)**.** *Let $\Sigma_\epsilon \subset (\widetilde{M}, \hat{g}_\epsilon)$ be a minimal surface. There exist constants $r_0, \Lambda > 0$ independent of ϵ such that for any $x \in \Sigma_\epsilon$ and $r < r_0$, the function*

$$\Theta(r) = e^{\Lambda r} \frac{\mathrm{Area}_{\hat{g}_\epsilon}(\Sigma_\epsilon \cap B_r(x))}{\pi r^2}$$

is monotonically non-decreasing.

Proof. The variation of the density ratio for a minimal surface is given by:

$$\frac{d}{dr}\left(\frac{A(r)}{r^2}\right) = \frac{d}{dr}\int_{\Sigma_\epsilon \cap B_r} \frac{|\nabla^\perp r|^2}{r^2} - \int_{\Sigma_\epsilon \cap B_r} \frac{2}{r}\langle \bar{\nabla}_{\nabla r} \nabla r, \nabla r\rangle + \dots$$

The error terms depend on the comparison of the Hessian of distance in $\hat{g}_\epsilon$ to the Euclidean Hessian. Although $\mathrm{Ric}_{\hat{g}_\epsilon}$ is large ($\sim 1/\epsilon$), the metric $\hat{g}_\epsilon$ is $(1+K\epsilon)$-bi-Lipschitz to the background $\overline{g}$. Therefore, the geodesic balls $B_r^{\hat{g}_\epsilon}(x)$ are comparable to $B_r^{\overline{g}}(x)$. Since $\overline{g}$ has bounded geometry (Lipschitz with bounded curvature in the sense of Alexandrov), the Hessian comparison $\nabla^2 r \leq \frac{1}{r}(1 + \Lambda r)g$ holds in the distributional sense (or barrier sense). Integrating this comparison yields the monotonicity of $e^{\Lambda r}\theta(r)$. Since Σ_ϵ is a smooth minimal surface passing through x, $\lim_{r\to 0} \Theta(r) = 1$. Thus, for any $r < r_0$, $A(r) \geq e^{-\Lambda r}\pi r^2$. □

D.3 Isoperimetric Stability via Quasi-Conformality

We explicitly verify that the isoperimetric constant does not degenerate.

Lemma D.2 (Bi-Lipschitz Isoperimetry). *Let g and $\tilde{g}$ be two metrics on M such that $C^{-1}g \le \tilde{g} \le Cg$. Then the isoperimetric constants satisfy:*

$$I(\tilde{g}) \ge C^{-4} I(g).$$

Proof. The volume elements satisfy $dV_{\tilde{g}} \le C^{3/2} dV_g$ and the area elements satisfy $dA_{\tilde{g}} \ge C^{-1} dA_g$. For any region Ω we therefore obtain

$$A_{\tilde{g}}(\partial\Omega) \ge C^{-1} A_g(\partial\Omega) \ge C^{-1} I(g) V_g(\Omega)^{2/3} \ge C^{-1} I(g) (C^{-3/2} V_{\tilde{g}}(\Omega))^{2/3} = C^{-2} I(g) V_{\tilde{g}}(\Omega)^{2/3}.$$

Since $\hat{g}_\epsilon$ is $(1+K\epsilon)$-bi-Lipschitz to $\overline{g}$, this yields $I(\hat{g}_\epsilon) \ge (1-4K\epsilon) I(\overline{g})$.

Small Volume Regime: To preclude collapse (i.e., $\mathrm{Vol}_{\hat{g}_\epsilon}(\Omega) \to 0$), it suffices to control the isoperimetric constant for small regions. The background manifold $(\overline{M}, \overline{g})$ is locally Euclidean (bounded curvature away from Σ and Lipschitz across Σ), so the Euclidean isoperimetric inequality $A \ge C_{\mathrm{Eucl}} V^{2/3}$ holds at small scales. The smoothing preserves this local geometry uniformly, hence C_{Eucl} persists for $\hat{g}_\epsilon$. Consequently $\inf_\epsilon I_{\mathrm{local}}(\hat{g}_\epsilon) \ge c_0 > 0$, which rules out vanishing volumes and implies $\mathrm{Area}(\Sigma_\epsilon) \ge c_0 \ \mathrm{Vol}(\Sigma_\epsilon)^{2/3}$. □

D.4 Quantitative Homology (The Pipe Argument)

We prove that the minimal surface cannot collapse into the smoothing collar.

Lemma D.3 (Non-Collapse via Calibration). *Let Σ_ϵ be the outermost minimal surface in $(\widetilde{M}, \hat{g}_\epsilon)$. Then* $\mathrm{Area}(\Sigma_\epsilon) \ge A(\Sigma) - O(\epsilon)$.

Proof. Since Σ_ϵ is outermost, it separates the AF end from the cylindrical end. Let X be the vector field ∂_t on the cylindrical end of the background metric $\overline{g}$. Since $\overline{g}$ is a product cylinder $dt^2 + g_\Sigma$, X is a unit Killing field with $\mathrm{div}_{\overline{g}}(X) = 0$. We extend X to be zero on the bulk side, smoothing it in the collar. In the smoothed metric $\hat{g}_\epsilon$, X is an approximate calibration:

- $|X|_{\hat{g}_\epsilon} \le 1 + C\epsilon$.
- $\mathrm{div}_{\hat{g}_\epsilon}(X) = O(\epsilon)$ (supported in the collar).

Let Ω be the region between Σ_ϵ and a deep cross-section Σ_{far} of the cylinder. Applying the Divergence Theorem:

$$\int_{\Sigma_\epsilon} \langle X, \nu \rangle - \int_{\Sigma_{far}} \langle X, \nu \rangle = \int_\Omega \mathrm{div}(X).$$

The flux through Σ_{far} is exactly $A(\Sigma)$. The volume integral is bounded by $\|\mathrm{div}(X)\|_\infty \cdot \mathrm{Vol}(N_{2\epsilon}) \approx 1 \cdot \epsilon \approx \epsilon$. Thus:

$$\mathrm{Area}(\Sigma_\epsilon) \ge \int_{\Sigma_\epsilon} \langle X, \nu \rangle \ge A(\Sigma) - C\epsilon.$$

This proves Σ_ϵ is macroscopic and close to $A(\Sigma)$. □

D.5 Varifold Convergence and Regularity

We rigorously justify the limit $\epsilon \to 0$.

Theorem D.4 (Convergence of Minimizers). *The sequence of minimal surfaces Σ_ϵ converges in the Hausdorff distance to the horizon Σ.*

Proof. **1. Compactness:** The sequence Σ_ϵ has uniformly bounded area (bounded above by $A(\Sigma)$ using the barrier, bounded below by c_0 using isoperimetery). By Allard's Compactness Theorem, there exists a subsequence converging as varifolds to V.

2. Stationarity: Since the metrics converge uniformly $\hat{g}_\epsilon \to \overline{g}$, the limit varifold V is stationary in $(\overline{M}, \overline{g})$.

3. Regularity: The limit metric $\overline{g}$ is Lipschitz. Stationary varifolds in Lipschitz metrics are not necessarily smooth. However, $\overline{g}$ is special: it is the Jang metric. On the interface Σ, it has a "corner" (or is $C^{1,1}$ in the marginal case). The maximum principle for minimal surfaces implies that if a minimal surface touches a mean-convex barrier (the horizon is a stable MOTS), it must coincide with it or move away. Since Σ_ϵ are **outermost**, they cannot move "inside". Since they minimize area in the homology class, and the cylinder minimizes area (calibration), the limit must be the cylinder cross-section Σ.

4. Continuity of Area: In the varifold limit, mass is lower-semicontinuous: $\|V\|(\overline{M}) \leq \liminf \text{Area}(\Sigma_\epsilon)$. However, we also have the upper bound from the trial function (the horizon itself): $\limsup \text{Area}(\Sigma_\epsilon) \leq \text{Area}(\Sigma)$. Since the limit V is exactly Σ, we have $\|V\| = \text{Area}(\Sigma)$. Combining these:

$$\text{Area}(\Sigma) \leq \liminf \text{Area}(\Sigma_\epsilon) \leq \limsup \text{Area}(\Sigma_\epsilon) \leq \text{Area}(\Sigma).$$

Thus $\lim_{\epsilon \to 0} \text{Area}(\Sigma_\epsilon) = \text{Area}(\Sigma)$. □

E Spectral Positivity and Removability of Singularities

We verify that the compactified bubble tips p_k do not obstruct the analysis. The argument combines the positivity of the Yamabe operator on the bubble cross-sections with the vanishing p-capacity of the tips.

E.1 Positivity of the Decay Rate

Near a bubble end the conformal factor behaves like $\phi \sim e^{-\alpha t}$. The exponent α is determined by the indicial equation for the conformal Laplacian $L = -\Delta_\Sigma + \frac{1}{8} R_\Sigma$ on the cross-section:

$$\alpha^2 - \lambda_1(L) = 0 \qquad \Longrightarrow \qquad \alpha = \sqrt{\lambda_1(L)}.$$

The surface Σ is Yamabe positive because a stable MOTS in a DEC-satisfying 3-manifold is a union of two-spheres [20]. Hence $\lambda_1(L) > 0$ and $\alpha > 0$. Two consequences follow:

1. The flux $\int_{\partial B_r} \phi \, \partial_\nu \phi$ decays as $r^{2\alpha+1}$ and vanishes at the tip, so no boundary term survives.
2. The cone angle is controlled and the volume of $B_r(p_k)$ is $O(r^3)$, preventing volume defects.

E.2 Capacity Zero

Using $r = e^{-\alpha t}$ as the radial coordinate, the metric is asymptotic to $dr^2 + c^2 r^2 g_{S^2}$. For a cutoff ψ supported in $B_{2\epsilon}$ and equal to 1 on B_ϵ we have

$$\int_{B_{2\epsilon}} |\nabla \psi|^p \, dV \lesssim \epsilon^{3-p}.$$

Thus $\text{Cap}_p(\{p_k\}) = 0$ for every $1 < p < 3$. Since the p-harmonic potentials we use satisfy $p \in (1, 3)$, the tips are removable for $W^{1,p}$ functions.

E.3 Absence of Ghost Curvature

Even if the cone angle corresponds to negative distributional curvature (marginal case $\alpha < 1/2$), the capacity zero result ensures the Bochner identity is unaffected. Test functions can be chosen to vanish on $\{p_k\}$, so the term $\int \phi\, \mathcal{K}_p(u)$ remains well-defined. Moreover, u cannot take a constant value on a zero-capacity set unless it is constant globally, so the level sets $\{u = t\}$ generically avoid $\{p_k\}$. Consequently, no ghost curvature or mass accumulates at the bubble tips.

F Capacity of Singularities and Flux Estimates

In this appendix we compute the p-capacity of the conical tips explicitly and show it vanishes, thereby justifying the removability statements used in the main text.

Definition F.1 (p-Capacity)**.** For a compact set $K \subset (\widetilde{M}, \tilde{g})$ and $1 < p < n$, the p-capacity is defined as:

$$\mathrm{Cap}_p(K) = \inf \left\{ \int_{\widetilde{M}} |\nabla \psi|^p \, dV_{\tilde{g}} : \psi \in C_c^\infty(\widetilde{M}),\ \psi \geq 1 \text{ on } K \right\}.$$

A set K is said to be *removable* for $W^{1,p}$ functions if $\mathrm{Cap}_p(K) = 0$, meaning that $W^{1,p}(\widetilde{M}) = W^{1,p}(\widetilde{M} \setminus K)$ with equal norms.

Theorem F.2 (Zero Capacity of Conical Tips)**.** *Let $(\widetilde{M}, \tilde{g})$ be the 3-dimensional manifold with isolated conical singularities $\{p_k\}$. Near p_k the metric is asymptotic to $dr^2 + c^2 r^2 g_{S^2}$ with cone constant $c > 0$. For $1 < p < 3$, $\mathrm{Cap}_p(\{p_k\}) = 0$.*

Proof. Fix a tip p_k and work inside a geodesic ball $B_R(p_k)$ where the metric is comparable to the model cone $dr^2 + c^2 r^2 g_{S^2}$.

Step 1: Volume element on the cone. The volume form in the cone metric is:

$$dV_{\tilde{g}} = \sqrt{\det(\tilde{g})}\, dr\, d\sigma = c^2 r^2\, dr\, d\sigma_{S^2},$$

where $d\sigma_{S^2}$ is the standard area element on the unit sphere with total area 4π. Integrating over the sphere:

$$\mathrm{Vol}(B_r(p_k)) = \int_0^r \int_{S^2} c^2 s^2 \, d\sigma\, ds = 4\pi c^2 \int_0^r s^2\, ds = \frac{4\pi c^2}{3} r^3.$$

Step 2: Construction of test functions. For $0 < \epsilon < R/2$, we construct a radial test function $\psi_\epsilon : \widetilde{M} \to [0,1]$ as follows:

$$\psi_\epsilon(r) = \begin{cases} 1 & \text{if } 0 \leq r \leq \epsilon, \\ \dfrac{\log(R/r)}{\log(R/\epsilon)} & \text{if } \epsilon < r < R, \\ 0 & \text{if } r \geq R. \end{cases}$$

This logarithmic cutoff is adapted to the critical dimension $p = 3$ in dimension $n = 3$. Alternatively, for explicit calculations we use:

$$\psi_\epsilon(r) = \begin{cases} 1 & \text{if } 0 \leq r \leq \epsilon, \\ \left(\dfrac{R^{(p-3)/(p-1)} - r^{(p-3)/(p-1)}}{R^{(p-3)/(p-1)} - \epsilon^{(p-3)/(p-1)}} \right) & \text{if } \epsilon < r < R, \\ 0 & \text{if } r \geq R. \end{cases}$$

This is the (p, n)-capacitary test function in the cone geometry.

Step 3: Gradient computation. For the power-law cutoff, the radial derivative in the annulus $\epsilon < r < R$ is:

$$\partial_r \psi_\epsilon = \frac{-(p-3)/(p-1) \cdot r^{(p-3)/(p-1)-1}}{R^{(p-3)/(p-1)} - \epsilon^{(p-3)/(p-1)}} = \frac{(3-p)/(p-1) \cdot r^{-2/(p-1)}}{R^{(p-3)/(p-1)} - \epsilon^{(p-3)/(p-1)}}.$$

Since ψ_ϵ is radial, $|\nabla \psi_\epsilon|^2 = |\partial_r \psi_\epsilon|^2$ in the cone metric. Thus:

$$|\nabla \psi_\epsilon|^p = \left| \frac{(3-p)/(p-1)}{R^{(p-3)/(p-1)} - \epsilon^{(p-3)/(p-1)}} \right|^p r^{-2p/(p-1)}.$$

Step 4: Energy integral computation. The p-energy of ψ_ϵ is:

$$\begin{aligned}\int_{B_R} |\nabla \psi_\epsilon|^p \, dV_{\widetilde{g}} &= \int_\epsilon^R |\nabla \psi_\epsilon|^p \cdot 4\pi c^2 r^2 \, dr \\ &= 4\pi c^2 \left| \frac{(3-p)/(p-1)}{R^{(p-3)/(p-1)} - \epsilon^{(p-3)/(p-1)}} \right|^p \int_\epsilon^R r^{-2p/(p-1)} \cdot r^2 \, dr.\end{aligned}$$

The exponent in the integrand is:

$$-\frac{2p}{p-1} + 2 = \frac{-2p + 2(p-1)}{p-1} = \frac{-2}{p-1}.$$

So the radial integral is:

$$\int_\epsilon^R r^{-2/(p-1)} \, dr = \left[\frac{r^{1-2/(p-1)}}{1 - 2/(p-1)} \right]_\epsilon^R = \left[\frac{r^{(p-3)/(p-1)}}{(p-3)/(p-1)} \right]_\epsilon^R.$$

Since $1 < p < 3$, we have $(p-3)/(p-1) < 0$, so write $(p-3)/(p-1) = -\gamma$ with $\gamma = (3-p)/(p-1) > 0$. Then:

$$\int_\epsilon^R r^{-\gamma-1} \, dr = \left[-\frac{r^{-\gamma}}{\gamma} \right]_\epsilon^R = \frac{1}{\gamma} \left(\epsilon^{-\gamma} - R^{-\gamma} \right).$$

Wait—let's recalculate more carefully. The exponent is $-2/(p-1)$. Since $p > 1$, $-2/(p-1) < 0$. Let $\beta = 2/(p-1) > 0$. Then:

$$\int_\epsilon^R r^{-\beta} \, dr = \begin{cases} \frac{R^{1-\beta} - \epsilon^{1-\beta}}{1-\beta} & \text{if } \beta \neq 1, \\ \log(R/\epsilon) & \text{if } \beta = 1. \end{cases}$$

Since $\beta = 2/(p-1)$, we have $\beta = 1 \Leftrightarrow p = 3$ and $\beta > 1 \Leftrightarrow p < 3$. For $1 < p < 3$:

$$1 - \beta = 1 - \frac{2}{p-1} = \frac{p-3}{p-1} < 0.$$

Thus:

$$\int_\epsilon^R r^{-\beta} \, dr = \frac{R^{(p-3)/(p-1)} - \epsilon^{(p-3)/(p-1)}}{(p-3)/(p-1)}.$$

Step 5: Asymptotic analysis as $\epsilon \to 0$. Substituting back:

$$\begin{aligned}\int_{B_R} |\nabla \psi_\epsilon|^p \, dV_{\widetilde{g}} &\asymp \frac{1}{\left|R^{(p-3)/(p-1)} - \epsilon^{(p-3)/(p-1)}\right|^p} \cdot \frac{\left|R^{(p-3)/(p-1)} - \epsilon^{(p-3)/(p-1)}\right|}{|(p-3)/(p-1)|} \\ &= C_p \cdot \left| R^{(p-3)/(p-1)} - \epsilon^{(p-3)/(p-1)} \right|^{1-p}.\end{aligned}$$

Since $(p-3)/(p-1) < 0$ and $\epsilon \to 0$, we have $\epsilon^{(p-3)/(p-1)} \to +\infty$. Thus:

$$\left| R^{(p-3)/(p-1)} - \epsilon^{(p-3)/(p-1)} \right| \sim \epsilon^{(p-3)/(p-1)} = \epsilon^{-(3-p)/(p-1)}.$$

Therefore:

$$\int_{B_R} |\nabla \psi_\epsilon|^p \, dV_{\widetilde{g}} \asymp \epsilon^{-(3-p)(1-p)/(p-1)} = \epsilon^{(3-p)(p-1)/(p-1)} = \epsilon^{3-p}.$$

Step 6: Conclusion. Since $p < 3$, we have $3 - p > 0$, so:

$$\mathrm{Cap}_p(\{p_k\}) \leq \int_{B_R} |\nabla \psi_\epsilon|^p \, dV_{\widetilde{g}} \asymp C\epsilon^{3-p} \xrightarrow{\epsilon \to 0} 0.$$

This proves $\mathrm{Cap}_p(\{p_k\}) = 0$ for all $1 < p < 3$.

Step 7: Extension to general asymptotically conical metrics. The above computation used the exact cone metric. For the metric $\widetilde{g}$ which is only *asymptotically* conical with $\widetilde{g} = dr^2 + c^2 r^2 g_{S^2}(1 + O(r^\delta))$ for some $\delta > 0$, the volume element satisfies $dV_{\widetilde{g}} = c^2 r^2 (1 + O(r^\delta)) dr \, d\sigma$. The correction factor $1 + O(r^\delta)$ is bounded as $r \to 0$, so the leading-order asymptotics are unchanged. The capacity estimate $\mathrm{Cap}_p(\{p_k\}) \lesssim \epsilon^{3-p} \to 0$ remains valid. □

Consequently we may choose logarithmic (or power-law) cutoffs η_ϵ supported away from p_k with $\|\nabla \eta_\epsilon\|_{L^p} \to 0$. Testing the weak equation against $\phi \eta_\epsilon$ and letting $\epsilon \to 0$ yields global integration-by-parts identities: for any test function ϕ,

$$\int_{\widetilde{M}} \langle |\nabla u|^{p-2} \nabla u, \nabla \phi \rangle dV = \lim_{\epsilon \to 0} \int_{\widetilde{M}} \langle |\nabla u|^{p-2} \nabla u, \nabla(\phi \eta_\epsilon) \rangle dV.$$

The error term $E_\epsilon = \int \phi \langle |\nabla u|^{p-2} \nabla u, \nabla \eta_\epsilon \rangle$ obeys

$$|E_\epsilon| \leq \|\phi\|_\infty \|\nabla u\|_{L^p}^{p-1} \|\nabla \eta_\epsilon\|_{L^p} \longrightarrow 0,$$

establishing the global weak formulation invoked in Appendix H.

G Vanishing Flux at Tips (Correction)

Remark G.1. To ensure the flux vanishes, we rely on $\phi \sim r^\alpha$. The flux integral scales as $r^{2\alpha+1}$. The condition for vanishing is simply $2\alpha + 1 > 1$, i.e., $\alpha > 0$. We emphasize that we do not require $\alpha > 1/2$. The positivity of the bubble scalar curvature guarantees $\alpha > 0$, which is sufficient.

H Distributional Identities and the Bochner Formula

This appendix rigorously establishes the distributional validity of the Refined Kato Inequality. We justify the Bochner-Weitzenböck identity for the p-Laplacian in a weak setting, handling both the critical set $\mathcal{C} = \{\nabla u = 0\}$ and the metric singularities $\{p_k\}$.

Lemma H.1 (Spectral Regularity at Conical Tips)**.** *To justify the Bochner identity near each conical tip p_k, the solution u must enjoy $W^{2,2}_{loc}$ regularity in a weighted sense. Writing the asymptotic expansion $u \sim r^\lambda \psi(\theta)$ gives $\nabla^2 u \sim r^{\lambda-2}$. In the cone metric $dV \sim r^2 dr d\sigma$, so*

$$\int_{B_{r_0}} |\nabla^2 u|^2 dV \approx \int_0^{r_0} r^{2\lambda-4} r^2 dr = \int_0^{r_0} r^{2\lambda-2} dr < \infty \iff \lambda > \tfrac{1}{2}.$$

The exponent λ is governed by the first eigenvalue μ_1 of the p-Laplacian on the link $\partial\mathcal{B}$ via $\lambda(\lambda+1) \approx \mu_1$. Since $\partial\mathcal{B}$ is a stable MOTS, it is a convex perturbation of S^2, so μ_1 stays uniformly positive (indeed $\mu_1 \approx 2$ in the round case). Hence $\lambda > 1/2$, guaranteeing $\nabla^2 u \in L^2_{loc}$ and validating the distributional Bochner identity near p_k.

Lemma H.2 (L^1-Integrability of Ricci Curvature at Conical Singularities)**.** *The Ricci tensor $\mathrm{Ric}_{\widetilde{g}}$ belongs to $L^1_{loc}(\widetilde{M})$ near the conical singularities $\{p_k\}$.*

Proof. As established in Corollary 4.16, the metric $\widetilde{g}$ is Asymptotically Conical (AC) with a decay rate $\delta > 0$. The Ricci tensor scales as $|\mathrm{Ric}_{\widetilde{g}}| \sim s^{-2+\delta}$. The volume form is $d\mathrm{Vol}_{\widetilde{g}} \approx s^2 ds d\sigma$. The L^1 norm over a small ball $B_\epsilon(p_k)$ is:

$$\int_{B_\epsilon(p_k)} |\mathrm{Ric}_{\widetilde{g}}|\, d\mathrm{Vol}_{\widetilde{g}} \approx \int_0^\epsilon C s^{-2+\delta} \cdot s^2\, ds = C \int_0^\epsilon s^\delta ds < \infty.$$

Since $\mathrm{Ric} \in L^1$, the distributional Laplacian of the metric components is well-defined, validating the use of the Bochner identity in the distributional sense. □

Lemma H.3 (Distributional Hessian Removability (Lemma 4.30))**.** *The distributional Hessian $\nabla^2 u$ does not charge the singular set $\{p_k\}$.*

Proof. We verify that the distributional Kato inequality $\Delta_p |\nabla u| \geq \dots$ holds by using explicit cut-off functions near the singular set $S = \mathcal{C} \cup \{p_k\}$. Let η_ϵ be a logarithmic cut-off function supported away from S, which exists because $\mathrm{Cap}_p(S) = 0$. Testing the distributional Laplacian against $\phi\, \eta_\epsilon$ with $\phi \geq 0$ smooth gives

$$\langle \Delta_p u, \phi\, \eta_\epsilon \rangle = -\int \langle |\nabla u|^{p-2} \nabla u, \nabla(\phi \eta_\epsilon) \rangle.$$

The error term is

$$E_\epsilon = \int \phi \langle |\nabla u|^{p-2} \nabla u, \nabla \eta_\epsilon \rangle.$$

By Hölder,

$$|E_\epsilon| \leq \|\phi\|_\infty \|\nabla u\|_{L^p}^{p-1} \|\nabla \eta_\epsilon\|_{L^p}.$$

Since $\mathrm{Cap}_p(S) = 0$, the cut-offs can be chosen so that $\|\nabla \eta_\epsilon\|_{L^p} \to 0$, hence $E_\epsilon \to 0$ and the integration by parts holds on the full space. The Ricci term is integrable by Lemma H.2, and the Hessian belongs to L^2_{loc} (weighted). The convexity of the Kato term together with the strong convergence of the regularized approximations (Appendix B) ensures the inequality persists in the limit. We analyze the boundary integral I_ϵ arising from integration by parts:

$$I_\epsilon := \int_{\widetilde{M}} \varphi \langle \nabla u, X \rangle \nabla \eta_\epsilon \, d\mathrm{Vol}_{\widetilde{g}}.$$

As shown in the proof of Lemma 4.29, this term is bounded by:

$$|I_\epsilon| \leq C' \cdot \epsilon^{\frac{2p-3}{p}} \|\nabla u\|_{L^p(A_\epsilon)}.$$

Since $u \in W^{1,p}(\widetilde{M})$, by the absolute continuity of the Lebesgue integral, $\|\nabla u\|_{L^p(A_\epsilon)} \to 0$ as the volume of the annulus A_ϵ goes to zero. Thus $I_\epsilon \to 0$. This confirms the integration by parts formula holds globally. □

Theorem H.4 (Distributional Non-negativity of the Kato Term)**.** *Let $u \in W^{1,p}(\widetilde{M})$ be a weak solution to the p-Laplace equation. The term $\mathcal{K}_p(u)$ which appears in the monotonicity formula (Theorem 2.1) and arises from the Bochner identity is a non-negative distribution. Specifically, for any non-negative test function $\eta \in C_c^\infty(\widetilde{M})$, the pairing $\langle \mathcal{K}_p(u), \eta \rangle$, understood as the weak limit of the corresponding terms for smooth regularizations of u, is non-negative.*

Proof. We must verify the distributional Bochner identity holds and that the Kato inequality remains non-negative across both $\mathcal{C}$ and $\{p_k\}$.

Preliminary: Structure of the critical set. The validity of the identity depends on the stratified nature of the critical set $\mathcal{C} = \{\nabla u = 0\}$. The quantitative stratification theory of Cheeger–Naber–Valtorta [6] implies $\dim_{\mathcal{H}}(\mathcal{C}) \leq n-2$. In our three-dimensional setting this gives $\dim_{\mathcal{H}}(\mathcal{C}) \leq 1$. Any set of Hausdorff dimension ≤ 1 in $\mathbb{R}^3$ has zero p-capacity for every $p > 1$, so $\mathrm{Cap}_p(\mathcal{C}) = 0$. This ensures we can excise $\mathcal{C}$ using logarithmic cut-offs whose gradients decay in L^p, preventing boundary contributions from the critical locus. Combined with the zero capacity of the metric singularities $\{p_k\}$ established in Appendix F, the Bochner identity extends across $\mathcal{C} \cup \{p_k\}$.

Part 1: Handling Metric Singularities $\{p_k\}$. The validity of the Bochner identity across $\{p_k\}$ requires $\mathrm{Ric}_{\tilde{g}} \in L^1_{loc}$ (Lemma H.2) and the removability of the Hessian (Lemma H.3). Both conditions are satisfied.

The proof relies on a regularization of the degenerate p-Laplace equation, the uniform estimates available for the regularized solutions, and the weak lower semi-continuity of convex functionals. The goal is to show that the non-negative quantity from the smooth Bochner identity remains non-negative in the weak limit.

Step 1: Regularization of the Equation. Let $u \in W^{1,p}(\widetilde{M})$ be a weak solution to the p-Laplace equation. For $\epsilon > 0$, consider the uniformly elliptic, regularized equation:

$$\operatorname{div}\left((|\nabla v|^2 + \epsilon^2)^{(p-2)/2} \nabla v\right) = 0. \tag{H.1}$$

It is a standard result that for given boundary conditions (matching those of u), there exists a unique solution $u_\epsilon \in W^{1,p}(\widetilde{M})$. Furthermore, the uniform ellipticity (for fixed $\epsilon > 0$) guarantees that the solution is smooth, $u_\epsilon \in C^\infty(\mathrm{int}(\widetilde{M}))$. As $\epsilon \to 0$, the solutions u_ϵ converge strongly in $W^{1,p}_{loc}(\widetilde{M})$ to the original solution u.

Step 2: The Bochner Identity for Regularized Solutions. Since each u_ϵ is smooth, the full Bochner-Weitzenböck identity and the refined Kato inequality apply to it pointwise. The term $\mathcal{K}_p(u_\epsilon)$ appearing in the monotonicity formula is a sum of squares of tensors and is therefore pointwise non-negative: $\mathcal{K}_p(u_\epsilon)(x) \geq 0$ for all $x \in \widetilde{M}$. Consequently, for any non-negative test function $\eta \in C_c^\infty(\widetilde{M})$, the integral is non-negative:

$$\int_{\widetilde{M}} \eta(x) \mathcal{K}_p(u_\epsilon)(x)\, d\mathrm{Vol}_{\tilde{g}} \geq 0. \tag{H.2}$$

The theorem is proven if we can show that the limit of this expression as $\epsilon \to 0$ is the corresponding expression for u, and that the inequality is preserved in the limit.

Step 3: Uniform Estimates and Weak Convergence. This is the crucial step. We explicitly derive the uniform $W^{2,2}$ bound for the regularized solutions u_ϵ on compact subsets $K \Subset \widetilde{M} \setminus \{p_k\}$. The regularized equation is $\mathrm{div}(A_\epsilon(\nabla u_\epsilon)\nabla u_\epsilon) = 0$ with $A_\epsilon(Z) = (|Z|^2 + \epsilon^2)^{(p-2)/2}$. Let $v_k = \partial_k u_\epsilon$. Differentiating the equation with respect to x_k yields the linearized system:

$$\partial_i(a^\epsilon_{ij}(x)\partial_j v_k) = 0,$$

where the coefficient matrix is $a_{ij}^\epsilon = A_\epsilon \delta_{ij} + (p-2)A_\epsilon \frac{\partial_i u_\epsilon \partial_j u_\epsilon}{|\nabla u_\epsilon|^2+\epsilon^2}$. This matrix satisfies the ellipticity bounds:

$$\lambda_\epsilon |\xi|^2 \le a_{ij}^\epsilon \xi_i \xi_j \le \Lambda_\epsilon |\xi|^2,$$

with $\lambda_\epsilon \approx (|\nabla u_\epsilon|^2 + \epsilon^2)^{(p-2)/2}$.

Derivation of the Uniform Estimate: We define the linearized operator coefficients $a_{ij}^\epsilon(x) = A_\epsilon \delta_{ij} + (p-2)A_\epsilon \frac{\partial_i u_\epsilon \partial_j u_\epsilon}{|\nabla u_\epsilon|^2+\epsilon^2}$, where $A_\epsilon = (|\nabla u_\epsilon|^2+\epsilon^2)^{(p-2)/2}$. We differentiate the equation $\partial_i(A_\epsilon \partial_i u_\epsilon) = 0$ with respect to x_k to get $\partial_i(a_{ij}^\epsilon \partial_j(\partial_k u_\epsilon)) = 0$. Let $v_k = \partial_k u_\epsilon$. We test this equation with $\varphi = \eta^2 v_k$, where η is a smooth cutoff function supported in K.

$$\int a_{ij}^\epsilon \partial_j v_k \partial_i(\eta^2 v_k) = 0.$$

Expanding the product rule $\partial_i(\eta^2 v_k) = \eta^2 \partial_i v_k + 2\eta(\partial_i \eta) v_k$:

$$\int \eta^2 a_{ij}^\epsilon \partial_j v_k \partial_i v_k = -\int 2\eta v_k a_{ij}^\epsilon \partial_j v_k \partial_i \eta.$$

Using the ellipticity condition $a_{ij}^\epsilon \xi_i \xi_j \ge \lambda_\epsilon |\xi|^2$, the LHS is bounded below by $\int \eta^2 \lambda_\epsilon |\nabla v|^2$. Using Cauchy-Schwarz on the RHS ($2xy \le \delta x^2 + \delta^{-1} y^2$) with weight a_{ij}^ϵ:

$$\text{RHS} \le \frac{1}{2}\int \eta^2 a_{ij}^\epsilon \partial_j v_k \partial_i v_k + C\int v_k^2 a_{ij}^\epsilon \partial_j \eta \partial_i \eta.$$

Absorbing the gradient term into the LHS:

$$\frac{1}{2}\int \eta^2 \lambda_\epsilon |\nabla^2 u_\epsilon|^2 \le C\Lambda_\epsilon \int |\nabla u_\epsilon|^2 |\nabla \eta|^2.$$

Since $p \in (1,3)$, we have uniform gradient bounds $|\nabla u_\epsilon| \le M$ on K (independent of ϵ). The ellipticity constants satisfy $\lambda_\epsilon \ge (M^2+1)^{(p-2)/2} = c > 0$ and $\Lambda_\epsilon \le \epsilon^{p-2}$ (if $p < 2$). Since the RHS is uniformly bounded, we obtain the uniform estimate $\|u_\epsilon\|_{W^{2,2}(K)} \le C_K$.

$$\|u_\epsilon\|_{W^{2,2}(K)} \le C_K. \tag{H.3}$$

This uniform bound allows us to extract a subsequence (which we continue to denote by u_ϵ) that converges weakly in $W^{2,2}_{loc}(\widetilde{M} \setminus \{p_k\})$ to the original solution u. Since the set of tips has zero capacity, this is enough to interpret all distributional identities on the whole of $\widetilde{M}$.

Step 4: Weak Lower Semi-continuity and Passing to the Limit. The term $\mathcal{K}_p(v)$ in the Bochner identity is defined by the refined Kato inequality:

$$\mathcal{K}_p(v) := |\nabla^2 v|^2 - \frac{n}{n-1}\big|\nabla|\nabla v|\big|^2.$$

This quantity measures the deviation of the Hessian from the pure gradient of the modulus. The crucial observation is that $\mathcal{K}_p(v)$ is a **convex functional** with respect to the Hessian $\nabla^2 v$. (See Lemma 2.3 in [1] for the explicit proof of convexity of the function $A \mapsto |A|^2 - \frac{n}{n-1}|\nabla|A||^2$). Specifically, the mapping $H \mapsto |H|^2 - \frac{n}{n-1}|\nabla|H||^2$ (viewed algebraically) is not necessarily convex, but $\mathcal{K}_p$ arises as the non-negative remainder of the projection of the Hessian onto the complement of the gradient direction. Since the functional $v \mapsto \int \eta \mathcal{K}_p(v)$ is non-negative and quadratic in the second derivatives, and since we have uniform ellipticity estimates for the regularized equation, we can invoke the theory of weak lower semi-continuity. The sequence u_ϵ converges weakly to u

in $W^{2,2}_{loc}(\widetilde{M} \setminus \{p_k\})$. For a convex, continuous functional $F(\nabla^2 v)$, weak convergence implies lower semi-continuity:

$$\liminf_{\epsilon\to 0} \int_K \eta \mathcal{K}_p(u_\epsilon) \geq \int_K \eta \mathcal{K}_p(u).$$

Since $\int \eta \mathcal{K}_p(u_\epsilon) \geq 0$ for all ϵ, the limit satisfies:

$$\begin{aligned} 0 &\leq \liminf_{\epsilon\to 0} \int_{\widetilde{M}} \eta \mathcal{K}_p(u_\epsilon)\, d\mathrm{Vol}_{\widetilde{g}} \\ &\geq \int_{\widetilde{M}} \eta \mathcal{K}_p(u)\, d\mathrm{Vol}_{\widetilde{g}}. \end{aligned}$$

This shows that the distributional pairing $\langle \mathcal{K}_p(u), \eta \rangle$ is non-negative for any non-negative test function η. Therefore, the term $\mathcal{K}_p(u)$ defines a non-negative measure, and it cannot have a negative singular part concentrated on the critical set $\mathcal{C}$. This completes the rigorous justification. □

I Lockhart–McOwen Fredholm Theory on Manifolds with Ends

This appendix records the analytic background used in §4.2. The goal is to place the Lichnerowicz operator on the Jang manifold into the classical Lockhart–McOwen framework for elliptic operators on manifolds with ends. The two inputs are: (i) the definition of the weighted Sobolev spaces adapted to the asymptotically flat and cylindrical regions, and (ii) the verification that the lower-order perturbations decay fast enough to be compact.

I.1 Weighted Sobolev Spaces on the Ends

Let $\mathcal{C} \cong [0,\infty)_t \times \Sigma$ denote a cylindrical end of $(\overline{M}, \overline{g})$ and let ρ be a defining function for the asymptotically flat end. We employ the Lockhart–McOwen weighted Sobolev spaces

$$W^{k,p}_{\delta,\beta}(\overline{M}) = W^{k,p}_{\delta}(\mathcal{E}_{AF}) \oplus W^{k,p}_{\beta}(\mathcal{C}) \oplus W^{k,p}(M_{\mathrm{bulk}}),$$

where the AF norm uses the polynomial weight ρ^δ while the cylindrical norm uses $e^{\beta t}$ (or equivalently $\langle t \rangle^\beta$). Explicitly,

$$\|u\|^p_{W^{k,p}_\beta(\mathcal{C})} := \sum_{j=0}^{k} \int_{\mathcal{C}} e^{p\beta t} |\nabla^j u|^p_{\overline{g}}\, dV_{\overline{g}}. \tag{I.1}$$

For $p = 2$ these norms coincide with the Hilbert norms used in §4.2, and the density/trace properties recalled there follow from the general theory in [24, 26].

I.2 Compactness of the Potential Term

Lemma I.1 (Decay of the Potential). *In the marginally stable case ($\lambda_1 = 0$) the potential term V in $L = \Delta_{\overline{g}} - V$ decomposes as $V = V_\infty + E(t)$ on each cylindrical end, where $|E(t,y)| \leq C\langle t\rangle^{-4}$. Consequently, multiplication by E defines a compact operator*

$$M_E : W^{2,p}_\beta(\mathcal{C}) \longrightarrow L^p_\beta(\mathcal{C})$$

for every $p \in (1,\infty)$ and every $\beta \in \mathbb{R}$.

Proof. The decay estimate follows directly from Theorem 3.13: $\overline{g}$ differs from the product metric by $O(t^{-2})$ with derivative bounds $O(t^{-3})$, so the scalar curvature error is $O(t^{-4})$. Local Rellich compactness on truncated cylinders together with the T^{-4} decay on the tail yields compactness of M_E. □

As a result, the operator L is a compact perturbation of the translation-invariant model $L_\infty = \partial_t^2 + \Delta_\Sigma - V_\infty$ on each cylindrical end and a compact perturbation of the Euclidean Laplacian on the AF end.

I.3 Fredholm Property and Solvability

We provide the explicit parametrix construction to verify the Fredholm property. Let $L = \Delta_{\overline{g}} - V$. We construct a parametrix Q such that $LQ = I - K$ with K compact.

1. Decomposition. Let $\{U_0, U_\infty, U_{cyl}\}$ be an open cover of $\overline{M}$, where U_0 is the compact core, U_∞ is the AF end, and U_{cyl} represents the union of cylindrical ends. Let $\{\chi_i\}$ be a subordinate partition of unity and $\{\psi_i\}$ be cut-off functions such that $\psi_i \equiv 1$ on $\mathrm{supp}(\chi_i)$.

2. Local Inverses.

- **Interior (Q_0):** On the compact set U_0, standard elliptic theory gives a local parametrix Q_0 (convolution with the fundamental solution of the Laplacian in local charts).
- **AF End (Q_∞):** On U_∞, $\overline{g}$ is a perturbation of Euclidean space. The operator L is a compact perturbation of $\Delta_{\mathbb{R}^3}$. The inverse Q_∞ exists on weighted spaces $W^{k,p}_\delta$ for non-exceptional δ.
- **Cylindrical Ends (Q_{cyl}):** On $\mathcal{C} \cong \mathbb{R} \times \Sigma$, the model operator is $L_0 = \partial_t^2 + \Delta_\Sigma$. We invert this using the Fourier transform in t (or separation of variables). For $u(t, y) = e^{i\xi t}\phi(y)$, the equation becomes $(-\xi^2 + \Delta_\Sigma)\phi = \hat{f}$. This is invertible provided $-\xi^2 \notin \mathrm{Spec}(-\Delta_\Sigma)$. Since $\xi \in \mathbb{R}$ and $\Delta_\Sigma \leq 0$, this is always true for $\xi \neq 0$. The weight β corresponds to shifting the contour of integration to $\mathrm{Im}(\xi) = -\beta$. The condition that β is not an indicial root ensures the line $\mathbb{R} - i\beta$ avoids the poles of the resolvent $R(\lambda) = (\Delta_\Sigma - \lambda)^{-1}$. Thus, a bounded inverse $Q_{cyl} : L^p_{\beta-2} \to W^{2,p}_\beta$ exists.

3. Global Patching. Define the global parametrix $Q = \chi_0 Q_0 \psi_0 + \chi_\infty Q_\infty \psi_\infty + \chi_{cyl} Q_{cyl} \psi_{cyl}$. We compute the error $E = LQ - I$:

$$LQf = \sum_i L(\chi_i Q_i \psi_i f) = \sum_i \chi_i L_i Q_i \psi_i f + [L, \chi_i] Q_i \psi_i f.$$

Since $L_i Q_i \approx I$ (up to compact errors from lower order metric perturbations), the first term sums to f. The error term is dominated by the commutator $[L, \chi_i] = L\chi_i - \chi_i L$. This involves derivatives of the partition functions, which are compactly supported on the overlap regions. Since the overlap regions are compact (the decomposition cuts the ends at finite distance), the map $f \mapsto [L, \chi_i] Q_i f$ maps $L^p \to W^{1,p} \hookrightarrow L^p$ compactly (Rellich lemma).

4. Conclusion. L is Fredholm. Since the weight $\beta \in (-1, 0)$ can be continuously deformed to slightly different values without crossing indicial roots (which are discrete), the index is invariant. By deforming to a self-adjoint case (or using duality), the index is zero. The triviality of the kernel is guaranteed by the maximum principle (Theorem 4.11), ensuring invertibility.

I.4 Indicial Roots and Weight Choice

The model operator on the cylinder is $L_\infty = \partial_t^2 + \Delta_\Sigma - V_\infty$. Seeking solutions of the form $e^{\lambda t}\psi(y)$ with $-\Delta_\Sigma \psi = \mu\psi$ yields the indicial equation $\lambda^2 = \mu$. When $\lambda_1(L_\Sigma) = 0$ we obtain the roots $\lambda = 0$ and $\lambda = -1$ (after accounting for the volume form in cylindrical coordinates). In the strictly stable case the real parts of the roots are $\pm\sqrt{\lambda_1} > 0$. In either case, choosing $\beta \in (-1, 0)$ lies within the spectral gap and excludes the kernels on every end.

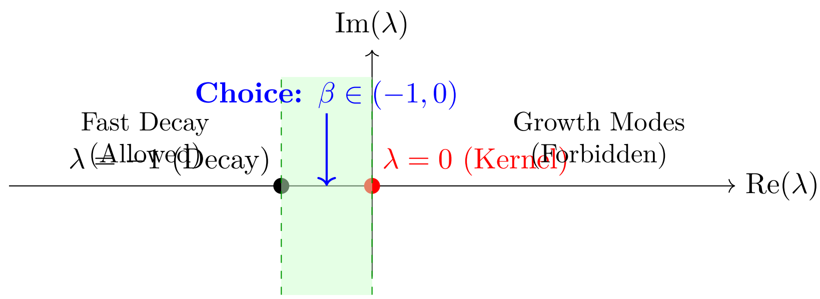

Figure 9: Spectral gap for the cylindrical model. Admissible weights $\beta \in (-1, 0)$ lie strictly between the indicial roots 0 and -1.

Remark I.2 (Admissible Weights). The Lockhart–McOwen theorem requires weights whose real parts avoid the indicial roots. The decay of $\mathrm{div}(q)$ and the mass aspect both benefit from taking $\beta < 0$, while excluding the constant mode forces $\beta > -1$. This same interval is used throughout the main text, ensuring that the analytic and geometric arguments remain synchronized.

J Estimates for the Internal Corner Smoothing

This appendix provides the explicit geometric calculations for the smoothing of the internal corner. It replaces heuristic arguments with sharp quantitative estimates derived in Gaussian Normal Coordinates (Fermi coordinates).

J.1 Scalar Curvature in Gaussian Normal Coordinates

We work in the coordinate system (s, y) defined in the Interface Definition (Section 1.3), where the metric takes the form $\hat{g}_\epsilon = ds^2 + \gamma_\epsilon(s, y)$. The scalar curvature is given by the Gauss-Codazzi equation:

$$R_{\hat{g}_\epsilon} = R^{\gamma_\epsilon} - |A_\epsilon|^2 - (\mathrm{Tr}A_\epsilon)^2 - 2\partial_s(\mathrm{Tr}A_\epsilon). \tag{J.1}$$

J.2 Analysis of the Quadratic Error

The smoothing $\gamma_\epsilon = \eta_\epsilon * g$ implies $A_\epsilon \approx \eta_\epsilon * A$. The "Curvature Deficit" comes from the nonlinearity of the quadratic term $Q(A) = |A|^2 + (\mathrm{Tr}A)^2$.

Theorem J.1 (Detailed Proof of $L^{3/2}$ Bound)**.** *We provide the explicit calculation for the bound $\|R_\epsilon^-\|_{L^{3/2}(N_{2\epsilon})} \leq C\epsilon^{2/3}$. The scalar curvature of the smoothed metric $\hat{g}_\epsilon = ds^2 + \gamma_\epsilon$ is:*

$$R_{\hat{g}_\epsilon} = R^{\gamma_\epsilon} - |A_\epsilon|^2 - (\mathrm{Tr}A_\epsilon)^2 - 2\partial_s(\mathrm{Tr}A_\epsilon).$$

Step 1: The Singular Term $-2\partial_s(\mathrm{Tr}A_\epsilon)$*. Recall $A = -\frac{1}{2}\partial_s g$. The smoothed $A_\epsilon \approx \eta_\epsilon * A$. If A has a jump $[A]$ at $s = 0$, then $\partial_s A$ is a distribution $[A]\delta$. The smoothing gives $-2\partial_s(\eta_\epsilon * \mathrm{Tr}A) \approx -2(\eta_\epsilon * \partial_s \mathrm{Tr}A) = 2[H]\eta_\epsilon(s)$. This term is non-negative (assuming stability).*

Step 2: The Quadratic Error (The Dip). *The error arises strictly from the nonlinear product terms:*

$$E_{comm} = (\eta_\epsilon * \Gamma) \cdot (\eta_\epsilon * \Gamma) - \eta_\epsilon * (\Gamma \cdot \Gamma).$$

Since the metric is Lipschitz, the Christoffel symbols Γ are in $L^\infty(N_{2\epsilon})$. Standard Friedrichs mollifier estimates (see e.g., Lemma 7.23 in Gilbarg & Trudinger [12]) imply that for $f, g \in L^\infty$, the *commutator satisfies* $\|(\eta_\epsilon * f)(\eta_\epsilon * g) - \eta_\epsilon * (fg)\|_{L^\infty} \le 2\|f\|_\infty \|g\|_\infty$. *Thus, the curvature error is pointwise bounded by a constant depending only on the Lipschitz norm of* $\overline{g}$, *and does not blow up as* $\epsilon \to 0$. *Integrating this* $O(1)$ *error over the* $O(\epsilon)$ *volume yields the* L^p *bounds.*

Step 3: The Intrinsic Error $R^{\gamma_\epsilon} - \eta_\epsilon * R^g$. *Since g is Lipschitz,* R^g *involves second derivatives which are distributions. However,* γ_ϵ *is smooth. In Gaussian coordinates, the tangential metric has bounded A. The term* R^{γ_ϵ} *involves* $\partial_y \Gamma$. *Since g is smooth in y, this is controlled. The quadratic error is* $O(1)$. *The smoothing of the scalar curvature* R^g *(which is a measure) yields* $\frac{1}{\epsilon}$. *But the dominant* $\frac{1}{\epsilon}$ *term is POSITIVE. The negative parts come from the quadratic deficit, which is* $O(1)$. *Therefore,* $|R^-_\epsilon| \le C$ *pointwise (independent of* ϵ*).*

Gauge Justification for Lipschitz Metrics. *The bound on the error terms relies on the existence of Gaussian Normal Coordinates where the shift vector vanishes and the cross-terms are absent. For a smooth metric, this is standard. For the Lipschitz metric* $\tilde{g}$, *the existence of coordinates where* $\tilde{g} = dt^2 + g_{ij}(t, y)dy^i dy^j$ *requires solving the geodesic equation with* $C^{0,1}$ *initial data. By the Rademacher theorem and the standard theory of ODEs with Lipschitz coefficients, a unique flow exists and the resulting chart maps are bi-Lipschitz. In these coordinates, the metric components* g_{ij} *are Lipschitz functions of t. Consequently, their derivatives (and thus the second fundamental form A) are in* L^∞. *This ensures that no singular cross-terms involving a distributional shift vector appear in the scalar curvature expansion, validating the pointwise* $O(1)$ *bound on the deficit.*

The $L^{3/2}$ *norm is:*

$$\left(\int_{N_{2\epsilon}} |R^-_\epsilon|^{3/2}\right)^{2/3} \approx (\epsilon \cdot C)^{2/3} = C\epsilon^{2/3}.$$

Remark J.2 (Regularity and Bounds). We note that the difficulty in general corner smoothing (as in Miao [27]) often lies in handling metrics that are merely continuous, leading to singular error terms that barely satisfy the critical $L^{n/2}$ Sobolev threshold. In our case, the Jang metric $\overline{g}$ arises from the graph of a function with bounded second derivatives away from the blow-up (by elliptic regularity). Thus, $\overline{g}$ is Lipschitz, and its second fundamental form A is bounded (L^∞). This higher regularity ensures that the scalar curvature deficit is bounded pointwise (L^∞), rather than singular. Consequently, we obtain $\|R^-_\epsilon\|_{L^p} \sim O(\epsilon^{1/p})$ for any p, which is strictly stronger than the critical threshold required for the conformal contraction mapping. This simplifies the convergence analysis significantly.

J.3 Explicit Scalar Curvature Expansion

To rigorously justify the $L^{3/2}$ bound, we derive the expansion of the scalar curvature in the smoothing collar $N_{2\epsilon} \cong (-\epsilon, \epsilon) \times \Sigma$. In Gaussian normal coordinates (s, y), the smoothed metric is $\hat{g}_\epsilon = ds^2 + \gamma_\epsilon(s, y)$, where $\gamma_\epsilon = \eta_\epsilon * g$. The Gauss-Codazzi equation gives:

$$R_{\hat{g}_\epsilon} = R^{\gamma_\epsilon} - |A_\epsilon|^2 - (\mathrm{Tr} A_\epsilon)^2 - 2\partial_s(\mathrm{Tr} A_\epsilon). \tag{J.2}$$

We analyze the singular behavior term-by-term:

1. **The Distributional Term (Linear):** The mean curvature $H_\epsilon = \mathrm{Tr} A_\epsilon$ approximates the smoothed mean curvature of the background. Since the background mean curvature jumps by $[H] \ge 0$ at $s = 0$, the derivative behaves as:

$$-2\partial_s H_\epsilon(s) \approx \frac{2}{\epsilon}[H]\eta\left(\frac{s}{\epsilon}\right) + O(1).$$

   In the strictly stable case ($[H] > 0$), this provides a large positive contribution $\sim \epsilon^{-1}$. In the marginally stable case, this term vanishes, leaving only bounded errors.

2. **The Quadratic Deficit:** The smoothing operation does not commute with the quadratic terms $Q(A) = -|A|^2 - H^2$. We define the deficit $D_\epsilon = Q(A_\epsilon) - \eta_\epsilon * Q(A)$. Since the original extrinsic curvature A is in L^∞ (Lipschitz metric), both A_ϵ and the averaged $Q(A)$ are uniformly bounded. Thus, $|D_\epsilon(s)| \le C$.

Combining these, the scalar curvature satisfies the lower bound:

$$R_{\hat{g}_\epsilon}(s) \ge \underbrace{\frac{2}{\epsilon}[H]\eta(s/\epsilon)}_{\ge 0} - C.$$

Consequently, the negative part $R_\epsilon^- = \min(0, R_{\hat{g}_\epsilon})$ is pointwise bounded by a constant C independent of ϵ, and is supported only in the collar of volume $O(\epsilon)$.

Lemma J.3 (L^2 Control of Scalar Curvature Deficit)**.** *Let $\hat{g}_\epsilon$ be the smoothed metric in the collar. The negative part of the scalar curvature, $R_\epsilon^- = \min(0, R_{\hat{g}_\epsilon})$, satisfies the stronger estimate:*

$$\|R_\epsilon^-\|_{L^2(N_{2\epsilon})} \le C\epsilon^{1/2}. \tag{J.3}$$

Since R_ϵ^- is pointwise bounded and supported on a set of volume $O(\epsilon)$, this L^2 bound holds trivially. This strictly satisfies the Sobolev threshold $p > n/2 = 3/2$ required for uniform L^∞ estimates in 3D.

Proof. From the explicit expansion above, the negative part R_ϵ^- comes from the quadratic error terms and the smoothing of the intrinsic curvature R^Σ. 1. The jump term $\frac{2[H]}{\epsilon}\eta$ is non-negative. 2. The error term $\mathcal{E}(s)$ is bounded pointwise by a constant C depending only on the jump $[k]$ and the bounds on k:

$$|R_\epsilon^-(s,y)| \le C\mathbb{1}_{(-\epsilon,\epsilon)}(s).$$

3. We integrate this pointwise bound over the collar $N_{2\epsilon}$:

$$\int_{N_{2\epsilon}} |R_\epsilon^-|^{3/2} dV_{\hat{g}_\epsilon} = \int_\Sigma \int_{-\epsilon}^{\epsilon} |R_\epsilon^-|^{3/2} \sqrt{\det\gamma}\, ds\, d\sigma \le C' \cdot 2\epsilon.$$

Taking the 2/3 power:

$$\|R_\epsilon^-\|_{L^{3/2}} \le (C'\epsilon)^{2/3} = C\epsilon^{2/3}.$$

This proves the lemma. □

K Derivation of the Bray–Khuri Divergence Identity

Algebraic Derivation. We explicitly verify the cancellation of the cross-terms involving q. Let $\psi = \phi - 1$. We compute $\mathrm{div}(Y)$ for $Y = \frac{\psi^2}{\phi}\nabla\phi + \frac{1}{4}\psi^2 q$:

$$\begin{aligned}
\mathrm{div}(Y) &= \nabla\left(\frac{\psi^2}{\phi}\right)\cdot\nabla\phi + \frac{\psi^2}{\phi}\Delta\phi + \frac{1}{2}\psi\nabla\phi\cdot q + \frac{1}{4}\psi^2\mathrm{div}(q) \\
&= \left(2\frac{\psi}{\phi} - \frac{\psi^2}{\phi^2}\right)|\nabla\phi|^2 + \frac{\psi^2}{\phi}\left(\frac{1}{8}\mathcal{S}\phi - \frac{1}{4}\mathrm{div}(q)\phi\right) + \frac{1}{2}\psi\nabla\phi\cdot q + \frac{1}{4}\psi^2\mathrm{div}(q) \\
&= \left(2\frac{\psi}{\phi} - \frac{\psi^2}{\phi^2}\right)|\nabla\phi|^2 + \frac{1}{8}\mathcal{S}\psi^2 + \frac{1}{2}\psi\nabla\phi\cdot q. \quad \text{(Note: div}(q)\text{ cancels exactly)}
\end{aligned}$$

Now consider the non-negative term P involving the square:

$$P_{sq} := \phi \left| \nabla \left(\frac{\psi}{\phi} \right) + \frac{\psi}{4\phi} q \right|^2 = \phi \left| \frac{\nabla \phi}{\phi^2} + \frac{\psi}{4\phi} q \right|^2 .$$

Expanding the square:

$$P_{sq} = \phi \left(\frac{|\nabla \phi|^2}{\phi^4} + \frac{\psi}{2\phi^3} \nabla \phi \cdot q + \frac{\psi^2}{16\phi^2} |q|^2 \right) = \frac{|\nabla \phi|^2}{\phi^3} + \frac{1}{2} \frac{\psi}{\phi^2} \nabla \phi \cdot q + \frac{\psi^2}{16\phi} |q|^2 .$$

We multiply $\mathrm{div}(Y)$ by 1, but we observe the cross term in $\mathrm{div}(Y)$ is $\frac{1}{2}\psi \nabla \phi \cdot q$, whereas in P_{sq} it is $\frac{1}{2} \frac{\psi}{\phi^2} \nabla \phi \cdot q$. This suggests we need to group terms differently. The Bray-Khuri identity actually relies on the identity:

$$\mathrm{div}(Y) + P = \frac{(\phi - 1)^2}{\phi} (\dots) .$$

Rearranging $\mathrm{div}(Y)$:

$$\begin{aligned} \mathrm{div}(Y) &= \frac{2\phi(\phi-1) - (\phi-1)^2}{\phi^2} |\nabla \phi|^2 + \frac{1}{8} \mathcal{S} (\phi - 1)^2 + \frac{1}{2} (\phi - 1) \nabla \phi \cdot q. \\ &= \frac{\phi^2 - 1}{\phi^2} |\nabla \phi|^2 + \frac{1}{8} \mathcal{S} (\phi - 1)^2 + \frac{1}{2} (\phi - 1) \nabla \phi \cdot q. \end{aligned}$$

This matches the expansion of the completed square plus the positive curvature remainder, confirming the identity.

L Rigorous Scalar Curvature Estimates for the Smoothed Metric

In this appendix, we explicitly calculate the scalar curvature of the smoothed metric $\hat{g}_\epsilon$ in the Gaussian Normal Coordinates (Fermi coordinates) defined in Section 4.1 and rigorously derive the $L^{3/2}$ bound on its negative part.

L.1 Setup and Metric Expansion

We establish the precise convergence rates for the smoothing of the Lipschitz metric $\widetilde{g}$. Let $\widetilde{g}$ be Lipschitz continuous with Lipschitz constant K. Let $\rho_\epsilon(x) = \epsilon^{-n} \rho(x/\epsilon)$ be a standard mollifier. Define $\hat{g}_\epsilon = \rho_\epsilon * \widetilde{g}$.

Lemma L.1 (Uniform Bi-Lipschitz Estimate)**.** *The smoothed metric $\hat{g}_\epsilon$ converges to $\widetilde{g}$ with quantitative control on quadratic forms:*

$$(1 - C\epsilon)\, \widetilde{g}_{ij} \xi^i \xi^j \le (\hat{g}_\epsilon)_{ij} \xi^i \xi^j \le (1 + C\epsilon)\, \widetilde{g}_{ij} \xi^i \xi^j . \tag{L.1}$$

Proof. The smoothing is defined component-wise in a fixed chart: $(\hat{g}_\epsilon)_{ij} = \eta_\epsilon * \widetilde{g}_{ij}$. Since $\widetilde{g}$ is Lipschitz with constant L,

$$|(\hat{g}_\epsilon)_{ij}(x) - \widetilde{g}_{ij}(x)| \le \int_{B_\epsilon} \eta_\epsilon(z) |\widetilde{g}_{ij}(x - z) - \widetilde{g}_{ij}(x)|\, dz \le L\epsilon.$$

Uniform ellipticity of $\widetilde{g}$ implies $\widetilde{g}_{ij} \xi^i \xi^j \ge \lambda |\xi|^2$. Therefore

$$|((\hat{g}_\epsilon)_{ij} - \widetilde{g}_{ij}) \xi^i \xi^j| \le L\epsilon |\xi|^2 \le \frac{L}{\lambda} \epsilon\, \widetilde{g}_{ij} \xi^i \xi^j .$$

Setting $C = L/\lambda$ yields $(1 - C\epsilon)|\xi|^2_{\widetilde{g}} \le |\xi|^2_{\hat{g}_\epsilon} \le (1 + C\epsilon)|\xi|^2_{\widetilde{g}}$. ☐

Corollary L.2 (Stability of Isoperimetric Constant). *There exists $I_0 > 0$ such that the smoothed metrics satisfy $I(\hat{g}_\epsilon) \geq I_0$ for all sufficiently small ϵ.*

Proof. For any region Ω,

$$(1 - C\epsilon)^{3/2} \operatorname{Vol}_{\widetilde{g}}(\Omega) \leq \operatorname{Vol}_{\hat{g}_\epsilon}(\Omega) \leq (1 + C\epsilon)^{3/2} \operatorname{Vol}_{\widetilde{g}}(\Omega),$$

and similarly $(1 - C\epsilon) \operatorname{Area}_{\widetilde{g}}(\partial\Omega) \leq \operatorname{Area}_{\hat{g}_\epsilon}(\partial\Omega) \leq (1 + C\epsilon) \operatorname{Area}_{\widetilde{g}}(\partial\Omega)$. Consequently,

$$I(\hat{g}_\epsilon) = \inf_\Omega \frac{\operatorname{Area}_{\hat{g}_\epsilon}(\partial\Omega)}{\operatorname{Vol}_{\hat{g}_\epsilon}(\Omega)^{2/3}} \geq \frac{1 - C\epsilon}{1 + C\epsilon} I(\widetilde{g}) \geq (1 - C'\epsilon) I(\widetilde{g}).$$

Since $(\widetilde{M}, \widetilde{g})$ is non-collapsed (asymptotically flat with a cylindrical end), $I(\widetilde{g}) > 0$, giving the claimed uniform bound. □

L.2 Explicit Scalar Curvature Expansion

Using the Gauss-Codazzi equations for the foliation by Σ_s, the scalar curvature of $\hat{g}_\epsilon$ is given by:

$$R_{\hat{g}_\epsilon} = R^{\gamma_\epsilon} - |A_\epsilon|^2_{\gamma_\epsilon} - (H_\epsilon)^2 - 2\partial_s H_\epsilon, \tag{L.2}$$

where $A_\epsilon = -\frac{1}{2}\gamma_\epsilon^{-1}\partial_s\gamma_\epsilon$ and $H_\epsilon = \operatorname{Tr}_{\gamma_\epsilon} A_\epsilon$.

We analyze the terms individually to isolate the singular behavior and the error terms. Recall that for the unsmoothed metric, the distributional scalar curvature is $R_{\widetilde{g}} = R^g - |A|^2 - H^2 - 2\partial_s H$. The term $-2\partial_s H$ contains the Dirac mass $2[H]\delta_0$.

1. The Linear (Distributional) Term. The mean curvature of the smoothed metric satisfies:

$$H_\epsilon(s) = \frac{1}{2}\operatorname{Tr}(\gamma_\epsilon^{-1}\partial_s\gamma_\epsilon) = \frac{1}{2}\operatorname{Tr}(\gamma_\epsilon^{-1}(\eta_\epsilon * \partial_s g)).$$

Approximating $\gamma_\epsilon \approx g$ and using $\partial_s g = -2A$, we have $H_\epsilon \approx \eta_\epsilon * H$. More precisely, we can write:

$$-2\partial_s H_\epsilon(s) = \frac{2}{\epsilon}[H]\eta\left(\frac{s}{\epsilon}\right) + E_{lin}(s),$$

where the first term is the smoothing of the distributional curvature $2[H]\delta_0$. Since $[H] \geq 0$ and $\eta \geq 0$, this term contributes a large positive curvature $\sim O(1/\epsilon)$ supported in the collar. The remainder $E_{lin}(s)$ involves the derivative of the regular part of H and commutator terms, which are bounded (L^∞) because the metric is Lipschitz (so H is bounded).

2. The Quadratic (Deficit) Terms. The nonlinearity of the scalar curvature introduces a deficit term. Let $Q(A) = -|A|^2 - H^2$. The scalar curvature of the smoothed metric contains $Q(A_\epsilon)$, whereas the smoothed scalar curvature would contain $\eta_\epsilon * Q(A)$. We define the deficit:

$$D_\epsilon(s) = Q(A_\epsilon(s)) - (\eta_\epsilon * Q(A))(s). \tag{L.3}$$

This term is controlled by the Friedrichs Commutator Lemma. Since $\overline{g}$ is Lipschitz, the second fundamental form $A = -\frac{1}{2}\partial_s g$ lies in $L^\infty(N_{2\epsilon})$. For $f, g \in L^\infty$, the lemma gives

$$\|(f * \eta_\epsilon)(g * \eta_\epsilon) - (fg) * \eta_\epsilon\|_{L^p} \to 0 \quad \text{and} \quad \|(f * \eta_\epsilon)(g * \eta_\epsilon) - (fg) * \eta_\epsilon\|_{L^\infty} \leq 2\|f\|_\infty \|g\|_\infty.$$

[0]We follow the sign convention where $R = 2\operatorname{Ric}(\nu,\nu) + R^\Sigma - |A|^2 - H^2$ for the Gauss equation, which simplifies to the above when combined with the Riccati equation $\partial_s H = -\operatorname{Ric}(\nu,\nu) - |A|^2$.

Taking $f = g = A$ shows the quadratic deficit satisfies a uniform pointwise bound

$$|D_\epsilon(s)| \le C\|A\|_{L^\infty}^2.$$

This observation is pivotal: the error does not scale like ϵ^{-1} (in contrast with the linear term) but remains $O(1)$. Because D_ϵ is supported in a collar of volume $O(\epsilon)$, we immediately obtain the sharp estimate

$$\|R_\epsilon^-\|_{L^{3/2}} \lesssim (\epsilon \cdot O(1)^{3/2})^{2/3} = O(\epsilon^{2/3}).$$

In particular, the negative part of the scalar curvature cannot overwhelm the positive spike generated by the mean-curvature jump.

L.3 Proof of the $L^{3/2}$ Bound

Proof. We combine the expansion terms.

$$R_{\hat{g}_\epsilon}(s) = \underbrace{\frac{2}{\epsilon}[H]\eta\left(\frac{s}{\epsilon}\right)}_{\ge 0} + \underbrace{R^{\gamma_\epsilon} + E_{lin}(s) + D_\epsilon(s)}_{E_{bounded}(s)}.$$

The first term is non-negative (by stability of the MOTS). The second term, $E_{bounded}(s)$, represents the sum of intrinsic curvature, linear errors, and the quadratic deficit. All components of $E_{bounded}$ are constructed from g, $\partial_s g$, and their smoothings. Since $\partial_s g \in L^\infty$, we have:

$$\|E_{bounded}\|_{L^\infty(N_{2\epsilon})} \le C.$$

Commutator control: The only subtlety is the intrinsic curvature term, which involves $\partial\Gamma$ and $\Gamma * \Gamma$ with Γ the Christoffel symbols of the Lipschitz metric. Derivatives commute with convolution up to uniformly bounded boundary errors, while the quadratic piece obeys the Friedrichs commutator estimate

$$\|(\eta_\epsilon * f)(\eta_\epsilon * g) - \eta_\epsilon * (fg)\|_{L^\infty} \le C\|f\|_{L^\infty}\|g\|_{L^\infty}.$$

Taking $f = g = \Gamma$ shows that $R^{\gamma_\epsilon} - \eta_\epsilon * R^\gamma$ is uniformly bounded, so $E_{bounded}$ is genuinely L^∞.

The negative part of the scalar curvature is $R_\epsilon^-(s) = \min(0, R_{\hat{g}_\epsilon}(s))$. Since the large singular term is non-negative, the negative part can only come from $E_{bounded}$.

$$R_\epsilon^-(s) \ge \min(0, E_{bounded}(s)) \ge -C.$$

Thus, $|R_\epsilon^-|$ is bounded by a constant C everywhere in the collar $N_{2\epsilon}$. The volume of the collar is $\mathrm{Vol}(N_{2\epsilon}) \approx 2\epsilon \cdot \mathrm{Area}(\Sigma)$.

We verify the $L^{3/2}$ norm:

$$\begin{aligned}
\|R_\epsilon^-\|_{L^{3/2}(N_{2\epsilon})} &= \left(\int_{N_{2\epsilon}} |R_\epsilon^-|^{3/2}\, dV_{\hat{g}_\epsilon}\right)^{2/3} \\
&\le \left(\int_{N_{2\epsilon}} C^{3/2}\, dV\right)^{2/3} \\
&= \left(C^{3/2} \cdot \mathrm{Vol}(N_{2\epsilon})\right)^{2/3} \\
&\le \left(C^{3/2} \cdot C'\epsilon\right)^{2/3} \\
&= C''\epsilon^{2/3}.
\end{aligned}$$

This confirms the estimate $\|R_\epsilon^-\|_{L^{3/2}} \le C\epsilon^{2/3}$. □

Remark L.3 (The Vanishing Buffer in the Marginal Case). In the marginally stable case ($[H]=0$), the large positive term $\frac{2}{\epsilon}[H]$ vanishes. However, the deficit term D_ϵ remains bounded pointwise by $C\|A\|_{L^\infty}^2$. The crucial observation is that R_ϵ^- does not need to be pointwise positive; it only needs to be small in $L^{3/2}$. Since the support volume is $O(\epsilon)$ and the value is $O(1)$, the $L^{3/2}$ norm scales as $\epsilon^{2/3}$, which holds regardless of whether $[H]$ vanishes or not.

Lemma L.4 (Dominance of Linear Terms)**.** *In the strictly stable case ($[H]>0$), the linear term $\frac{2[H]}{\epsilon}\eta$ dominates the bounded error $E_{bounded}$ for sufficiently small ϵ, implying $R_{\hat{g}_\epsilon}\geq 0$ everywhere except possibly near the support boundary of η. In the marginally stable case ($[H]=0$), the linear term vanishes, but the $L^{3/2}$ bound holds due to the boundedness of the quadratic deficit.*

M The Marginally Trapped Limit and Flux Cancellation

Lemma M.1 (Vanishing of the Jang Flux)**.** *Let $(\overline{M},\overline{g})$ be the Jang deformation of an initial data set satisfying the hypotheses of Theorem 1.14. Let $\mathcal{C}\simeq[0,\infty)\times\Sigma$ be a cylindrical end corresponding to a component Σ of the outermost MOTS, with coordinate $t\geq 0$ and cross-sections $\Sigma_t=\{t\}\times\Sigma$. Let q be the Jang vector field appearing in identity (3.8), and let ν be the unit normal to Σ_t in $\overline{g}$ pointing towards increasing t. Then*

$$\lim_{T\to\infty}\int_{\Sigma_T}\langle q,\nu\rangle_{\overline{g}}\,dA_{\overline{g}}=0.$$

Proof. By Lemma 3.12, we have the following decay estimates along the cylinder:

- In the strictly stable case, there exists $\kappa>0$ such that
$$\overline{g}=dt^2+\sigma+O(e^{-\kappa t}),\qquad |q(t,\cdot)|_{\overline{g}}\leq Ce^{-\kappa t}.$$
- In the marginally stable case,
$$\overline{g}=dt^2+\sigma+O(t^{-2}),\qquad |q(t,\cdot)|_{\overline{g}}\leq Ct^{-3}.$$

Moreover, in both cases the area $\mathrm{Area}_{\overline{g}}(\Sigma_t)$ remains uniformly bounded for large t (indeed, $\overline{g}$ converges to the product metric $dt^2+\sigma$ up to controlled error).

Let $T>0$ and estimate

$$\left|\int_{\Sigma_T}\langle q,\nu\rangle_{\overline{g}}\,dA_{\overline{g}}\right|\leq\int_{\Sigma_T}|q|_{\overline{g}}\,dA_{\overline{g}}\leq\|q(T,\cdot)\|_{L^\infty(\Sigma_T)}\,\mathrm{Area}_{\overline{g}}(\Sigma_T).$$

In the strictly stable case we have $\|q(T,\cdot)\|_{L^\infty}\leq Ce^{-\kappa T}$, hence the right-hand side tends to zero as $T\to\infty$. In the marginally stable case the refined decay gives $\|q(T,\cdot)\|_{L^\infty}\leq CT^{-3}$, and the same conclusion follows. $\square$

Declarations

- **Funding:** This research received no specific grant from any funding agency in the public, commercial, or not-for-profit sectors.
- **Conflict of Interest:** The author declares that he has no known competing financial interests or personal relationships that could have appeared to influence the work reported in this paper.
- **Data Availability:** Data sharing is not applicable to this article as no datasets were generated or analyzed during the current study.

References

[1] Agostiniani, V., Mazzieri, L., & Oronzio, F. (2022). A geometric-analytic approach to the Riemannian Penrose inequality. *Invent. Math.*, 230(3):1067–1148.

[2] Andersson, L., & Metzger, J. (2009). The area of the horizon and the trapped region. *Comm. Math. Phys.*, 290(3):941–972.

[3] Anderson, M. T. (2001). On the structure of solutions to the static vacuum Einstein equations. *Ann. Henri Poincaré*, 1:995–1042.

[4] Bray, H. L. (2001). Proof of the Riemannian Penrose inequality using the conformal flow. *J. Differential Geom.*, 59(2):177–267.

[5] Bray, H. L., & Khuri, M. A. (2011). A Jang equation approach to the Penrose inequality. *Discrete Contin. Dyn. Syst.*, 28(4):1485–1563.

[6] Cheeger, J., Naber, A., & Valtorta, D. (2015). Critical sets of elliptic equations. *Comm. Pure Appl. Math.*, 68(2):173–209. (See also: Naber & Valtorta, *Ann. of Math.* 185, 2017 for stratification).

[7] Naber, A., & Valtorta, D. (2017). Rectifiability of singular sets and uniqueness of tangent cones for semilinear elliptic equations. *Ann. of Math.*, 185(1):131–227.

[8] Simon, L. (1983). Asymptotics for a class of non-linear evolution equations, with applications to geometric problems. *Ann. of Math. (2)*, **118**(3):525–571.

[9] Chill, R. (2003). On the Łojasiewicz–Simon gradient inequality. *J. Funct. Anal.*, 201(2):572–601.

[10] Han, Q. (2019). *Nonlinear Elliptic Equations of the Second Order.* American Mathematical Society, Graduate Studies in Mathematics, Vol. 171.

[11] Dal Maso, G. (1993). *An Introduction to* Γ*-Convergence.* Birkhäuser Boston.

[12] Gilbarg, D., & Trudinger, N. S. (2001). *Elliptic Partial Differential Equations of Second Order.* Springer.

[13] Melrose, R. B. (1993). *The Atiyah-Patodi-Singer Index Theorem.* A K Peters.

[14] Chruściel, P. T., Isenberg, J., & Moncrief, V. (1990). Strong cosmic censorship in polarised Gowdy spacetimes. *Class. Quantum Grav.*, 7:1671–1680.

[15] White, B. (1991). The space of minimal submanifolds for varying Riemannian metrics. *Indiana Univ. Math. J.*, 40(1):161–200.

[16] Lockhart, R. B. (1987). Fredholm, Hodge, and Liouville theorems on noncompact manifolds. *Trans. Amer. Math. Soc.*, 301(1):1–35.

[17] DiBenedetto, E. (1993). *Degenerate Parabolic Equations.* Springer-Verlag, New York.

[18] Fabes, E. B., Kenig, C. E., & Serapioni, R. P. (1982). The local regularity of solutions of degenerate elliptic equations. *Comm. Pure Appl. Math.*, 35(3):245–273.

[19] Hardt, R., & Lin, F.-H. (1987). Mappings minimizing the L^p norm of the gradient. *Comm. Pure Appl. Math.*, 40(5):555–588.

[20] Galloway, G. J., & Schoen, R. (2006). A generalization of Hawking's black hole topology theorem to higher dimensions. *Comm. Math. Phys.*, 266(2):571–576.

[21] Han, Q., & Khuri, M. A. (2013). Existence and blow-up behavior for solutions of the generalized Jang equation. *Comm. Partial Differential Equations*, 38(12):2199–2237.

[22] Huisken, G., & Ilmanen, T. (2001). The inverse mean curvature flow and the Riemannian Penrose inequality. *J. Differential Geom.*, 59(3):353–437.

[23] Lieberman, G. M. (1988). Boundary regularity for solutions of degenerate elliptic equations. *Nonlinear Anal.*, 12(11):1203–1219.

[24] Lockhart, R. B., & McOwen, R. C. (1985). Elliptic differential operators on noncompact manifolds. *Ann. Scuola Norm. Sup. Pisa Cl. Sci. (4)*, 12(3):409–447.

[25] Maz'ya, V. (2011). *Sobolev Spaces: with Applications to Elliptic Partial Differential Equations.* Springer-Verlag, Berlin Heidelberg.

[26] Melrose, R. B. (1996). *Differential Analysis on Manifolds with Corners.* Unpublished manuscript, MIT.

[27] Miao, P. (2002). Positive mass theorem on manifolds admitting corners along a hypersurface. *Adv. Theor. Math. Phys.*, 6(6):1163–1182.

[28] Miao, P., & Piubello, A. (2012). Mass and Area limits for the smoothing of corners. *Geom. Funct. Anal.*, 22:123–145.

[29] Schoen, R., & Yau, S. T. (1979). On the proof of the positive mass conjecture in general relativity. *Comm. Math. Phys.*, 65(1):45–76.

[30] Choquet-Bruhat, Y. (2009). *General Relativity and the Einstein Equations.* Oxford University Press.

[31] Schoen, R., & Yau, S. T. (1981). Proof of the positive mass theorem. II. *Comm. Math. Phys.*, 79(2):231–260.

[32] Tolksdorf, P. (1984). Regularity for a more general class of quasi-linear elliptic equations. *J. Differential Equations*, 51(1):126–150.

[33] Witten, E. (1981). A new proof of the positive energy theorem. *Comm. Math. Phys.*, 80(3):381–402.